

**This dissertation has been
microfilmed exactly as received**

66-14,196

**BLANCETT, Allen Leroy, 1938-
VOLUMETRIC BEHAVIOR OF HELIUM-ARGON
MIXTURES AT HIGH PRESSURE AND MODER-
ATE TEMPERATURE.**

**The University of Oklahoma, Ph.D., 1966
Engineering, chemical**

University Microfilms, Inc., Ann Arbor, Michigan

THE UNIVERSITY OF OKLAHOMA

GRADUATE COLLEGE

VOLUMETRIC BEHAVIOR OF HELIUM-ARGON MIXTURES AT
HIGH PRESSURE AND MODERATE TEMPERATURE

A DISSERTATION

SUBMITTED TO THE GRADUATE FACULTY

in partial fulfillment of the requirements for the

degree of

DOCTOR OF PHILOSOPHY

BY

ALLEN LEROY BLANCETT

Norman, Oklahoma

1966

VOLUMETRIC BEHAVIOR OF HELIUM-ARGON MIXTURES AT
HIGH PRESSURE AND MODERATE TEMPERATURE

APPROVED BY

Frank B. Campbell
Stanley E. Zabb, Jr.
Sheldon D. Christian
Charles
F. M. Townsend

DISSERTATION COMMITTEE

ACKNOWLEDGEMENTS

Completion of this work has been due in a large part to the efforts of many individuals and organizations who have assisted in various phases of the work. For their help, I express my sincere thanks. Special mention must be made, however, of those who contributed so significantly.

To Professor F. B. Canfield I owe a great deal. From the inception of the experimental design through the completion of this thesis he has consistently overlooked my shortcomings and helped me achieve whatever degree of success I had in the experimental and theoretical work.

Special thanks are offered also to Mr. K. R. Hall, who made my job of data treatment considerably simpler by his theoretical work and computer programming of the rather involved techniques utilized in the treatment.

Mr. M. Y. Shana'a contributed many valuable comments throughout the entire period of this work. Professor O. K. Crosser also contributed a good deal, particularly with regard to the solution of the temperature control problems in the cryostat.

Mr. Greg Clarke contributed invaluable assistance by checking all of the original pressure calculations, and

he also assisted in the construction of the experimental apparatus.

Dr. L. W. Brandt, of the United States Bureau of Mines Helium Research Center in Amarillo, made available the high-purity helium and provided for the composition analyses of all the gases used in this work.

Mr. Claude Miks, of Ruska Instrument Company, contributed many helpful comments concerning the operating techniques and characteristics of the Ruska instruments used in the experimental work.

Mr. David Monroe, of Monroe International, Inc., very helpfully arranged for the loan of a Monroe IQ Calculator, which proved to be of great value.

Mr. G. J. Scott was of inestimable value not only for his excellent machining skill, but also because of his continuous cooperation in the design changes that had to be made during the work.

A special debt of gratitude is owed the National Science Foundation, which supported the overall project with a research grant, and also supported me by means of a graduate fellowship during the first year of the work.

Above all, credit must go to my parents, who instilled in me the unwillingness to be satisfied with less than the best I could do, and to my wife, Gail, who, by her continued encouragement and assistance, has aided me immeasurably in my attempts to attain this goal.

TABLE OF CONTENTS

	Page
LIST OF TABLES	vii
LIST OF ILLUSTRATIONS	ix
 Chapter	
I. INTRODUCTION	1
II. REVIEW OF PREVIOUS WORK.	8
P-V-T Behavior of Argon.	8
P-V-T Behavior of Helium	11
Helium-Argon and Similar Mixtures.	13
III. DESCRIPTION OF EXPERIMENTAL APPARATUS.	15
Cryostat	15
Burnett Cell	32
Magnetic Pump.	41
Temperature Measurement.	42
Pressure Measurement	46
Pressure Generation.	59
Vacuum System.	60
Valves and Tubing.	61
IV. EXPERIMENTAL PROCEDURE	64
Temperature Equilibration of Cryostat.	64
Initiation of Experimental Runs.	67
Sequential Arrangement of Runs.	68
Evacuation and Purging.	68
Charging of the Burnett Cell.	70
Final Pressure Adjustment	74
Final Temperature Adjustment	74
Final Leak Check Before Run.	75
Initial Pressure Measurement	76
Expansion and Subsequent Pressure Measurements.	77

Chapter	Page
V. EXPERIMENTAL DIFFICULTIES.	81
Temperature Control.	81
Constant Refrigerating Effect	82
Location of Fan, Heater, and Vaporizer	84
Valves	85
Low Temperature Valves	87
Effect of Temperature on Circuitry of Cryo-PNI	89
Overpressure Indication.	92
VI. DATA ANALYSIS.	95
Gases Used	95
Calculation of the Pressures	97
Treatment of the Data.	97
Previous Methods.	98
Present Method of Analysis.	100
VII. DISCUSSION OF RESULTS.	107
Reliability of the Fitted Equations.	107
Comparison with Other Investigators.	116
Error Analysis	123
Estimated Errors.	129
VIII. APPLICATIONS OF THE DATA	132
Second Virial Coefficients	132
Pure-Component and Mixture Second Virial Coefficients	132
Interaction Second Virial Coefficients.	136
Third Virial Coefficients.	137
Pure-Component and Mixture Third Virial Coefficients	137
Interaction Third Virial Coefficients	143
LITERATURE CITED	145
APPENDICES	
A. EFFECT OF INCOMPLETE EVACUATION OF V_b	A-1
B. TEMPERATURE MEASUREMENT.	B-1
C. PRESSURE MEASUREMENT	C-1
D. EFFECT OF PRESSURE ON THE CELL CONSTANT.	D-1

LIST OF TABLES

Table	Page
1. Results of Composition Analyses.	96
2. The Compressibility Factors for Helium at the Experimental Pressures	108
3. The Compressibility Factors for Mixture A at the Experimental Pressures.	109
4. The Compressibility Factors for Mixture B at the Experimental Pressures.	110
5. The Compressibility Factors for Mixture C at the Experimental Pressures.	111
6. The Compressibility Factors for Mixture D at the Experimental Pressures.	112
7. The Compressibility Factors for Pure Argon at the Experimental Pressures.	113
8. Coefficients in the Series $z = PV/RT =$ $1 + B/V + C/V^2 + \dots$ For V in cm^3/mole	114
9. Differences Between the Experimental Com- pressibility Factors and Those Calculated from the Fitted Equations for Pure Helium. . .	117
10. Differences Between the Experimental Com- pressibility Factors and Those Calculated from the Fitted Equations for Mixture A. . . .	118
11. Differences Between the Experimental Com- pressibility Factors and Those Calculated from the Fitted Equations for Mixture B. . . .	119
12. Differences Between the Experimental Com- pressibility Factors and Those Calculated from the Fitted Equations for Mixture C. . . .	120
13. Differences Between the Experimental Com- pressibility Factors and Those Calculated from the Fitted Equations for Mixture D. . . .	121

Table	Page
14. Differences Between the Experimental Compressibility Factors and Those Calculated from the Fitted Equations for Pure Argon . . .	122
15. Average Differences Between the Experimental Compressibility Factors and Those Calculated from the Fitted Equations.	123
16. Comparison of the Experimental Argon Compressibility Factors with Those of Other Investigators.	124
17. Comparison of the Experimental Helium Compressibility Factors with Those of Other Investigators.	125
18. Second Virial Coefficients for Helium, Argon, and Four Mixtures, in cm^3/mole	134
19. Comparison of Selected Values for the Second Virial Coefficients of Helium and Argon. . . .	135
20. The Second Interaction Virial Coefficient, B_{12} , for Helium-Argon Mixtures	136
21. Third Virial Coefficients for Helium, Argon, and Four Mixtures, in $(\text{cm}^3/\text{mole})^2$	143
22. The Third Interaction Virial Coefficients, $C_{\text{He-He-Ar}}$ and $C_{\text{He-Ar-Ar}}$, in $(\text{cm}^3/\text{mole})^2$	144
C-1. Instrument Constants for Piston Gages.	C-6
C-2. Calibration Data for Piston Gage Weights	C-8

LIST OF ILLUSTRATIONS

Figure	Page
1. Experimental Apparatus	16
2. Burnett Apparatus with Evacuation and Pressure Generation Systems.	17
3. Cryostat	20
4. Two-Phase Separator.	23
5. Burnett Cell--Final Design, with Copper Gaskets and Set Screws	34
6. Internal Appearance of Burnett Cell before Final Modification and Assembly.	38
7. Magnetic Pump.	43
8. Pressure Measuring Apparatus	47
9. Range of Sensitivity for the Room-Temperature Pressure Null Indicator.	54
10. Variation of Maximum Sensitivity with Tem- perature, for Cryogenic Pressure Null Indicator.	56
11. Non-Linearity of Readout of Cryogenic Pressure Null Indicator, for Maximum Sensitivity at -183°C	57
12. Temperature Dependence of the Helium-Argon Interaction Second Virial Coefficient.	138
13. Variation of the Helium-Argon Mixture Second Virial Coefficient with Composition.	139
14. Variation of the Helium-Argon Mixture Third Virial Coefficient with Composition at 50°C	140

Figure	Page
15. Variation of the Helium-Argon Mixture Third Virial Coefficient with Composition at 0°C.	141
16. Variation of the Helium-Argon Mixture Third Virial Coefficient with Composition at -50°C.	142
C-1. Zero Shift of Cryogenic Pressure Null Indicator as a Function of Pressure for Three Temperatures. Room-Temperature Curve Presented by Ruska is Included for Comparison.	C-32

ADDITIONS AND CORRECTIONS

Following the treatment of the data and the preparation of the final copy of this dissertation, an error was found in one of the basic equations used for determining the effect of pressure on the cell constant. Equations D-1 and D-2 were originally developed from the relationships presented by Comings (10, p. 162-3). Professor S. E. Babb, of the University of Oklahoma's Department of Physics, has pointed out an error in one of these relationships. Comings' equation for longitudinal stress in a thick-walled cylinder with closed ends and both internal and external pressure is

$$\sigma_z = \frac{P_1}{K^2 - 1}$$

The equation should have been

$$\sigma_z = \frac{P_1 - K^2 P_2}{K^2 - 1}$$

as presented many years ago in A. E. H. Love's classic work, "A Treatise on the Mathematical Theory of Elasticity." As a result of this error, Comings' Equations 6-18, 6-19, and 6-20 are also incorrect.

When the corrected equation is used to describe the longitudinal stress component, Equations D-1 and D-2 in the present work will become

$$\frac{\delta L}{L} = \frac{P_i}{E} \left\{ \frac{R_i^2(1-2\mu) + R_e^2[(2\mu-1)(P_e/P_i)]}{R_e^2 - R_i^2} \right\} \quad (D-1)$$

$$\frac{\delta R_i}{R_i} = \frac{P_i}{E} \left\{ \frac{R_i^2(1-2\mu) + R_e^2[1+\mu+(\mu-2)(P_e/P_i)]}{R_e^2 - R_i^2} \right\} \quad (D-2)$$

When these corrected equations are substituted into Equation D-8, the resulting corrected Equation D-9 is

$$\frac{\delta V_c}{V_c} = \frac{P_i}{E} \left\{ \frac{3R_i^2(1-2\mu) + R_e^2[2(1+\mu) + (4\mu-5)(P_e/P_i)]}{R_e^2 - R_i^2} \right\} \quad (D-9)$$

and the simplification for equal internal and external pressure becomes

$$\frac{\delta V_c}{V_c} = 3 \frac{P}{E} (2\mu - 1) \quad (D-10)$$

This corrected form for Equation D-10 will lead to new values for Equations D-12, D-13, and D-14:

$$\frac{\delta V}{V} = -6.1 \times 10^{-7} P \quad (D-12)$$

$$(\delta V)_{\text{larger cell}} = -5.87 \times 10^{-6} P \quad (D-13)$$

$$(\delta V)_{\text{smaller cell}} = -2.94 \times 10^{-6} P \quad (\text{D-14})$$

The expressions for the cell constant N_j then become:

at 50°C,

$$N_j = N_\infty \left[\frac{1 - 2.41 \times 10^{-7} P_j}{1 - 3.40 \times 10^{-7} P_{j-1}} \right] \quad \text{for all pressures;} \quad (\text{D-35})$$

at 0°C,

$$N_j = N_\infty \left[\frac{1 - 2.63 \times 10^{-7} P_j}{1 - 3.74 \times 10^{-7} P_{j-1}} \right] \quad \text{if } P_{j-1} \leq 500 \text{ atm} \quad (\text{D-36})$$

$$= N_\infty \left[\frac{1 - 2.63 \times 10^{-7} P_j}{1 - 1.82 \times 10^{-5} - 3.36 \times 10^{-7} P_{j-1}} \right] \quad (\text{D-37})$$

if $P_{j-1} > 500$ atm;

at -50°C,

$$N_j = N_\infty \left[\frac{1 - 2.94 \times 10^{-7} P_j}{1 - 3.72 \times 10^{-7} P_{j-1}} \right] \quad \text{if } P_{j-1} \leq 500 \text{ atm} \quad (\text{D-38})$$

$$= N_\infty \left[\frac{1 - 2.94 \times 10^{-7} P_j}{1 - 2.41 \times 10^{-5} - 3.74 \times 10^{-7} P_{j-1}} \right] \quad (\text{D-39})$$

if $P_{j-1} > 500$ atm

When the values of 700, 400, and 250 atm are assumed for P_0 , P_1 , and P_2 , the change in cell constant with pressure will then be

$$\text{at } 50^{\circ}\text{C: } N_1/N_{\infty} = 1.000134$$

$$N_2/N_{\infty} = 1.0000869$$

$$\text{at } 0^{\circ}\text{C: } N_1/N_{\infty} = 1.000148$$

$$N_2/N_{\infty} = 1.0000839$$

$$\text{at } -50^{\circ}\text{C: } N_1/N_{\infty} = 1.000143$$

$$N_2/N_{\infty} = 1.000100$$

For the worst case, at 0°C , the change will be approximately 0.015 percent, rather than 0.0063 percent, as stated in Appendix D.

A re-treatment of the two runs for pure helium at 0°C resulted in the following comparison with selected values from Table 2, page 108

$$T = 273.15^{\circ}\text{K}$$

$$z = (PV/RT)$$

P (atm)	Original	Corrected
683.599	1.33969	1.33937
143.091	1.07494	1.07488
55.9640	1.02957	1.02955
534.047	1.26914	1.26890
116.508	1.06118	1.06113
29.0883	1.01541	1.01540

Thus it can be seen that the corrected values differ by 0.024 percent at the highest pressure, decreasing to

0.004 percent at about 100 atm. The correction of the above equations is therefore of importance.

As emphasized in the dissertation, the present treatment is only a preliminary one. Publication of the data will be withheld until the method of treatment has been improved as planned. In the meantime, the experimental pressure measurements remain valid.

VOLUMETRIC BEHAVIOR OF HELIUM-ARGON MIXTURES
AT HIGH PRESSURE AND MODERATE TEMPERATURE

CHAPTER I

INTRODUCTION

In 1936 E. S. Burnett of the U. S. Bureau of Mines Helium Plant and Cryogenic Laboratory in Amarillo, Texas, described a method for determining compressibility factors of gases without direct measurements of volume or mass (5). This thesis is a report of the construction of a Burnett apparatus and of its use in the determination of the volumetric behavior of the helium-argon system at 50, 0, and -50°C for pressures up to 680 atmospheres.

The results of this investigation include values of the compressibility factors ($z = PV/RT$) for helium, argon, and four mixtures having compositions of 21.99, 41.05, 59.35, and 80.00 mole percent helium in argon. Compressibility factors have been presented for the experimental pressures. Orthonormal polynomials have been utilized to obtain virial coefficients for the reciprocal volume series, and these coefficients have been interpreted to be those statistically

nearest the exact theoretical virial coefficients of the infinite series expansion.

The Burnett apparatus consists of two chambers of unspecified volume, V_a and V_b , connected by an expansion valve. A charging line and a pressure tap are connected to chamber A, and an exhaust line from chamber B leads to an atmospheric vent valve and a vacuum system. The entire apparatus is placed in a constant-temperature bath.

To carry out the desired measurements, chamber A is filled to the maximum pressure with the gas to be studied. When temperature equilibrium has been attained, the initial pressure is measured, and the gas is expanded into chamber B, which has been evacuated. Again the pressure is measured after the establishment of temperature equilibrium. The expansion valve is then closed, and chamber B is vented and evacuated. The process is repeated until the minimum desired pressure has been measured.

At the time of the initial pressure measurement, the following equation of state holds for the gas in V_a :

$$P_0(V_a)_0 = z_0 n_0 RT \quad (1)$$

where the subscripts indicate the values of the quantities before the first expansion.

After the first expansion, the equation of state for the same amount of gas in the total volume of the two chambers is

$$P_1(V_a + V_b)_1 = z_1 n_0 RT \quad (2)$$

When the expansion valve is closed and the contents of chamber B discarded, the pressure remains the same; the number of moles in chamber A will then be n_1 , so that the equation of state describing the system will be

$$P_1 (V_a)_1 = z_1 n_1 RT \quad (3)$$

If this process is continued, the equation of state before the j^{th} expansion is seen to be

$$P_{j-1} (V_a)_{j-1} = z_{j-1} n_{j-1} RT \quad (4)$$

and the equation which holds after the j^{th} expansion is

$$P_j (V_a + V_b)_j = z_j n_{j-1} RT \quad (5)$$

The relationship between compressibility factors at successive pressures is then found by dividing Equation 4 into Equation 5:

$$\frac{z_j}{z_{j-1}} = \frac{P_j (V_a + V_b)_j}{P_{j-1} (V_a)_{j-1}} \quad (6)$$

As a matter of convenience, the ratio of the total volume after the j^{th} expansion to the volume of chamber A before the j^{th} expansion is normally written in the simplified notation

$$N_j \equiv \frac{(V_a + V_b)_j}{(V_a)_{j-1}} \quad (7)$$

where N_j is called the cell constant for the j^{th} expansion. With this simplification, Equation 6 becomes

$$\frac{z_j}{z_{j-1}} = \frac{P_j N_j}{P_{j-1}} \quad (8)$$

When this equation is applied to the first expansion, the result after slight rearrangement is

$$\frac{z_1}{P_1} = N_1 \left(\frac{z_0}{P_0} \right) \quad (9)$$

For the second expansion,

$$\begin{aligned} \frac{z_2}{P_2} &= N_2 \left(\frac{z_1}{P_1} \right) \\ &= N_1 N_2 \left(\frac{z_0}{P_0} \right) \end{aligned} \quad (10)$$

In like manner, the compressibility factor after the j^{th} expansion can be expressed as

$$z_j = P_j N_1 N_2 N_3 \dots N_j (z_0/P_0) \quad (11)$$

Thus it is seen that the compressibility factor following a given expansion can be determined from a knowledge of the measured pressures, the initial compressibility factor, z_0 , and each of the cell constants up to and including the one for that expansion.

Deformation of the two chambers and the associated apparatus will occur at the high pressures, causing the cell constants, N_j , to be a function of the pressures before

and after an expansion. The theory of elasticity can be used to estimate the deformation in terms of the volume at zero pressure (Appendix D); therefore, if the zero-pressure cell constant can be determined, each of the cell constants at higher pressure can be estimated very closely from that value.

From Equation 8, it is seen that the cell constant at zero pressure (which is the cell constant as the number of expansions becomes infinite) is simply the limit of the ratio, P_{j-1}/P_j , at zero pressure, where $z_j = z_{j-1} = 1$.

$$N_{\infty} = \lim_{P \rightarrow 0} \frac{P_{j-1}}{P_j} \quad (12)$$

Therefore, if expansions are carried out to low pressure, the value of N_{∞} will be obtained by extrapolation of this pressure ratio to zero pressure. In practice, the extrapolation is performed most accurately if the expansions are made with a gas for which the compressibility factor is quite linear with pressure, such as helium.

The remaining quantity to be determined is the initial compressibility factor, z_0 . After the value for the cell constant at zero pressure, N_{∞} , has been determined, Equation 11 is used to obtain z_0 . In particular, the limit of $P_j N_1 N_2 \dots N_j$ at zero pressure is equal to P_0/z_0 , z_j being equal to 1 at zero pressure. An extrapolation similar to the one above is used to determine P_0/z_0 . When the

initial pressure P_0 is divided by P_0/z_0 , the value of z_0 results, and the remainder of the compressibility factors for that run follow from Equation 11.

For studies of theoretical interest, the compressibility factor can be expressed as an infinite series in density, or reciprocal volume,

$$z = 1 + B/V + C/V^2 + D/V^3 + \dots \quad (13)$$

where B, C, D, \dots are called the second, third, fourth, ... virial coefficients. This series expansion, which has been called the Leiden expansion, is of interest because the coefficients can be related, by means of statistical mechanics, to the intermolecular potential energy of the gases. According to the statistical mechanical development, the virial coefficients depend only upon the temperature and the potential energy of interaction. In addition, the second virial coefficient, B , is a measure of the interaction of pairs of molecules in the limit of zero macroscopic density; the third virial coefficient is a measure of three-molecule interactions in the zero-density limit, and so on (21, p. 132).

Slight rearrangement of Equation 13 shows one method for determining the second and third virial coefficients.

$$(z - 1)V = B + C/V + D/V^2 + \dots \quad (14)$$

When the quantity $(z-1)V$ is plotted versus $1/V$, its limit as $1/V$ approaches zero will be the second virial coefficient,

B :

$$B = \lim_{1/V \rightarrow 0} (z-1)V \quad (15)$$

The third virial coefficient is equal to the slope of $(z-1)V$ at zero pressure, and it can also be obtained by a limiting technique:

$$C = \lim_{1/V \rightarrow 0} [(z-1)V - B]V \quad (16)$$

This method of obtaining B and C requires extremely accurate compressibility data at low densities.

Other methods used in the determination of virial coefficients from compressibility data are discussed in Chapter VI.

CHAPTER II

REVIEW OF PREVIOUS WORK

Previous work of interest in this review will be of two general types--those reported results concerning the P-V-T behavior of the pure components helium and argon, and those concerning the P-V-T behavior of helium-argon mixtures and similar mixtures.

P-V-T Behavior of Argon

The volumetric behavior of argon has been reported by numerous investigators, and although discrepancies exist among some of the data sets, the agreement is generally considered to be adequate.

Compressibility data on argon prior to 1961 have been summarized in the excellent book edited by Cook (11). The Cryogenic Data Center of the National Bureau of Standards has recently published a bibliography (39) of approximately 11,000 references for the thermophysical properties of the cryogenic fluids, including argon, which seems to cover the reported work through 1964. These two compilations were used extensively in the present literature survey and were found to be quite complete. Another earlier source

of information was the book by Din (15), which included comments concerning the probable validity of the various earlier sets of reported data.

Briefly summarizing the early work, the compressibility of argon has been reported by Onnes and Crommelin (42, 43) at the University of Leiden; by Holborn and co-workers (22, 23, 24, 25) at the Reichsanstalt in Berlin; by Masson and co-workers (32) at the University of Durham; and by P. W. Bridgman (4) at Harvard. More recently, Michels and co-workers (33, 34, 35) at the Van der Waals Laboratory in Amsterdam have reported the experimental compressibility measurements for argon, as have Schneider and co-workers (49, 50) of the National Research Council Laboratories in Ottawa, and Getzen (17) at the Massachusetts Institute of Technology.

The Leiden measurements were made for several temperatures between 20 and -150°C , with maximum pressure of about 60 atm at the higher temperatures, decreasing to about 13 atm at -150°C . Din mentioned that "discrepancies between the Leiden and Reichsanstalt data have been recognized for some time and are attributed by Masson to a fault in the Leiden technique." Whalley, Lupien, and Schneider (50) also point out this disagreement, saying that it is apparently caused by incorrect Leiden values due to "side-trapping in one limb of the piezometer after measuring the volume at one atmosphere pressure."

The Berlin data cover the temperature range from -100 to 400°C for pressures between 0 and 100 atm, and at 0 and 100°C the maximum pressure was 200 atm. Cragoe (12) indicated that the results were not worked up correctly, and Whalley et al. (50) have recalculated the experimental results, giving "a rather extended discussion of the Berlin data since the PVT properties of a number of gases below 0°C and above 150°C are known only from these measurements." The 300 and 400°C isotherms were both rejected by Whalley et al. in their assessment of the best values for the second and third virial coefficients for argon.

The Durham data were obtained over the temperature range 25-174°C for pressures between 5 and 125 atm. Measured values of PV were not presented, but the virial coefficients were given, along with the mean deviation of PV.

The early compressibility measurements at Amsterdam (35) covered the range from 0 to 150°C in 25° intervals, for pressures between 20 and 2900 atm. The more recent work (34) extended the range of coverage to -155°C for pressures up to 1050 atm and densities up to 640 Amagat (the Amagat density is the ratio of the volume of a fixed mass of gas at 0°C and 1 atm pressure to the volume of the same amount of gas at the given conditions). The measurements of Michels' group have often been considered among the most accurate available.

The Ottawa data cover the temperature range 0-600°C for pressures from 10 to 80 atmospheres. Second and third

virial coefficients have been reported and compared with the earlier work.

Getzen's results from M.I.T. cover temperatures from 0 to 300°C, with a density range from 0 to 10 moles per liter with maximum pressure of 400 atm. His results are reported in the book by Cook.

Bridgman's work has been carried out principally at high pressures, in some cases up to 15,000 atm. A few values are reported at temperatures from -90 to -150°C, and at 0, 25, and 55°C several values are reported for the volume of one gram of argon.

Second virial coefficients of argon have been reported by Kerr (29) at Ohio State, based on his measurements from 25 to -190°C at pressures between 0.4 and 1.1 atm. Oishi (40) has measured the compressibility of argon at 0 and 100°C at pressures below 2 atm in an attempt to determine second virial coefficients more accurately than had been done earlier.

Rogovaya and Kaganer (45) have reported compressibilities of argon from -25 to -183° at pressures to 200 atm.

Fender and Halsey (16) have carried out measurements on argon between 80 and 125°K at low pressures, and Crain (12) has measured the P-V-T behavior of argon from 143 to 273°K at pressures to 500 atm.

P-V-T Behavior of Helium

Helium is probably the most completely investigated of all the gases. Fortunately, the book by Cook (11) presents

a thorough review of the volumetric and thermodynamic properties of helium reported prior to 1960, and Canfield (6) has added a little further information. Therefore, only the highlights of the work will be mentioned here.

As with argon, early measurements of the compressibility of helium were begun by Onnes (41) in Leiden, and continued by other investigators in that laboratory during the following years. Holborn and Otto (22) also reported data on helium, as did Michels and Wouters (36) in Amsterdam, and Wiebe, Gaddy, and Heins (52) at the U. S. Department of Agriculture's Fixed Nitrogen Research Laboratory. Schneider (46) at Ottawa, White and co-workers (51) at Ohio State University, and Miller and co-workers (54) at the University of Pennsylvania have added to the available information on helium. Canfield (6) has recently contributed valuable measurements of the behavior of helium between 0 and -140°C at pressures to 500 atm.

In spite of the accuracies claimed by all of these investigators, comparison of their results shows that the agreement among the various sources is not as good as the claimed limits of error would indicate. The reported second virial coefficients based on work prior to 1962 have been compared by White et al. (51), by Witonsky and Miller (54), and by Canfield, Leland, and Kobayashi (8). In general, it is found that the results obtained at Leiden are systematically lower than those of other workers at all

temperatures above -150°C . White and Canfield report the highest second virials, and Schneider agrees reasonably well with White's values where the temperature ranges overlap. Other values fall between these and the Leiden values.

Keesom (28) has presented a set of "adopted" values based on work prior to 1942. Later work by Canfield, by Witonsky, and by Stroud, Miller and Brandt (47) indicates that perhaps Keesom's evaluation of the data should be reconsidered in the light of more recent work.

Helium-Argon and Similar Mixtures

Despite the theoretical interest in mixtures of simple molecules such as helium and argon, this system has not been investigated extensively. Tanner and Masson (48) have carried out the most extensive of the existing measurements, reporting seven isotherms between 25 and 174°C up to 125 atm, with two different mixtures at each temperature. Michels and Boerboom (33) have determined the interaction second virial coefficient, B_{12} , for this system at 25°C , and Magasanik (31) has determined it at 50, 75, and 100°C . Knobler, Beenakker, and Knapp (30) have reported a value for B_{12} at -183°C .

Perhaps the most complete collection of references on pertinent mixture data is the recent NBS Bibliography mentioned earlier (39). The references are there, but they are often difficult to recognize as such. A more satisfactory compilation of such mixture data has been presented

recently by Canfield (7), who summarized the data currently available for the study of the volumetric behavior of simple gas mixtures.

CHAPTER III

DESCRIPTION OF EXPERIMENTAL APPARATUS

This chapter includes the description of the more important parts of the apparatus. The major part of the experimental apparatus is shown in Figure 1. To the left of the barricade is the cryostat, suspended from an angle-iron framework which supported all of the apparatus within the cryostat. To the right are two piston gages with weights, a resistance bridge, a pressure null indicator, and several other pieces of equipment which were used to control and measure the temperature and pressure of the gas in the Burnett cell. Not shown in Figure 1 is the diaphragm compressor which was used to generate the pressures required during the experimental investigations. Figure 2 is a schematic representation of the Burnett apparatus and its connections with the vacuum pump and the diaphragm compressor.

Cryostat

The cryostat developed for this work was a gas-bath cryostat which was originally designed for operation between -200 and 50°C. A report of the design of this cryostat has been published recently (3). A more detailed discussion is now presented.

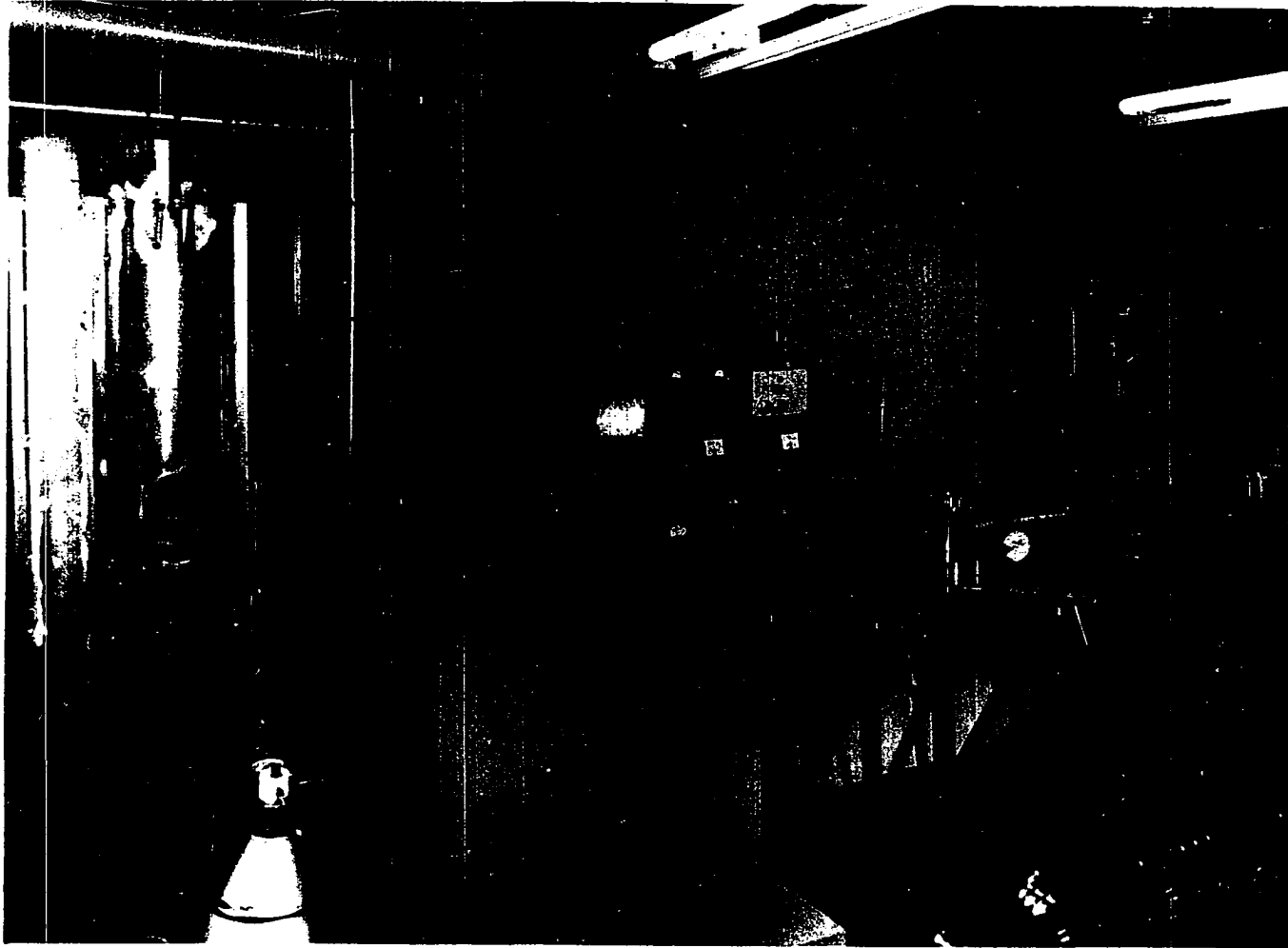


Figure 1. Experimental Apparatus

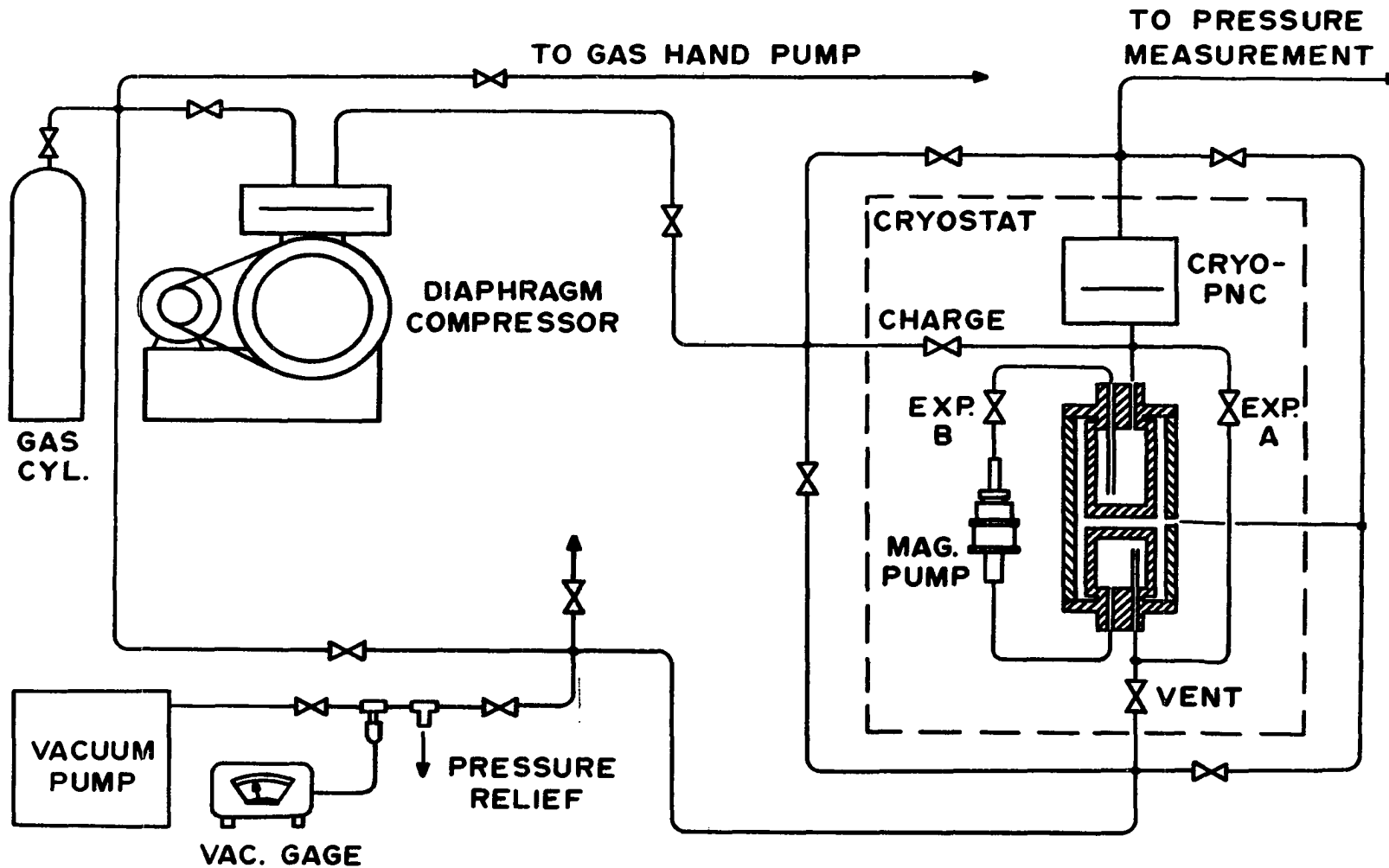


Figure 2. Burnett Apparatus with Evacuation and Pressure Generation Systems

During the early stages of this work one of the goals was to design and construct a cryostat which would allow continuous temperature control at any temperature between the above limits, within 0.002°C or better.

Cryostats which could be controlled to this extent were in operation at other laboratories, but none were found which did not have a number of shortcomings. Many suitable refrigerants were toxic, flammable, or expensive, requiring elaborate safety precautions and refrigerant recovery techniques. Viscous dissipation of energy was quite important for stirring liquid baths at low temperatures, and cooldown requirements were often excessive in the larger liquid baths. The major shortcoming, however, was that, when operating between room temperature and the normal boiling point of nitrogen, two or more different bath fluids had to be used, each one introducing its own problems and requiring a temporary shutdown of the equipment while the liquids were changed.

Because of these shortcomings of liquid baths, the decision was made to try to build a gas-bath cryostat. As originally envisioned, this cryostat was to use liquid nitrogen as a refrigerant at all temperatures, and the nitrogen boil-off vapor was to become the bath fluid. Later developments showed that at the highest temperature studied in this work (50°C) compressed air from the laboratory line was quite satisfactory as a refrigerant and bath fluid.

With the gas-bath cryostat, no problems of toxicity and flammability were involved, and a bath fluid recovery

system was unnecessary. Viscous dissipation due to stirring was quite low compared with a liquid system, and the low heat capacity of the system reduced cooldown losses. The cryostat was constructed largely from standard components and offered ease of operation over the entire temperature range. The low heat capacity of the bath fluid gave a rapid response time with small amounts of controlled heat; however, heat transfer to objects in the bath was slower than in liquid baths. The working space available for equipment was a cylindrical space 5-3/4 inches in diameter and 22 inches in length.

Physical Description of Cryostat

The outer container of the cryostat was an aluminum cylinder 22 inches in diameter and 46 inches long, lined with a three-inch layer of Styrofoam (Figure 3). A sheet-aluminum cylinder 14 inches in diameter acted as a radiation shield and vapor baffle and separated the foamed insulation from a 12-inch outside diameter strip-silvered glass dewar (H. S. Martin & Son, No. M-203200, 800 mm depth). Inside this dewar, about four inches above the bottom, was a circulating fan which supported a second aluminum radiation shield and vapor baffle 7-5/8 inches in diameter, extending upward to within one inch of a Styrofoam plug in the top of the dewar. Between this inner radiation shield and the inside of the dewar was a vaporizer into which the liquid nitrogen refrigerant was metered through a valve on top of

the cryostat. The fan, a temperature controller sensing element and a bare wire control heater were all supported on four threaded 1/4-inch stainless steel rods suspended from the top of the cryostat. Two diametrically opposed windows in the shields and foam permitted visual observation of the fan. An O-ring seal between the body and the top of the cryostat kept out moist air and made possible the future operation of the cryostat at pressures from ambient to the nitrogen triple point.

Refrigeration and Temperature Control

One of the most challenging problems encountered in the development of the cryostat involved the refrigeration system. At a control temperature of 0°C the nitrogen consumption was slightly more than one-third liter per hour. This necessitated very close regulation of the nitrogen flow rate for precise temperature control because of the low heat capacity of the gas bath.

Canfield's work with liquid baths (6) had led to the assumption that close control of refrigerant flow could be obtained by varying the pressures both in the cryostat and in the liquid nitrogen storage dewar to give an easily regulated pressure drop through the transfer line. Developments soon showed that this assumption was not valid. Surging two-phase flow was found to be unavoidable in this kind of transfer, in which the nitrogen was transferred vertically upward, then across and down to a lower point in a well-insulated transfer line (Figure 1).

Various attempts were made to minimize or damp out the short-term effects of these surges, but these effects were large enough in comparison to the bath's small heat capacity to cause temperature fluctuations of several hundredths of a degree at the higher temperatures.

These flow control problems were solved by the installation of a valve which metered the flow of liquid nitrogen from a two-phase separator at the discharge end of the transfer line (Figure 4). A small positive pressure in the storage dewar caused the liquid nitrogen to flow upward through the transfer line, and its flow rate was regulated by a float valve which controlled the liquid level in the separator. The nitrogen vapor generated by heat leak into the transfer line and the separator was vented from the separator, leaving a constant level of saturated liquid nitrogen above the metering valve. In this manner, the flow rate of nitrogen into the cryostat could be controlled very closely.

After being metered through the valve at a constant rate the nitrogen dropped through a 1/2-inch diameter thin-wall stainless steel tube into the vaporizer located between the evaporating liquid and the gas. The heat transfer area of the vaporizer was more than adequate to permit the high rate of heat transfer at the lowest temperature of operation. At the higher temperatures, a tapered bottom on the vaporizer helped to equalize the circumferential distribution of the small amount of liquid nitrogen in it.

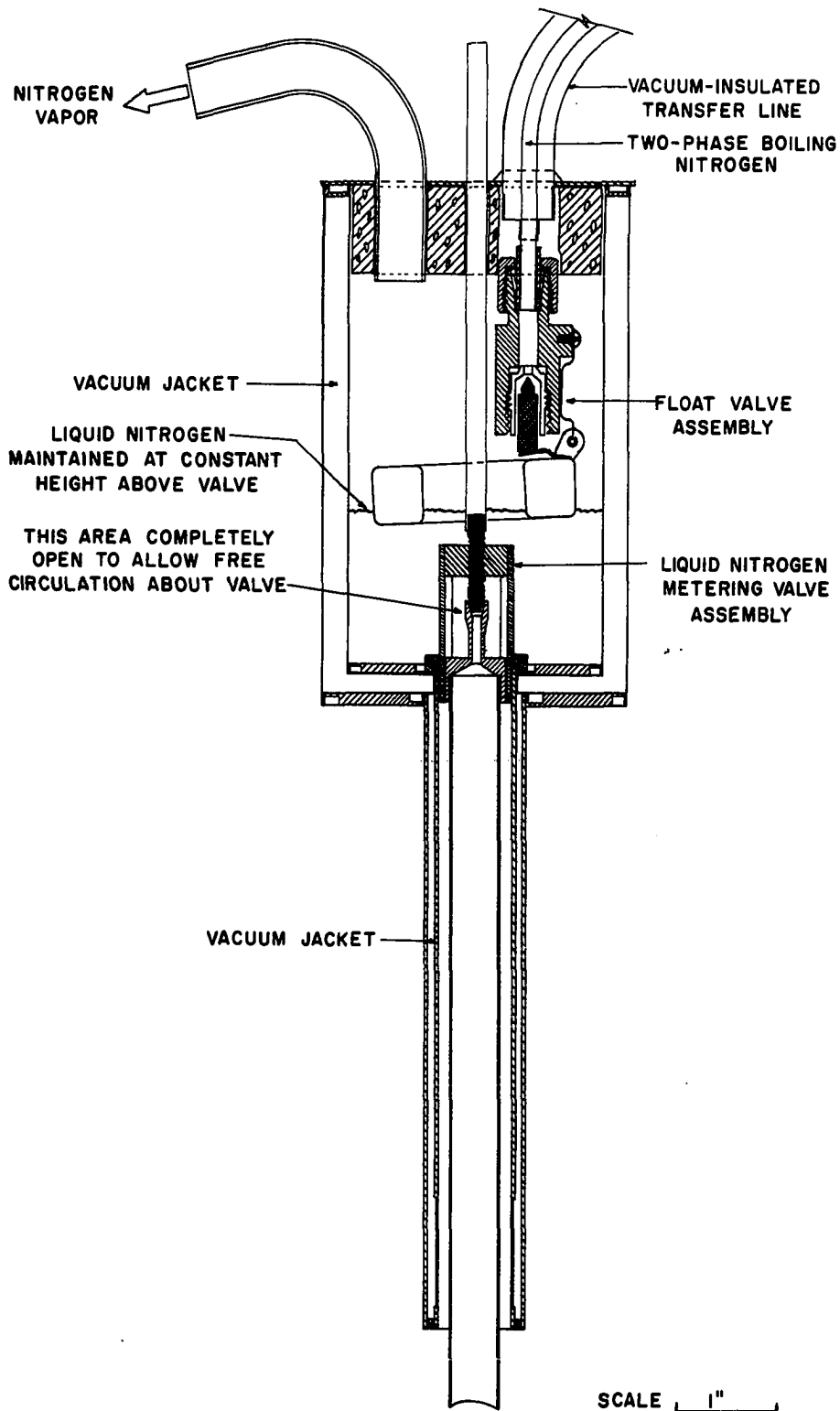


Figure 4. Two-Phase Separator

The nitrogen vapor coming out of the vaporizer became part of the bath fluid, giving a net outward flow of gas from the dewar, eliminating any chance for frosting due to leakage of moist room air into the cryostat. The vapor leaving the dewar passed up through holes in the Styrofoam plug, cooled the area above, and then was deflected downward by the outer aluminum shield. As it flowed down between the dewar and the shield it cooled them, then passed through holes in the bottom of the shield. From there it rose between the shield and the foam insulation where more of its available refrigeration was used up before it left the cryostat. By utilizing the refrigeration available in the excess gas, the nitrogen usage was reduced significantly.

As mentioned earlier, the refrigerant used at control temperatures of 0 and -50°C was liquid nitrogen, and at 50° , compressed air. In each case the flow rate of the refrigerant was chosen by trial to give just enough excess cooling to be overbalanced with a control heater operating between 0 and 20 watts, generally giving a time-average heating effect of 5 watts or less.

Refrigerant Transfer System: For operation of the cryostat at 0 and -50° the liquid nitrogen was transferred from a 50-liter storage dewar through the insulated transfer line to the two-phase separator on top of the cryostat. The dewar was fitted with a multi-purpose nylon pressuring head. This pressuring head allowed the dewar to be refilled from

the Linde LS-110 pressurized dewars at the same time the nitrogen was being transferred from the 50-liter dewar to the cryostat, thus permitting continuous operation of the cryostat without a temperature upset. A spring-loaded pressure relief ball-and-seat assembly was included in the head, and for additional safety to prevent dewar rupture in case of an accidental overpressure, the head was attached to the neck of the dewar with a short length of automobile radiator hose. During the early stages of the work an accidental buildup of pressure in the dewar caused the rubber hose to pop up off the neck, allowing the excess pressure to be relieved. Heat transfer through the nylon head was small enough that the rubber hose always remained flexible except during the refilling operation, and at this time the excess vapor was vented not only through the pressure relief mechanism but also through a manually-operated valve which was closed at the conclusion of the refill. A small pressure gauge was used to indicate the pressure in the dewar, which was normally kept at about 3-4 psig by adjustment of the pressure relief spring.

The slow rate of usage of liquid nitrogen in the cryostat (from 1/3 liter to 2-1/2 liters per hour) necessitated the use of a well-insulated transfer line in order to cut down on the unwanted loss of liquid due to boiloff outside the cryostat. The transfer line which was built to satisfy this requirement consisted of an inner tube of 3/16-inch

thin-wall Invar tubing separated from a jacket of 1/2-inch thin-wall stainless steel tubing by triangular Teflon spacers, with the annulus sealed on both ends and evacuated for minimum heat leak during transfer. The total length of the tube was slightly less than seven feet, and two right-angle bends were necessary. Initial attempts at bending the double-tube assembly after filling it with water and freezing with dry ice (solid CO_2 "snow") were unsuccessful because of the formation of numerous bulges and a few ruptures in the Invar tube where the dry ice snow had not been evenly applied. Because of its slight shrinkage on solidification and its freezing point of about 5°C , benzene was then used with very satisfactory results. The shrinkage did, however, require the elevation of one end of the tubing to prevent the formation of voids as the benzene froze.

One of the problems which arose after several hours of continuous transfer of liquid nitrogen was the apparent slow plugging of the metering valve in the two-phase separator. Although no complete investigation of this problem was ever made, it manifested itself by causing a very slow upward drift of the cryostat temperature--at a rate of approximately 0.001° per hour. This could be made relatively unimportant by closing the valve and then re-opening it, which seemed to clean off the seat (possibly, solid CO_2 was accumulating) because the cryostat temperature once again would return to the earlier set point. This manual adjustment,

although annoying, was not too critical in terms of valve positioning, so by repeating this procedure at appropriate intervals a few times a day, the cryostat temperature was controlled within acceptable limits. A sintered-glass bubbler tip was attached to the lower end of the transfer tube in the 50-liter dewar, but it apparently did not filter out all of the small solid particles. For a more satisfactory continuous transfer, a second filter has been recommended for further experimental work with this cryostat. The first one should remove most of the "junk" in the liquid nitrogen, and the second should take out the remainder of the tiny particles which tend to plug the metering valve.

When the cryostat was operated at 50°C, the refrigerant used was compressed air from the laboratory lines. A pressure regulator was used to provide a constant pressure of about 7 psig. From the outlet of the regulator, the air was carried through 30-35 feet of flexible plastic tubing, in which the small amount of oil and water in the air dropped out. The air was then introduced into the cryostat, discharging from a tube at the bottom of the dewar.

Liquid nitrogen could have been used as a refrigerant at 50°, but an expense of this magnitude was not justified in view of the satisfactory results obtained with the compressed air.

Temperature Control: At each of the experimental temperatures the refrigerant was introduced into the cryostat

in a slight excess at a closely controlled rate. This excess of cooling was then overcome by adding a small amount of heat by means of a bare-wire heater whose rate of heat generation was regulated by a Hallikainen Model 1053 Thermotrol, a commercial proportional-plus-reset electronic temperature controller. The signal to the Thermotrol was obtained with a Rosemount Model 104N48AAC sensor which had a platinum resistance element encased in a 1/4-inch diameter stainless steel sheath. The sensor was mounted midway up inside the inner aluminum shield, so that the tip would be located near the midpoint of the Burnett cell. The cooling excess was just enough to be overbalanced with a time-average heating effect of five watts or less.

The control heater was made of coiled 25-gage Nichrome wire strung between the sides of a four-inch Transite frame. It was mounted just below the circulating fan so that all of the gas would pass directly over and through the heater coils, then mix thoroughly before passing up through the inner shield.

The heater was divided into three segments for either series or parallel connection. When connected in series, the heater wattage could be adjusted by means of an external variable resistor between 10 and 100 watts. A 1000-watt heater was made available for quick warm-up of the cryostat by switching to a parallel connection. This was convenient in the early stages of development of the cryostat.

In line with the findings reported by Canfield (6), there were a few features which were found to be necessary

for good temperature control. The most important of these was a constant refrigerating effect, which was attained only after several failures of ideas which seemed, a priori, to be based on perfectly sound reasoning. The final solution, the two-phase separator with a level control mechanism inside and a metering valve at the bottom, was a very satisfactory means of ensuring a constant refrigerating effect. Vigorous stirring of the bath was also found to be important, but not so critical in the gas bath as it seems to be in a liquid bath. Finally, a bare-wire heater was needed to provide rapid heating of the gas in the bath. Time lags in the heating were essentially eliminated because of the intimate contact between the bare wire and the vigorously-moving gas passing through the heater just below the inlet to the circulating fan.

Circulation of the Bath Fluid: Vigorous circulation of the gas bath was assured by the use of a Diehl Mil-B-4-1 vaneaxial fan which was modified by replacing the standard bearings with BarTemp low temperature bearings. Power input to the fan increased from about 15 watts at the higher temperatures to about 30 watts at the lower ones. The rated air flow for this fan at room temperature was 120 cfm at free delivery.

Of particular importance in temperature control was the assurance of constant fan speed and electrical dissipation. A natural choice of motor suitable for these requirements

was a synchronous motor, but at the time the search for cryostat fans was being made, a satisfactory fan-synchronous motor combination was not found. It was quite simple, however, to use a strobe light for visual determination of constant speed of the induction motors commonly used for gas circulation. Speed and dissipation were found to be sufficiently constant down to about -150°C .

At lower temperatures the fan was on the verge of instability; with the application of normal line voltage (117 volts), the amperage of the fan varied randomly as much as 20 percent. A slightly higher voltage (125-135 volts) reduced this variation, but a slightly lower voltage allowed the speed to drop to about one-third of full speed. Once the fan had been allowed to slow down at these low temperatures, the normal line voltage was not enough to bring the speed back to normal. The fan would operate at this reduced, essentially constant speed until the applied voltage was raised enough to return it to full speed. The higher voltage was applied to the fan until the windings warmed up enough that it was able to regain its full speed, after which the voltage could be reduced gradually to its original level.

Operating Characteristics

Liquid nitrogen consumption for steady-state operation of the cryostat varied from between one-third and one-half liter per hour at 0°C to about two and one-half liters per

hour at -183°C . These figures represent only the amount of nitrogen that actually entered the cryostat--transfer losses and boiloff in the two-phase separator are not included.

A time-average control heater dissipation of two to ten watts at 0° and one to five watts at -183°C was enough to give the desired temperature control. Higher wattages increased both the local temperature variations and the positional temperature gradients.

The bath temperature was measured with a Leeds and Northrup Model 8164 capsule-type platinum resistance thermometer. A movable support for this thermometer was employed to determine the radial and longitudinal temperature gradients in the working space of the cryostat before the experimental equipment was introduced.

Local temperature variations sensed by the bare platinum resistance thermometer in the empty cryostat could be reduced to $\pm 0.03^{\circ}\text{C}$ by careful adjustment of the refrigerant flow rate and control heater dissipation. The periods of these variations were in the range of one to five minutes.

The extent of temperature control indicated by these numbers is a conservative estimate of the control possible within a mass of experimental equipment. For example, the cryostat normally contains the experimental Burnett cell roughly five inches in diameter and fourteen inches high, a differential pressure cell four inches in diameter and four and one-half inches high, an electromagnetic gas pump,

and four high pressure valves. With all this mass in the cryostat, the temperature in either end of the pressure cell was found to vary only by a few thousandths down to -90°C . Steady-state gradients from top to bottom in the cell were 0.012° at -50° , 0.015° at 0° , and 0.03° at $+50^{\circ}\text{C}$. Larger gradients existed at lower temperatures, but modifications proposed in Chapter V are expected to result in gradients of this size or smaller at all temperatures down to the vicinity of the nitrogen triple point.

The empty cryostat could be cooled from 0° to -183° in one hour, and temperature control could normally be attained within another hour. With all the above-mentioned equipment in the cryostat, cooldown from room temperature to -183° required about four hours and temperature control was attained in another three hours.

The cryostat was built with the intention of evacuating it in future work. A large vacuum pump or ejector connected to the cryostat would permit operation at lower temperatures approaching the nitrogen triple point (-210°C).

Burnett Cell

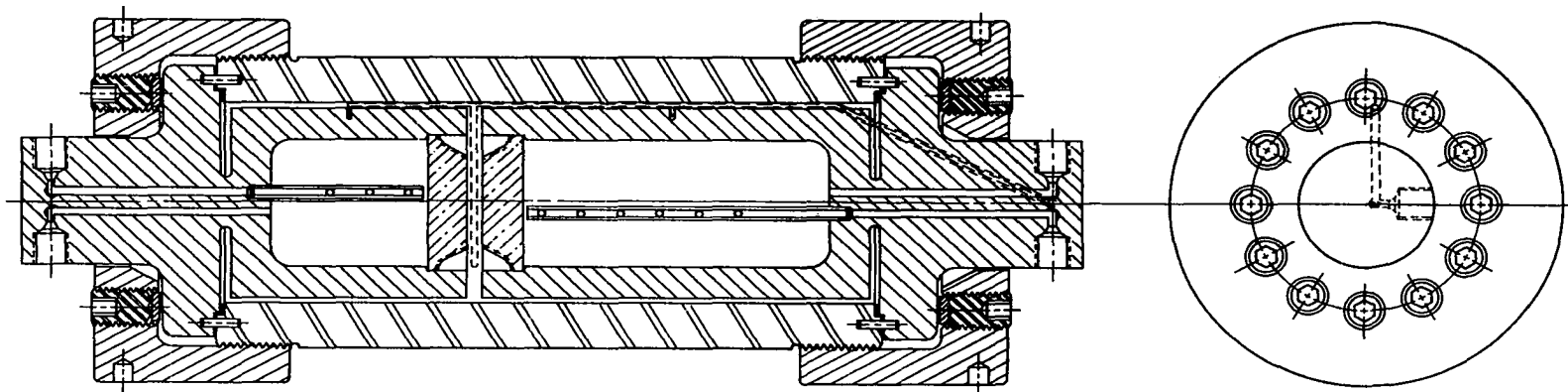
The Burnett cell used in this experimental work was a double-wall pressure bomb designed especially to reduce the volume distortion with pressure. The importance of this reduction of distortion is made readily apparent by an error analysis of the Burnett method. This error analysis, given in Chapter VII, shows that due to the

uncertainties in the prediction of elastic distortion of metals, all possible efforts should be made to eliminate this distortion.

With this in mind, the initial objective of the design was the development of a constant volume two-cell pressure bomb for use over the pressure range 0 to 1000 atmospheres, for all temperatures between 50 and -200°C .

As shown in Figure 5, the main feature of this design was the manner in which the two internal volumes were contained in a pressure jacket. Because of the small diameter of the neck connecting each volume with its flanged sealing region, the pressure jacket surrounded approximately 99 percent of the area of each cell. Limitations on the maximum allowable length of the bomb and minimum desirable cell volumes precluded the use of other means of surrounding the cells more completely with the pressure jacket. The effect of pressure on the volumes of the two internal cells is given in Appendix D.

Each end of the bomb was sealed with an annealed copper gasket. When the bomb was first constructed, the end closures were machined to accept Teflon-coated, vented, hollow metal O-rings. The mating surfaces were machined very precisely according to the manufacturer's recommended dimensions, and were highly polished. Each of the inner cells was pinned to the outer sleeve to prevent rotation between the mating sealing surfaces as the end caps were tightened.



SCALE: 1 2 3 4 5 INCHES

Figure 5. Burnett Cell--Final Design, with Copper Gaskets and Set Screws

In spite of all the precautions taken to ensure success, the O-rings were judged to be unsatisfactory for this application. Three successive sets of O-rings gave similar results--they sealed perfectly for the first pressure cycle, but on each subsequent pressure cycle a leak occurred at a lower pressure than before. Disassembly of the bomb always revealed the same thing. The O-rings were deformed just as pictured in the manufacturer's literature, the O-ring grooves were still highly polished, and no obvious reason for the leakage could be found. Therefore, the use of these O-rings for this particular application was considered to be unsatisfactory.

The possibility of unsatisfactory performance of the O-rings had been considered in the original design, so modifications were possible. Earlier experience with the use of copper gaskets for metal-to-metal seals at these pressures and temperatures indicated that a thin annealed copper gasket should be essentially foolproof for this job. The copper needed to be annealed so that it would flow at sufficiently low loading, and it had to be thin in order that the differential contraction between the unlike metals at the joint would not be enough to cause a leak when the temperature was cycled between 50 and -200°C . The two end pieces of the cell were modified accordingly, and copper gaskets were made from annealed sheet 0.031 inches thick.

When the O-rings were used, the end caps of the cell had to be pulled down just enough to make an initial

seal, according to the manufacturer's instructions. The vented, hollow design of the O-rings was supposed to make them self-energized so that any increase in the pressure created a better seal because of the unsupported-area effect. At any rate, the screwed caps were quite sufficient for this type of loading. When the decision was made to use copper gaskets, however, the screwed caps became marginal because of the pull-down torque required to create the initial gasket load required for the seal at high pressure. The galling and frictional characteristics of the metal in the cell (Monel Alloy K-500)* were very bad for the high loading required. The end closures were therefore modified by drilling and tapping twelve evenly-spaced 1/2-20NF holes in each cap at the mid-radius of the gasket. Oval-point socket set screws in this size were found to be available only on special order, so standard cup-point set screws were used. To eliminate the severe galling problem experienced earlier with the Monel Alloy K-500 and to obtain a better load distribution, bearing pads were made of hardened drill rod. Beneath each set screw was placed one of these pads, a disc 1/8 inch thick with a diameter of 7/16 inch.

The use of this bomb in the Burnett apparatus required that some means of determining the cell temperatures be included. For this reason, in the outer end of each cell was drilled a cylindrical hole just large enough for the insertion of the Leeds and Northrup capsule-type platinum

* Trademark of International Nickel Company.

resistance thermometer. Initially, one of these thermometers was placed in each of the two holes in order to measure the steady-state longitudinal temperature gradient in the bomb. In the later experimental work, however, the temperature of the larger cell was measured with a resistance thermometer, and a difference thermocouple was used to indicate the approach to temperature equilibrium between the two cells. The length of thermocouple wire necessary to allow for assembly and disassembly of the bomb without disturbing the thermocouple connections was coiled into the small space between the two cells. Silicone rubber was used to mount the thermocouple junctions in small holes in the cells.

The holes for the thermometer, the method of mounting the thermocouple junctions, and the general appearance of the interior of the Burnett cell are shown in Figure 6. This picture was made prior to the first assembly of the cell, and shows the O-rings which were later found to be unsatisfactory for this job. The nuts on either end are shown in their original condition, before being drilled and tapped for the set screws which were necessary in sealing the copper gaskets used later.

A major step in the Burnett method is the expansion of the gas under study from a cell at high pressure to an evacuated cell, followed by the attainment of temperature and pressure equilibrium between the two cells. In an expansion of the gas from the larger cell at high pressure

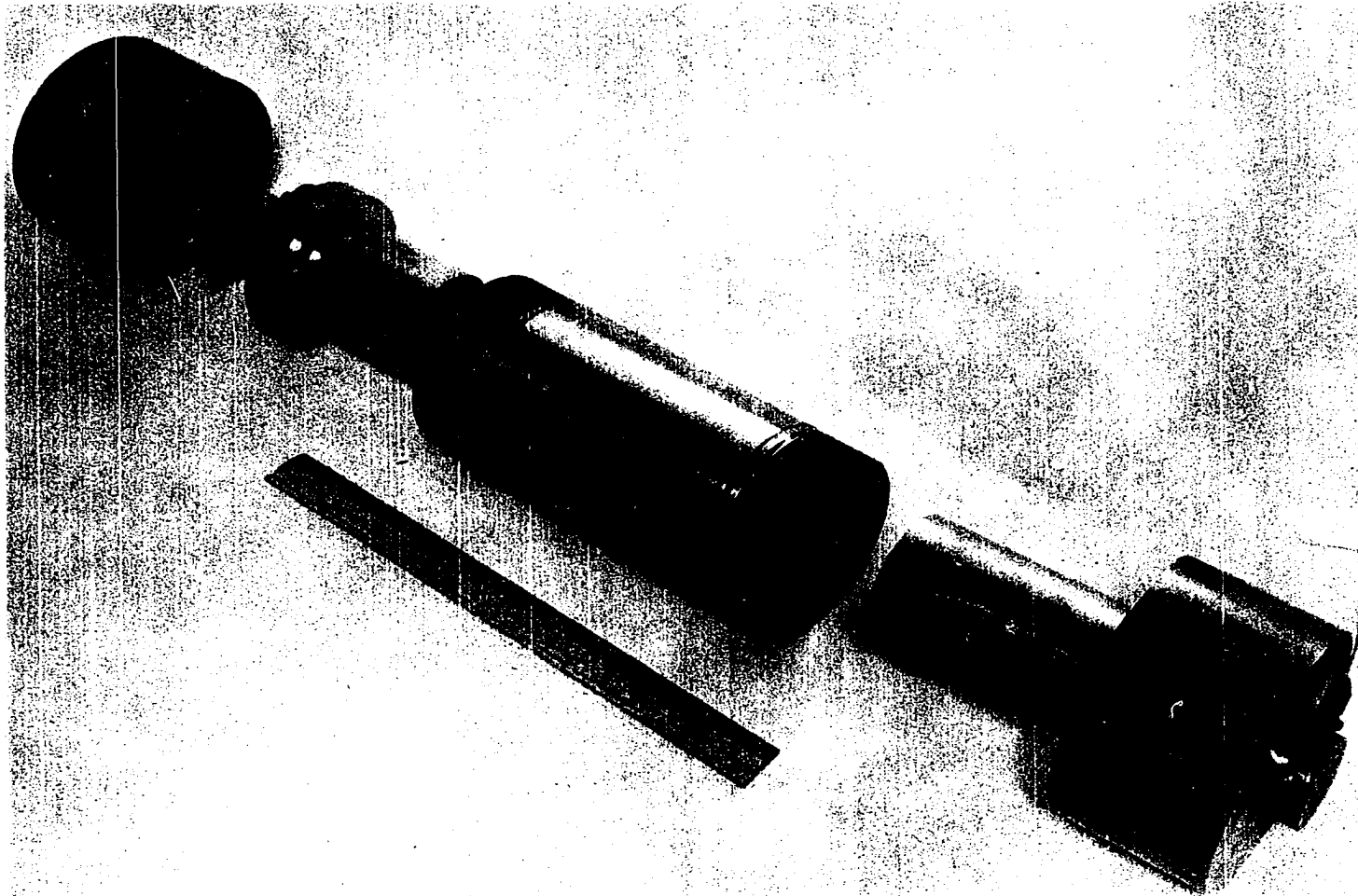


Figure 6. Internal Appearance of Burnett Cell Before Final Modification and Assembly

to the smaller, evacuated cell, there is normally a cooling of the larger cell and a warming of the smaller one. To help increase the speed of equilibration between the cells following an expansion, the larger cell was placed above the smaller one to take advantage of natural convection, and the gas was circulated between the cells by the electromagnetic pump mentioned in the following section. To ensure rapid mixing of the gas in both cells, sparging tubes were force-fit into the proper holes in the cells, as shown in Figure 5.

As mentioned above, the bomb was made of Monel Alloy K-500 (K-Monel) forged bar stock, annealed after forging for optimum machinability and low temperature impact strength, and ultrasonically tested for soundness of forging. It was machined and welded in the annealed condition.

The end plugs in the two cells were inert-gas (argon) welded, using Monel "64" filler rod*. It was found to be extremely important that 50 percent of the molten pool consist of filler rod--otherwise, cracking of the weld upon cooling was quite probable. Prior to welding, the cells were cleaned and scrubbed very carefully with the following sequence of solvents: benzene, acetone, denatured alcohol, and trichloroethylene.

The welded parts were stress-relieved at about 870-980°C. All parts were then age-hardened for optimum low-temperature properties as recommended by the manufacturer

* Trademark of International Nickel Company.

(19). The resulting hardness was 25 on the Rockwell "C" scale. Following heat treating, all parts were pickled as recommended by the manufacturer (19). The very tenacious oxide coating that remained after the pickling was removed from the outer surfaces by brushing. The internal surfaces of the two cells were cleaned as well as possible by repeated vigorous flushings with hot soapy water until no loose particles could be found in the wash water. All pieces were then cleaned with the same series of solvents as listed above, and the cell assembled.

When the screws, holes, bearing pads, and cell end pieces were all well covered with molybdenum disulfide lubricant, the set screws were cross-torqued to 28 foot-pounds, which was about four times the theoretical torque needed. A leak-check with helium at room temperature showed the cell to be leak-tight to 12,000 psi. Earlier hydrostatic tests had been made up to 15,000 psi, and the maximum experimental pressure was to be 10,000 psi, so the 12,000 psi test was considered acceptable.

As a final leak check, the cell was pressured up with helium to 12,000 psi at -183°C . The pressure was monitored for two hours with no apparent pressure drop. At these conditions, a drop of 0.1 psi would have been readily apparent. Thus the Burnett cell was considered leak-proof to 12,000 psi at all temperatures between -183 and $+50^{\circ}\text{C}$.

Magnetic Pump

The double-wall feature of the pressure bomb minimized distortion, but at the same time it introduced another important problem--the two walls with a gas space between them caused the rate of equilibration between the two cells to be much too slow following an expansion. In order to increase this rate of equilibration, some means for exchanging the gas between the two cells was thought desirable.

Another problem which had to be considered for later work at lower temperatures was the possibility of nonhomogeneities in the two volumes of the Burnett cell following an expansion. To eliminate this problem, circulation of the fluid between the two volumes was again desirable.

An electromagnetic pump was built to circulate the gas, and it worked quite well. The stringent requirement for this pump was that it had to operate at the cell temperature, inside the cryostat. It therefore had to be small, and it had to operate at pressures up to 1000 atmospheres and at temperatures down to -200°C . A qualitative flow detector was necessary in order that the proper operation of the pump could be assured during the experimental work, and the need for complete evacuation of the entire experimental apparatus had to be considered.

The pump which was built to satisfy all of these requirements has been described elsewhere (9). Operation of this pump during the experimental investigations is

discussed in Chapter IV. A drawing of the pump is presented as Figure 7.

Temperature Measurement

The temperature of the gas in the Burnett cell was determined by using a Leeds & Northrup G-2 Mueller Bridge to measure the resistance of a Leeds & Northrup Model 8164 capsule-type platinum resistance thermometer. The thermometer was inserted in a thermometer well in the upper end of the Burnett cell.

The thermometer had been calibrated in 1963 by the National Bureau of Standards, at the oxygen boiling point, the ice point, the water boiling point, and the sulfur boiling point. It was also made consistent with the Mueller Bridge in this laboratory by calibration at the water triple point. Details of these calibrations and the interpolation formulas used are presented in Appendix B. With a current of 2.0 milliamps passing through the platinum resistance thermometer element, the sensitivity of the bridge was such that a change of a thousandth of a degree in the temperature of the element was detectable. When properly calibrated with the Mueller Bridge in use, the manufacturers guaranteed agreement with the International Temperature Scale to within $\pm 0.01^\circ\text{C}$.

The Mueller Bridge was also calibrated in 1963, by the Leeds & Northrup Company. Details of the calibration are included in Appendix B.

The L&N #8164 thermometer used in this work consisted of a platinum resistance element wound strain-free

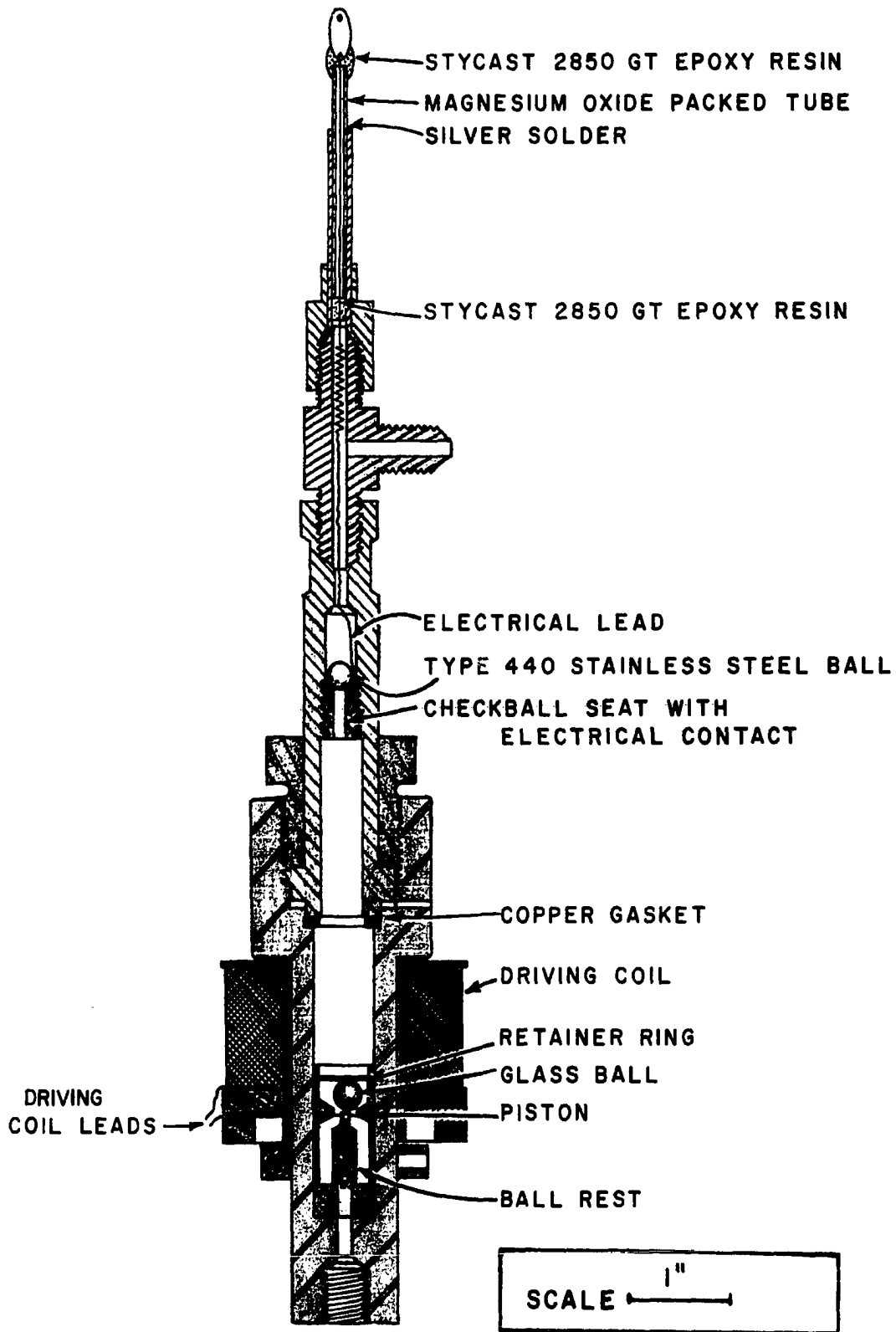


Figure 7. Magnetic Pump

on a mica cross and inserted in a platinum tube of 5.56 mm outside diameter with 0.25 mm wall. Four No. 28 platinum leads for current and potential connections passed through a glass seal on the upper end of the tube. Total length of the thermometer from the tip of the lower end of the tube to the outer end of the glass seal was 57.6 mm, or about 2-1/2 inches. The platinum tube was filled with helium.

The small size of the thermometer made possible its almost complete insertion in the Burnett cell. A thermometer well 1/4 inch in diameter and 1-11/16 inches deep was drilled in the outer end of each cell of the pressure bomb (Figure 5). The capsule-type thermometer could be placed in either of these holes so that when it touched the bottom of the hole, which was its normal position, the lower rim of the glass seal was less than 1/16 inch outside the cell. Thus only the glass seal and the lead wires were not surrounded by the metal of the pressure cell. The small lead wires minimized heat conduction to or from the thermometer so that its chances of indicating the true cell temperature were improved.

With the thermometer located in the thermowell of the upper cell, there was some uncertainty concerning the temperature of the lower cell because of earlier measurements of steady-state temperature gradients between the upper and lower ends of the pressure bomb. Prior to the start of the experimental data accumulation, two L&N #8164 thermometers were available for a short time. One of these was placed

in the thermowell of each cell, and the temperatures were measured when the cryostat had attained a steady state. A Leeds & Northrup 12-position Type 31-3 rotary selector switch was used for switching between the two thermometers during the measurements. The temperature of the lower thermometer was found to be higher at all three experimental temperatures, and the differences in the bottom and top temperatures were found to be: (1) at 50°C, 0.012°; (2) at 0°C, 0.015°; (3) at -50°C, 0.030°.

These temperatures were the temperatures at the outer end of the cells, in the vicinity of the thermowells. As such, they did not necessarily represent the exact temperature of the gas inside the cells. The lower thermometer's temperature was felt to be higher than the inside temperature, based on extensive temperature measurements which had been made earlier in the empty cryostat. Consequently, the temperature gradient between the inner volumes of the two cells was thought to be less than the measured gradient at the ends.

A difference thermocouple between the two cells helped make the temperature uncertainties less. A 1/16-inch diameter, 3/16-inch deep hole was drilled in the wall of each of the two cells in the pressure bomb, about at the mid-length of the cell. Into each of these holes was placed a copper-constantan junction. The constantan lead was between the two junctions, and the copper leads were led out of the annular space through the high-pressure tubing connection

to a second L&N rotary selector switch. By means of this switch, the galvanometer signal could be changed between the Mueller bridge output and the difference thermocouple EMF. When the second thermometer was no longer available, the difference thermocouple was used as an indicator of the approach to temperature equilibrium between cells following an expansion.

In spite of efforts to prevent the generation of thermal EMF's in solder joints, they were noticed at times during the temperature equilibration measurements with the thermocouple. Therefore the difference thermocouple was not accepted as the final indication of equilibration. The constancy of pressure in the cells was a much more sensitive check of equilibration, in combination with the temperature indication of the platinum resistance thermometer in the upper thermowell. Only after the temperature and pressure had both stabilized for twenty minutes or longer was the pressure measurement recorded.

Pressure Measurement

The pressure measuring apparatus is shown in Figure 8. Not included in this drawing is the marine barometer used in the measurements. The single piston gage toward the left of the drawing represents a pair of such gages, one for measuring high pressures and one for low ones. Pressure was transmitted between the Burnett cell and the piston gages by means of two diaphragm pressure null indicators (PNI's) in series.

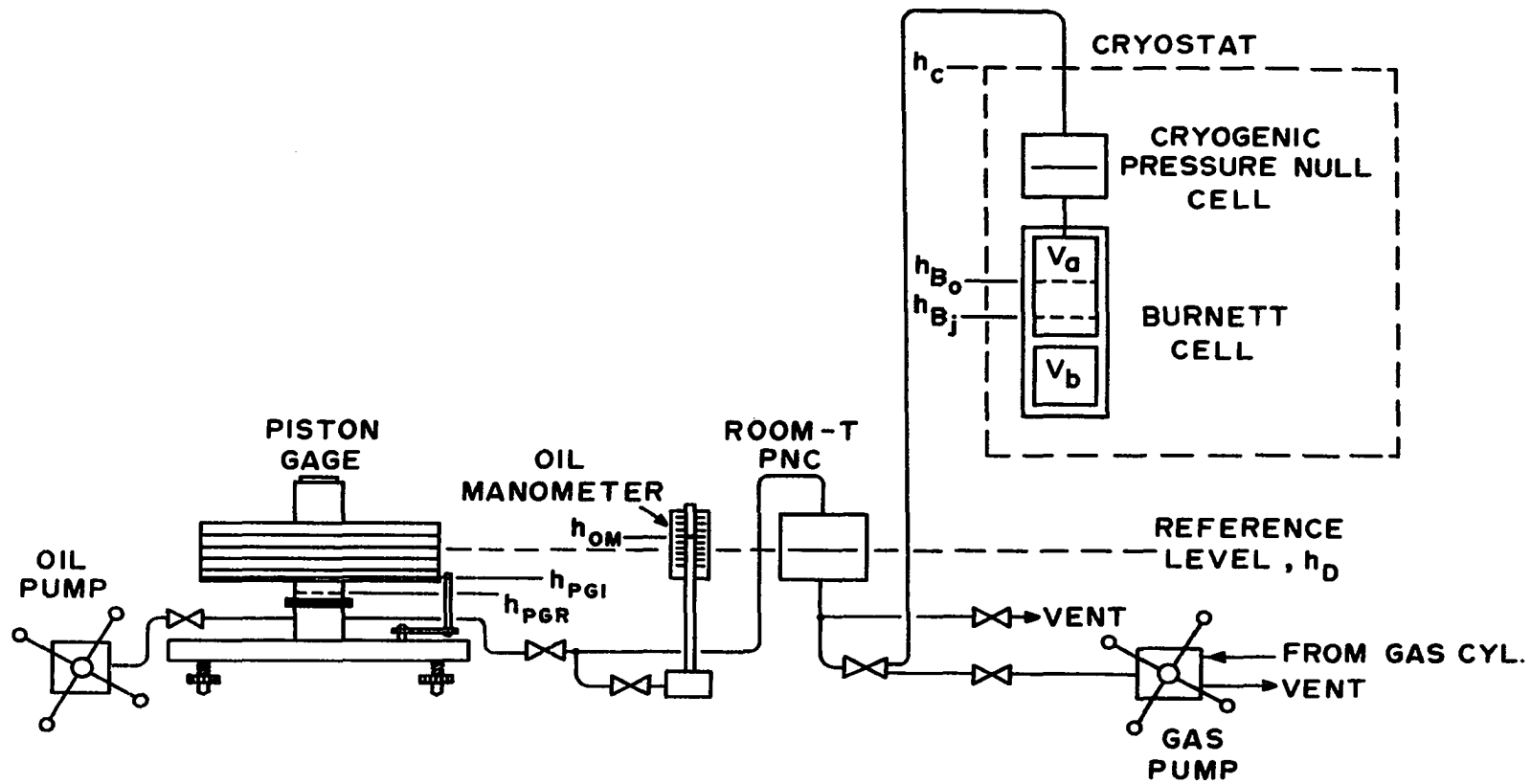


Figure 8. Pressure Measuring Apparatus

Piston Gages and Weights

The two piston gages used in this work were both Ruska Instrument Corporation's Model 2400. The low-pressure gage had a piston diameter of approximately 0.4 inches, and was used for all pressures between one-half and 165 atmospheres. The other gage had a piston approximately 0.18 inches in diameter, and was used for measuring all higher pressures to 700 atmospheres. One set of accurately calibrated weights was used with both gages. Calibration information for the piston gages and the weights is presented in Appendix C.

The accuracy of the gages is claimed by the manufacturers to be 0.01 percent of the reading or better; the piston area for each gage is reported by the National Bureau of Standards to be correct to one part in 10,000 at 25°C. Resolution of the gages has been claimed by Ruska to be five parts per million at full load, decreasing to 50 parts per million at empty weight; the minimum resolution at all of the calibrating test points was less than five parts per million.

All of the weights were constructed of type 303 stainless steel. Final calibration of the weights is reported in Table C-2. The weights were equivalent to Class "P" standard masses, and were calibrated against Class "S" standard masses as certified by the National Bureau of Standards*.

*N.B.S. Circular No. 3 (1918).

Pressure Null Indicators

In order to reduce the chance of misunderstanding in the discussions involving the pressure null indicators, a few of the names that have been chosen by this author should be defined. The term "pressure null cell" will be used to describe the high-pressure vessel containing a steel diaphragm and a differential transformer which senses the movement of the diaphragm as the pressure difference across the diaphragm changes. The term "electronic null indicator" will denote the circuitry which interprets the signal from the differential transformer and produces a corresponding signal which is sent to a 50-0-50 microammeter. The combination of a pressure null cell and an electronic null indicator will be called a "diaphragm pressure null indicator," or, more simply, a "pressure null indicator."

The pressure null indicator which was used to indicate pressure balance between the piston gage oil and the intermediate gas will be called the "room-temperature pressure null indicator," or "room-T PNI;" the one having its pressure null cell (PNC) in the cryostat where it separated the intermediate gas and the gas in the Burnett cell will be called the "cryogenic pressure null indicator," or "cryo-PNI." Room-T PNC and cryo-PNC will have the obvious meanings.

Previous workers have used different names to describe these things. For instance, not only Canfield (6) and Hoover (26), but also the manufacturer, describe the combination of the cell and the electronic circuitry as a

"differential pressure indicator." That terminology is appropriate if the indicator is used to measure small pressure differentials, as Hoover did. For describing the present system, however, that name is perhaps a bit misleading because in this work it was used solely as an indicator of pressure balance across the diaphragm. For this reason, the names selected above are felt to be the more descriptive of the actual function of the pressure null indicators.

Design Considerations: A fundamental restriction in the development of the equations for the Burnett method is the requirement of isothermal conditions for all of the gas whose properties are being measured. If the experimental apparatus does not permit all of this gas to be kept at the same temperature during the measurement, a correction must be made to account for the non-thermostatted portion of the gas to make the results consistent with the theory. This correction involves a considerable uncertainty in most cases, so that all possible efforts should be made to minimize or eliminate its necessity.

This problem was eliminated in the present apparatus by the use of a specially-designed cryogenic pressure null indicator. As the name implies, this pressure null indicator was made specifically for the purpose of operating at cryogenic temperatures. As a result of this special design it could be located inside the cryostat so that it could transmit the pressure from the thermostatted volume in the Burnett cell, to the remainder of the pressure measuring apparatus.

Locating the cryogenic pressure null indicator inside the cryostat solved one problem, but at the same time it introduced another one. The oil of the piston gages could not be used as a pressure transmitting fluid inside the cryostat, so a different fluid was required above the diaphragm of the cryogenic pressure null cell. This intermediate fluid then had to be separated from the piston gage oil in some manner. The obvious separating device was a second pressure null indicator. Therefore a second indicator (room-T PNI) was used for this purpose, and the equipment was designed so that the fluid used in the intermediate system could be the gas used in the Burnett cells. This arrangement was found to be quite satisfactory. The use of the second pressure null indicator eliminated the need for a high-pressure manometer such as the one used by Canfield (6), and in so doing, greatly reduced the errors in the hydraulic head corrections.

Description of Indicators: The pressure null indicators were made by Ruska Instrument Corporation of Houston, Texas. The room-temperature indicator (room-T PNI) was Ruska's Model 2416.1, which has been used successfully in many other laboratories. The cryogenic indicator (cryo-PNI) has been developed within the last three years, and Hoover (26) is the first investigator to report its successful use. Hoover's work and the present work indicate that this cryo-PNI (Model 222S) is a very satisfactory pressure null indicator for low-temperature, high-pressure work.

Each of the pressure null indicators was composed of a pressure null cell (PNC) and an electronic null indicator. The pressure null cells consisted of a type 302, full-hard stainless steel diaphragm 0.002 inches thick and 2 inches in effective diameter mounted inside a heavy stainless steel body. The body of the room-T cell was made of 416 stainless steel, and the body of the cryo-PNC was of high-strength alloy A-286*, which has good low-temperature properties.

In the upper chamber of the pressure null cell was a differential transformer. The core of this transformer was mounted on a stem which was attached to the diaphragm. A change in the pressure differential across the diaphragm caused a change in the position of the diaphragm which, in turn, caused a change in position of the transformer core relative to the transformer coil. The core-coil relationship caused an electrical output which was a function of the diaphragm position and thus the balance or differential of pressure across the diaphragm. This electrical output was then indicated by the electronic null indicator.

Accuracy and Sensitivity: According to the manufacturer's specifications, the pressure null indicators possessed the following accuracy and sensitivity:

"The accuracy of the null point is $\pm 1\frac{1}{2}$ scale divisions under the worst case of combined operating conditions of 10 percent line voltage variation, 20°C to 40°C temperature variation and over a period of 2 hours continuous operation."

*Trademark of Carpenter Steel Company

"The maximum sensitivity is one scale division for a pressure differential of 0.0001 psi. The sensitivity is continuously variable from zero up to maximum value."

Early work with the two null indicators created uncertainties concerning their maximum sensitivity. The sensitivity of the room-T PNI seemed to be better than that claimed by Ruska, and that of the cryo-PNI seemed to vary with temperature. An accurate knowledge of the sensitivities of these indicators was necessary for the best possible experimental pressure measurements, so the sensitivities were determined for the conditions of interest in this work.

The range of sensitivity for the room-T PNI is shown in Figure 9. This figure shows the continuous variability of sensitivities which was obtainable by adjustment of the sensitivity knob of the electronic null indicator. For any given position of this knob, the corresponding sensitivity was measured by exposing the lower side of the diaphragm to atmospheric pressure, and applying small increments of pressure above the diaphragm by means of an oil manometer which was in the piston gage oil system. A cathetometer was used to measure the oil heads. As well as could be determined, the sensitivity in psi per scale division was linear over the entire scale at all sensitivities. The maximum sensitivity was used during all of the experimental pressure measurements.

Only the maximum sensitivity of the cryo-PNI was used in the experimental pressure measurements; consequently,

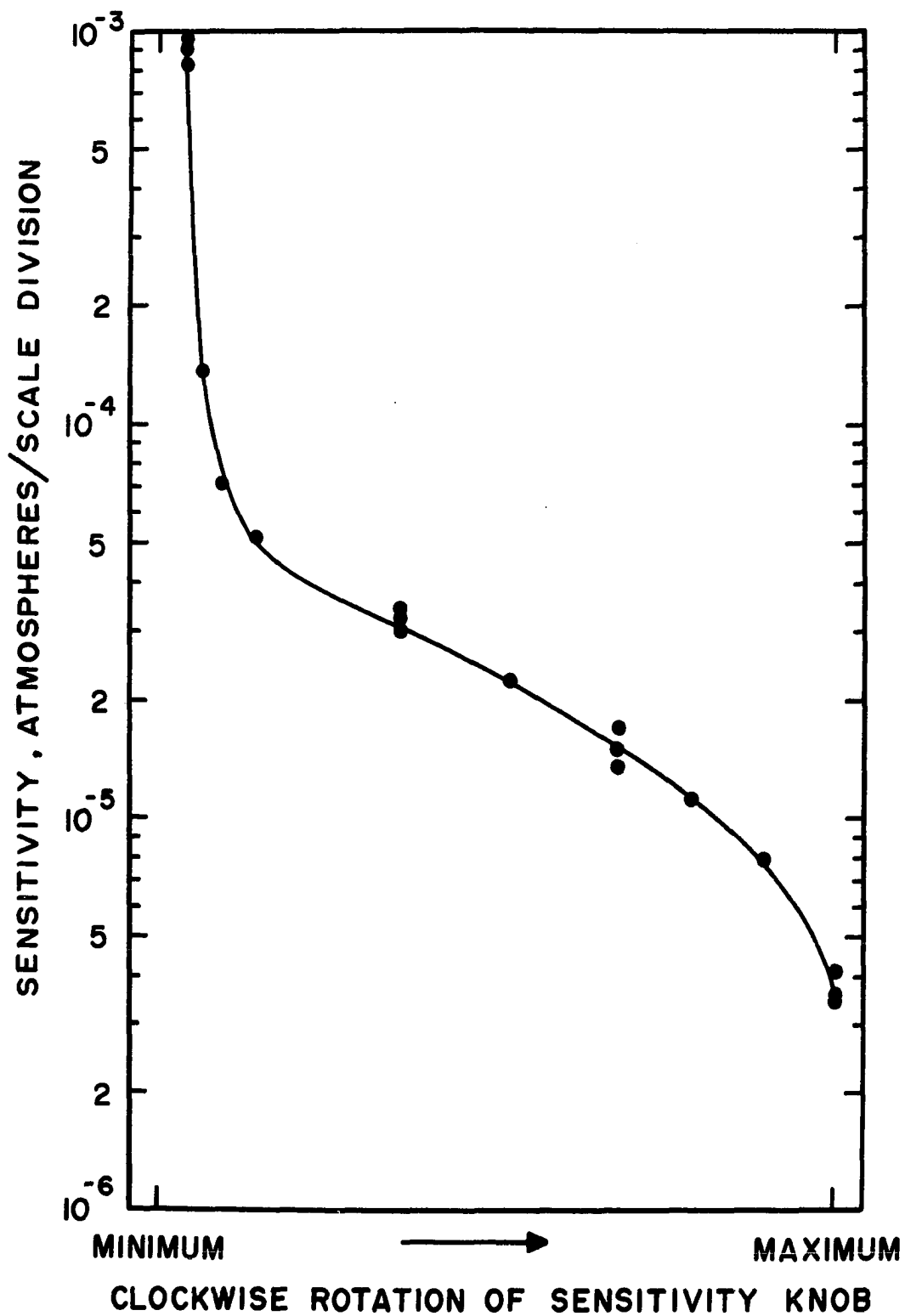


Figure 9. Range of Sensitivity for the Room-Temperature Pressure Null Indicator

the entire range of sensitivity for that indicator was not determined. As mentioned above, however, a variation of maximum sensitivity with cryostat temperature was apparent, and this was investigated for each of the three control temperatures of this work (50, 0, and -50°C), and at -183°C . The results are presented in Figures 10 and 11.

Figure 10 shows a linear readout in psi per scale division for temperatures of 50 and 0°C , but at -50° , a slight curvature is apparent near the extremities of the scale. The sensitivity is seen to vary progressively with temperature change, in such a manner that the indicator becomes less sensitive at lower temperature. Figure 11 shows that the readout has become completely nonlinear at -183°C , and that the maximum sensitivity at this temperature is much less than at -50°C . The difference in the scale of the ordinates of Figures 10 and 11 should be noted.

Also to be noted is the s-shape of the readout curve. Although it is not apparent in Figure 10, the readout at these three temperatures actually possesses a similar characteristic, but is much flatter in the middle part of the s-shape. This shape creates problems which must be understood for proper operation of the indicator. More about this characteristic is mentioned in Chapter V. The room-T PNI did not exhibit this characteristic.

Summarizing the sensitivity measurements, the following results were obtained:

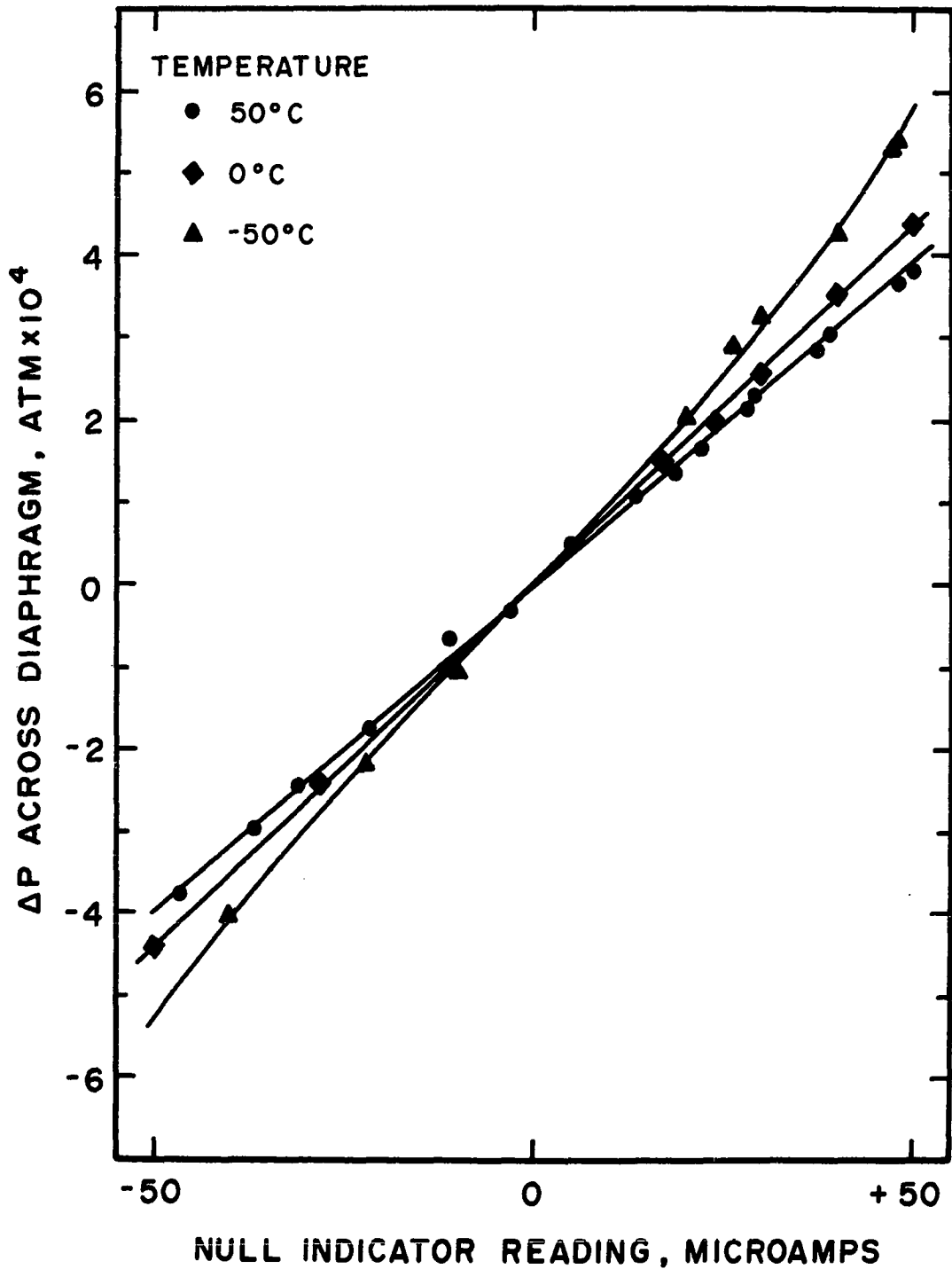


Figure 10. Variation of Maximum Sensitivity with Temperature, for Cryogenic Pressure Null Indicator

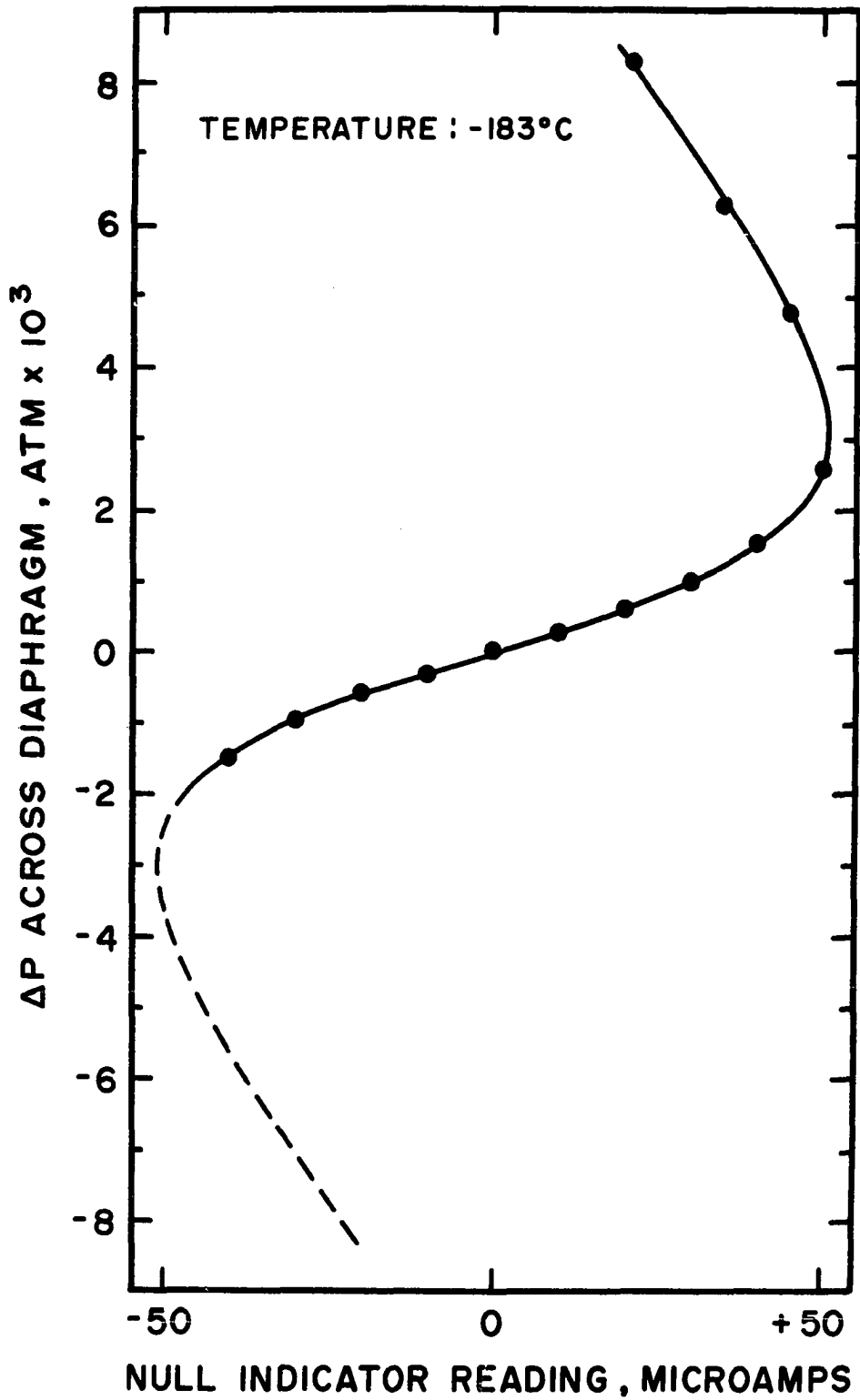


Figure 11. Non-Linearity of Readout of Cryogenic Pressure Null Indicator, for Maximum Sensitivity at -183°C

Ruska's reported value: 1×10^{-4} psi/scale division
(for both indicators)

Measured values:

	Temperature, <u>°C</u>	Maximum Sensitivity, <u>psi/scale division</u>
Room-T PNI	23	0.54×10^{-4}
Cryo-PNI	50	1.13×10^{-4}
	0	1.25×10^{-4}
	-50	1.55×10^{-4}
	-183	4.06×10^{-4}

It is seen that the maximum sensitivity of the room-T PNI was almost twice as good as claimed by Ruska. The cryo-PNI's sensitivity was not quite as good as claimed, and departed from the claimed value progressively as the temperature decreased. This decrease of sensitivity must be considered in work at low temperature, and all efforts should be made to minimize or eliminate the problem. This problem is mentioned more in detail in Chapter V.

The sensitivity measurements were all made at atmospheric pressure. The assumption was made that an increase of total pressure had no important effect on the sensitivities. The behavior of the null indicators during the experimental work showed this to be a reasonable assumption.

Despite the problems encountered in the use of the pressure null indicators, it is only fair to say that their behavior was absolutely delightful. The same could also be said of the piston gages.

Pressure Generation

A diaphragm compressor was used to compress the gases from standard cylinder pressures (2200 psi or less) to the desired pressures in the Burnett cell. A diaphragm compressor was chosen primarily because of its advantage of not allowing the gases to come in contact with the compressing fluids.

In view of the continuing and increasing needs anticipated at the time of purchase, the compressor selected was a Corblin #B2C1000 single-stage diaphragm compressor for non-corrosive gas service. The maximum permissible discharge pressure was 15,000 psi, the maximum permissible compression ratio was 20 to 1, and the speed was 400 rpm. The capacity was variable with suction and discharge pressure, and for this work it was always sufficient.

The overdesign of the compressor for this application made the charging of the experimental apparatus very fast. In fact, the flow rate of the gas from the gas cylinder to the compressor intake had to be cut down drastically to prevent overpressure of the cryogenic pressure null indicator by a pressure surge caused by too rapid filling of the apparatus. Only when the compression ratio exceeded about 10 did this cease to be a significant problem. Thus there was practically no delay caused by insufficient compressor capacity, and the gases could be taken from the cylinders at pressures down to as little as 500 psi and

compressed to the maximum experimental pressures of 10,000 psi in a single stage of compression.

Vacuum System

The vacuum system is shown in Figure 2. The principal purpose of the vacuum system was to evacuate volume V_b before an expansion, but it was also quite valuable because it could be used to assure that no leaks were present in the charge, vent, and both expansion valves of the Burnett apparatus.

The system vacuum was produced by a two-stage oil-lubricated vacuum pump having a rated shut-off pressure of 0.05 microns of mercury. This pump was connected to the remainder of the system with 1/2 inch copper water pipe. A flare joint was used to connect the pump to the system, but all of the other connections were sweat fittings, in accordance with the findings by Canfield concerning the difficulty of getting vacuum-tight flare fittings.

The pressure in the vacuum system was measured continuously by a thermocouple vacuum gage. This gage consisted of a heated thermoelectric junction which developed an EMF, which was in turn sent to a meter calibrated in units of pressure. As is the case with thermal conductivity gages in general, this gage responded to the total pressure of permanent gases and vapors.

The gage was calibrated against a small (5 microns to 5 mm scale) McLeod gage during the early stages of the work and later checked several times to ascertain its proper

operation. The calibration changed with composition of the gas in the system, but even after a new calibration at any particular composition, the gage would tend to drift by as much as two or three microns in the 0-5 micron range. Fortunately, that amount of drift was not prohibitive in this work, so the gage was considered acceptable.

The greatest advantage of the thermocouple gage over the McLeod gage was its continuous readout of the pressure. In addition, it was not as fragile as the McLeod gage and required no cold trap during its operation. Its advantage over other electrical gages was its ability to be cycled between atmospheric pressure and 1 micron with the filament energized.

For protection of the glass-encased vacuum-gage sensor, the vacuum system had a spring-loaded Circle Seal relief valve. This relief valve was greatly appreciated the few times a mistake was made of opening the valve to the vacuum system before the high pressure on the other side of the valve had been vented.

Valves and Tubing

With the exception of the vacuum system tubing, all tubing used in the present apparatus was 3/16-inch stainless steel tubing having a pressure rating of 15,000 psi. All the valves outside the cryostat were Ruska valves, and all fittings were Ruska fittings. These valves had single-piece stems with the threads inside the valve packing. Some of the difficulties encountered with the valves are mentioned in Chapter V.

The four valves used inside the cryostat were Autoclave Engineers Series 30V valves with two-piece stems. These 30,000 psi valves had two desirable features for this work. First, the two-piece stem greatly reduced the chance for scoring the valve stem when the valve was closed. In addition, the valve packing was below the stem's threads, so that no metal particles from the threads could enter the system.

The importance of this latter feature can be appreciated in the light of Hoover's comment concerning the rupture of the diaphragm of his cryo-PNI (26, p. C-2). After detecting a rupture, he found that "the foreign particles proved to be pieces of 'Teflon' tape which had been used at the pipe fittings." If Teflon thread tape will do this, the best way to prevent a rupture is to keep the system absolutely clean.

In order to get a tight seal between 700 atm and a full vacuum, the stems of the Autoclave valves had to be polished. After this was done, however, the valves were used successfully throughout the experimental work without additional problems. The stems were hand-polished in a lathe, with "crocus cloth" used in the final step. They were then "worked in" with molybdenum disulfide lubricant, as described in Chapter V.

The Teflon packing in the Autoclave valves provided a tight seal at all of the temperatures involved in this

work (50, 0, and -50°C). To get this leakproof seal, however, it was necessary to tighten the packing nuts to the point of deforming the packing washer. In one case, this washer was found to be deformed when the valve was disassembled.

For operation at -183°C , a tightening of the packing nut at room temperature did not insure leakproof packing at low temperature. Fortunately, this was not a problem in the present work, and showed up only as a sidelight in a low-temperature test of the Burnett cell.

CHAPTER IV

EXPERIMENTAL PROCEDURE

There are three requirements of the experimental procedure which must be met in order that the experimental results will be consistent with the equations which describe the Burnett method analytically. First, the equations are developed with the assumption that the temperature before an expansion is equal to the equilibrium temperature following the expansion. Second, it is assumed that the amount of gas in V_a before an expansion is the same as the amount in V_a plus V_b after the expansion. Third, it is assumed that the amount of gas in V_a is the same when the pressure measurement is being made as it is when V_a and V_b are isolated from one another by closure of the expansion valve following the pressure measurement.

The methods used to insure that the experimental procedure actually satisfied these requirements and other requirements mentioned later are described in the following sections.

Temperature Equilibration of Cryostat

The attainment of temperature control in the cryostat was relatively simple at any of the experimental temperatures

(-50, 0, and 50°C), but at 50°, the procedure was particularly easy. As mentioned in earlier discussions of the experimental equipment, liquid nitrogen was used as the refrigerant for operation at the two lower temperatures, and laboratory compressed air was used at the higher one. Unless otherwise noted, the following discussions will consider the procedure for attaining temperature control from the initial condition of having the cryostat at room temperature.

To bring the cryostat up to temperature control for a run at 50°C, the circulating fan, the Thermotrol, and the control heater were switched on, and the compressed air was introduced into the cryostat. The Thermotrol setting was adjusted to a predetermined position which would cause the cryostat to control within a degree or so of the desired temperature. The heater wattage was adjusted to the maximum of 110 watts, and the air pressure was regulated to between about 4 and 8 psig. The air was often withheld until the bath temperature was approaching the control temperature, but its earlier introduction didn't affect the rate of equilibration noticeably because of the small heat capacity of the gas bath.

The first step in cooling the cryostat to 0 or -50°C was to start the transfer of liquid nitrogen from the storage dewar to the two-phase separator on top of the cryostat. After the transfer line and the separator had cooled down,

a level of liquid nitrogen began to build up in the separator. At this time, the liquid nitrogen metering valve was opened several turns, the circulating fan was turned on, and the Thermotrol was adjusted to its predetermined setting for the proper control. The control heater was adjusted to its maximum wattage so that when the cryostat temperature approached the control value the heater would prevent excessive overshooting of the temperature. Some overshoot was actually desirable because of the slow rate of cooling of the Burnett cell compared with the cooling rate of the gas bath. A larger temperature difference between bath and cell helped speed up the equilibration.

As the temperature of the Burnett cell approached the desired level, the nitrogen metering valve was closed in a stepwise manner, and the heater wattage was reduced to about 20 watts. At the control temperature, the liquid nitrogen rate and the heater dissipation were adjusted so that the Thermotrol's fraction of ON-time was about 1/5. The time-average control wattage normally varied between 3 and 10 watts. The lower wattages produced smaller gradients in temperature, but the larger ones were easier to control.

When temperature control was attained in the cryostat, there was very little that could go wrong. At 50°C, no major problem ever arose. At 0 and -50°C, the main difficulty was the tendency for the temperature to drift upward by a few thousandths of a degree in several hours. This

drift was not very reproducible in magnitude, but it could be corrected by momentarily closing the liquid nitrogen metering valve and then re-opening it. The nitrogen seemed to carry tiny particles of solid which "plated out" on the valve seat, and which were removed by this simple adjustment. The sintered glass filter at the inlet of the transfer mechanism in the dewar was apparently permeable to these small particles. Fortunately, the filter did stop a lot of other contaminants which might have made the situation even worse. When the filter was removed from the dewar it was filled with a black residue which had accumulated during the transfer.

Initiation of Experimental Runs

The presence of the cryogenic pressure null cell inside the cryostat caused a considerable delay whenever the control temperature was changed before a run. The delay was due to the strong effect of temperature on the characteristics of the cryogenic pressure null indicator. The problems involved in making the adjustments to the circuitry to compensate for a change in the cryostat temperature are discussed later in the section on experimental difficulties.

The essential point to emphasize here is that the Burnett cell could not be charged while the cryostat was approaching the control temperature. Instead, the null indicator problems required that the temperature in the cryostat be within about a degree or less of the desired

control temperature before the null point adjustment and the circuitry adjustments could be made properly. This had to be done at atmospheric pressure. Only after the null indicator adjustments were made could the Burnett cell be charged with the gas to be studied.

Sequential Arrangement of Runs

Because of the ease of temperature control and the rapidity with which the temperature could be changed between successive runs, the most appropriate arrangement of the experimental runs was originally felt to be the completion of all runs for a given composition, followed by a change of composition. The null indicator problems were not considered bad enough to require that all runs for all compositions at a single temperature be made before the temperature was changed. Looking back on the problems involved, the wisdom of the original decision seems questionable, although the method used had its advantages.

One of these advantages was that the entire system had to be completely evacuated and purged only six times rather than eighteen times. For the first run at a given composition, the procedure described below was used, and for the other five runs at the same composition, the system required no special evacuation and purge to insure the proper composition.

Evacuation and Purging

The procedure followed when the composition was

changed took a considerable amount of time. The tubing was approximately 1/8-inch inside diameter, and the valves, Burnett cell, and pressure null cells had many very small clearances which evacuated very slowly. In addition to these problems, the diaphragm compressor had a check valve on both the inlet and the discharge line, and could not be evacuated above the diaphragm. It had to be purged repeatedly to ensure purity of the sample.

The first step before evacuation and purging was the adjustment of the room-temperature pressure null indicator to give a null reading for a pressure balance across the diaphragm at atmospheric pressure. After this was done, the external valves in the system were all closed and the system was evacuated to 100 microns pressure. To permit evacuation through the magnetic pump in the cryostat, the check ball on the upper seat was raised by means of the lifting magnet.

When the system pressure had dropped below 100 microns, the appropriate valves were closed to permit purging of the diaphragm compressor and the line between the gas cylinder and the gas hand pump on the instrument table. These were purged several times while the pressure in the remainder of the system was dropping still further. After the pressure had dropped below 10 microns, the evacuation valve was closed and the Burnett cell was repeatedly purged with the study gas. In order to prevent overpressure of the diaphragm

in the room-temperature pressure null cell, the valve isolating it from the rest of the system was closed before pressure was applied to the system. To prevent overpressure of the cryogenic pressure null cell's diaphragm, the pressure was applied slowly and the proper valves were opened wide to allow pressure equalization above and below the diaphragm as the pressure changed. Each time pressure was applied to the system during the purging steps, the gas was then vented through the various external valves so that all parts of the system would be purged.

The Burnett cell was purged at least three times, and after the last time the pressure was vented so that the remaining gas would be at approximately atmospheric pressure. Temperature equilibration was then necessary before the cryogenic PNI could be adjusted prior to the run. Following this equilibration, the proper adjustments were made, after which the system was ready for charging of the Burnett cell.

Charging of the Burnett Cell

Before the charging was begun, the two expansion valves in the cryostat were closed and the evacuation of the lower volume (V_p) was started. Next, the high-range piston gage was loaded with weights sufficient to create a pressure greater than the maximum pressure to be encountered during the charging. The valve between the room-temperature pressure null cell and the remainder of the system was opened, and a slight overpressure was applied to the top of this diaphragm.

The valve between the compressor and the Burnett cell was very carefully opened a tiny bit, and the cell was slowly pressured up to the pressure of the gas cylinder.

At this point one of the design features of the equipment became readily appreciated. The use of the study gas both in the Burnett cell and also in the intermediate gas system allowed them to be pressured up simultaneously with no particular care except that the process be carried out slowly. The reason for the required slowness was that it made much less probable the overpressure of either of the diaphragms in the two pressure null cells. Actually, the valve which permitted a direct path between the Burnett cell's interior (leading to the bottom side of the cryo-PNC diaphragm) and the intermediate gas system (above the diaphragm) insured against overpressure of the diaphragm if the increase of pressure occurred slowly enough to allow equilibration of pressure above and below the diaphragm by passage of gas through the valve.

Overpressure of the diaphragm in the room-T PNC was prevented by using the oil system hand pump to increase the pressure in the piston gage oil system above the diaphragm as the pressure of the intermediate gas below the diaphragm rose.

A large overpressure of either of the diaphragms was found to be acceptable if it always occurred from the top side. Because of the way the pressure null cells were

constructed, however, an overpressure of more than a few psi from the bottom caused a shift of the null point, which had been determined before the pressuring had begun. Not only was this undesirable from the standpoint of causing a possible rupture of the diaphragm when it was thus work-hardened, but in addition it led to problems concerning the knowledge of the exact null point in later measurements during the run.

If such an overpressure of the cryo-PNC's diaphragm did occur during the initial charging step of the run, the pressure below the diaphragm was reduced and that above it was increased, so that if the diaphragm had actually deformed during the overpressure from below, it might regain its original shape by the overpressure from above. Following this "compensating overpressure," the pressure in the entire system was reduced to atmospheric and the null point of the cryo-PNI was checked. This null point was usually the same as before, but if it was not, the compensating overpressure was applied repeatedly until successive checks of the null point gave identical results. The system was then pressured up again, but understandably a little more care was taken this time to go a little slower to prevent another overpressure.

After the system reached cylinder pressure, the diaphragm compressor was turned on. As mentioned in the description of equipment, the capacity of the compressor was much in excess of the present need, so to prevent too rapid

pressure buildup in the system, the valve between the gas cylinder and the compressor was opened only slightly to reduce the rate of charging. The valve between the compressor and the system was also opened only slightly so that it would act as a snubber to damp out the surges of pressure that occurred as the compressor operated. With these precautions, the cryo-PNC's diaphragm was relatively safe from overpressure. The pressure in the oil system, however, had to be increased as the system pressure rose, and occasionally a problem arose here.

If an overpressure from the bottom of the room-T diaphragm occurred, the same treatment as with the cryo-PNC was used, but it was much simpler. The valves and tubing were arranged so that the room-T PNC could be isolated from the rest of the gas system and the gas below the diaphragm vented to the atmosphere. Thus a compensating overpressure from the top of this diaphragm was easily applied by increasing the oil pressure with the hand pump. As before, the null point was then checked repeatedly until two successive results were the same. Then the intermediate gas pressure could be applied to the bottom of the diaphragm (after a higher oil pressure was applied above it) without venting the whole system and starting over on the charging.

As the pressure in the system approached the desired initial pressure for the run, the valve on the intake line to the compressor was closed down more to reduce further the

rate of charging. Finally it was closed and the compressor was turned off.

Final Pressure Adjustment

The pressure in the system always changed slightly as the Burnett cell and the other contents of the cryostat approached the control temperature. If this change was small, a final adjustment of the pressure was made with the gas hand pump on the instrument table. If the change of pressure was too large for this method, the compressor was once again turned on and the required amount of gas was added. As before, this was done very carefully to prevent overpressure of the diaphragm.

Final Temperature Adjustment

The initial set-point of the Thermotrol was normally within a tenth of a degree of the desired control temperature. Following the final pressure adjustment, the cryostat was allowed to come to temperature equilibrium at this initial set point. The temperature was measured, and from a knowledge of the variation of control temperature with a given change in the Thermotrol's setting, the final adjustment could be made to bring the cryostat to the desired temperature within a few thousandths of a degree. Sometimes a second adjustment was necessary, but in all cases the final temperature was within $\pm 0.002^{\circ}\text{C}$ of the reported temperature.

Final Leak Check Before Run

A continuous monitoring of the system pressure showed when the temperature equilibration was completed. When the pressure reached a stationary level, the valve between the Burnett cell and the intermediate gas system was closed, and the charging valve for the Burnett cell was closed. If a leak was present in either of these two places, its presence was shown immediately by a rapid change of the meter readout for the cryo-PNI caused by the change of pressure above or below the diaphragm. If no such change occurred, the gas outside the Burnett cell charging valve was vented to the atmosphere, and a vacuum was applied to the valve. The absence of a pressure rise in the vacuum line after the vacuum pump was isolated from it was considered sufficient evidence that the charging valve was not leaking. As a further indication, it was found that whenever the system was leak-tight, the pressure null indicators could be balanced at the system pressure, and over a period of several hours the cryo-PNI meter readout would oscillate about the null point as room temperature varied. Due to the high sensitivity of the pressure null indicators (from 3×10^{-6} atm/unit to 10.5×10^{-6} atm/unit) a very tiny leak on either side of the diaphragm would have been readily apparent.

The two expansion valves were shown to be leak-tight before a run by the fact that the cell pressure did not drop over a period of several hours, and also by the fact that

the lower volume, which was evacuating during the charging process, would hold its vacuum (<10 microns) when isolated from the vacuum pump

Initial Pressure Measurement

By the time the correct temperature was obtained in the cryostat and the system had been checked for leaks, the piston gage had been rotating under system pressure for a number of hours. It was therefore at equilibrium with respect to room temperature and system pressure. The gas in the Burnett cell was at temperature and pressure equilibrium also. A final balance of the piston gage pressure and the system pressure was made by adding or removing the required number of fractional gram weights to obtain a pressure balance, normally to within 1 part in 10^5 or better.

Both of the pressure null indicators had to be balanced simultaneously when the pressure measurement was made. The simultaneous balancing of the two PNI's at the same time the piston gage weights passed the reference level scribe mark was quite challenging. It was possible, however, and the results were most satisfactory.

When this condition was met, the weights on the piston gage were recorded, followed by a reading of the barometric pressure and the temperature of the barometer. The piston gage weights were then double-checked to make sure that they had been recorded properly.

Expansion and Subsequent Pressure Measurements

As described previously, chamber V_b had been evacuating during the initial pressure measurement. The vacuum gage by this time indicated a pressure less than 10 microns in this chamber. The vent valve was closed, and the check ball in the magnetic pump was lifted with the magnet to prevent its sticking on its seat during the expansion process. Expansion valve A was then opened very slightly, so that the gas in the upper chamber could expand into the lower chamber.

The arrangement of the two pressure null indicators, with the cell pressure below the diaphragm of one and the intermediate gas pressure below the diaphragm of the other, made the danger of overpressure from the bottom almost negligible during the expansion. The drop in the cell pressure created an overpressure from the top of the cryo-PNC diaphragm, and the resulting movement of this diaphragm caused a slight reduction in pressure of the intermediate gas, allowing an overpressure from the top of the room-T PNC diaphragm.

To minimize the amount of overpressure of either diaphragm during an expansion, a metering vent valve in the intermediate gas system was slightly opened to the atmosphere to allow a reduction of the pressure in this system as the cell pressure dropped. Unfortunately, this sometimes led to an overpressure of the cryogenic cell's diaphragm. Some of the resulting problems are discussed in the section

on experimental difficulties. In retrospect, it is felt that perhaps no intermediate gas should have been vented until the expansion was completed, so that the chances for venting too much would be greatly reduced. The danger of an excessive overpressure from the top of the diaphragm was probably of less importance than the drift in the null point of the pressure null indicator because of the overpressure from the bottom.

Eventually the expansion was completed, and the expansion valves were both opened up wide. The magnet was raised to allow the check ball of the magnetic pump to fall into its seat, and the magnetic circulating pump was switched on.

The magnetic pump was included in the apparatus for two reasons--not only did it speed up temperature equilibration following an expansion, but also it mixed the gases to reduce the probability of concentration inhomogeneities.

During an expansion, the upper chamber (V_a) cooled and the lower one (V_b) warmed up. With the magnetic pump circulating the gas between the two cells, the time required for equilibration was shortened. This shortening of the equilibration time was not automatic, however, because the operation of the pump introduced a certain amount of heat due to the electrical dissipation of the driving coil. Thus it was found desirable to turn off the pump before the equilibration was completed; otherwise, the equilibrium temperature

would be much too high. The proper time for turning off the pump was determined by experience, and it varied from one expansion to the next. At the lowest pressures of a run, temperature equilibration was found to be quicker without the use of the pump.

The problem of concentration inhomogeneities was not considered serious in the present work. Further work at lower temperatures has been planned, however, which will involve measurements near the two-phase region of mixtures. The magnetic pump is expected to be valuable as a mixing device in that work.

When the constancy of temperature and pressure in the cell indicated that the equilibration was complete, one of the expansion valves was closed tight and the other was adjusted until it was open about 1/8th of a turn. A pressure balance was then made as described for the initial pressure measurement, and corresponding readings were recorded.

The reasons for adjusting the expansion valves in the indicated manner before the pressure measurement should be clearly understood. The most obvious reason for closing the valves is that, as they are closed, the cell pressure will rise because of the reduction of the total cell volume. If the pressure measurement is made before they are closed, it will be noticeably incorrect. The less obvious reason is that whenever that final pressure balance is made, the

diaphragm will flex slightly, causing a change of volume of the upper chamber. If both of the expansion valves are completely closed during the final balancing, this volume change will cause the pressures in V_a and V_b to be unequal, and once again a noticeable error in the pressure measurement will occur. As a workable compromise between these two requirements, the expansion valves were adjusted as described above.

Following the measurement of pressure, the expansion valve which had remained open a fraction of a turn was then closed as the pressure balance was maintained. The fact that the pressure balance was maintained should not be overlooked, because it ensured the correct proportioning of the gas between V_a and V_b during the closure of the valve.

The gas in V_b was then vented to the atmosphere, and this chamber was evacuated until the pressure was less than 10 microns. The time required to attain this pressure was an excellent indication of the absence of leaks in the expansion valves. A second method used to check for expansion valve leaks was to monitor the pressure in V_a as the evacuation proceeded. This method was not always reliable, however, because of the temperature equilibrium upset that was caused by venting and evacuating V_b .

The expansion and evacuation process described above was continued, with a pressure measurement after each expansion, until the pressure was reduced to 2-3 atm. Generally, twelve expansions (thirteen pressures) were sufficient for this.

CHAPTER V

EXPERIMENTAL DIFFICULTIES

The successful construction and operation of the gas-bath cryostat and the other experimental equipment used in this work was accomplished only after several difficulties were encountered and resolved. In order that future investigators might be spared the same encounters, this chapter has been included.

The principal problems that arose were concerned with precision of temperature control and accuracy of pressure measurement. A part of the temperature control problem was the location of the circulating fan, the heater, and the liquid nitrogen vaporizer; the other part was the attainment of a constant refrigerating effect in the cryostat. Valves and fittings also presented difficulties.

Temperature Control

When the gas-bath cryostat design was still in the drawing-board stage, the desired limits of temperature variation in the cryostat were quite small (i.e., $\pm 0.002^{\circ}\text{C}$ or less). This small variation was to be obtained at any temperature between 0° and -183°C , and the control between

-140 and -183° was particularly important. As far as could be determined at that time, there was no gas-bath cryostat of comparable size (10 inches in diameter and 30 inches in length) which possessed this degree of temperature control.

Before this discussion becomes more involved, the fact should be pointed out that these goals were not completely attained. Repeated modifications were made to the equipment, each time producing a little better result; eventually, however, the money available for further modifications was exhausted. As a result, the control achieved at that time had to be accepted and the earlier plans modified to take advantage of the success up to then. The principal benefit of the earlier work was that a great deal of valuable information had been accumulated which should be useful to the investigator who continues the modifications.

Constant Refrigerating Effect

As is normally the procedure in this field, the temperature in the cryostat was to be controlled by introducing a slight excess of refrigeration and offsetting that slight excess with the proper amount of heat. Liquid nitrogen was to be used as the refrigerant, and a bare-wire heater was to supply the heat.

In order to get the desired temperature control with acceptably small temperature gradients in the cryostat, a small heat input from the heater was desirable. A

time-average heater dissipation of less than 10 watts (preferably 2 to 5 watts) was envisioned. This restriction in turn required that the refrigerating effect be essentially constant. This can be appreciated more fully by considering a maximum possible variation in heater dissipation amounting to 2 watts on either side of the time-average value. For operation at 0°C, 2 watts of cooling would be obtained with slightly more than 1/3 cc per minute, or about 4 percent of the total nitrogen usage in the cryostat. Due to the fact that the nitrogen was a two-phase fluid during the transfer, control of the flow to this extent was understandably quite difficult.

Subcooling of the nitrogen was considered, but then rejected. A vapor flow control valve placed in the vapor outlet line from the cryostat was notably unsuccessful for controlling the refrigerating effect. Other attempts were equally disappointing. Eventually the conclusion was made that the liquid and vapor should be separated outside the cryostat, and the liquid could then be metered into the cryostat at a closely controllable rate.

Fortunately, this conclusion was apparently right, because when the workable combination of two-phase separator and metering valve was finally constructed, the constant refrigerating effect resulted. The final design characteristics of this combination have been discussed in the description of experimental equipment. The principal

problem which remained was the nuisance caused by frosting of the separator because of improper design of the top closure. Compared with the earlier difficulties, this was a negligible bother.

Location of Fan, Heater, and Vaporizer

Temperature control in the cryostat was dependent upon the proper location of the circulating fan, the heater, and the liquid nitrogen vaporizer. But the location of these three elements had an even greater effect on the magnitude of the temperature gradients from point to point inside the cryostat. In fact, once the problem of obtaining a constant refrigerating effect was solved, the reduction of gradients replaced it as a major problem.

The description of these three components and their final location has been presented in the discussion of experimental equipment. The main thing that must be added here is that this "final" design and location was accepted because the expenditures of time and money had by this time passed the point of diminishing returns.

A great deal of work was done in trying to eliminate excessive temperature gradients over the desired temperature range (0 to -183°C). Reversal of gas flow in the dewar, interchange of fan and heater position, and a detailed check of velocity gradients inside the inner shield showed that the present arrangement was satisfactory for measurements down to about -90° , but below that temperature the gradients just could not be made small enough.

The information that was accumulated during these efforts indicated that if the heater, vaporizer, and fan were all located near one another at the top of the dewar, satisfactorily small gradients would result. At the time this paper was being written, the appropriate modifications were being made to test the validity of this tentative conclusion.

Valves

All of the valves used outside the cryostat were Ruska valves with one-piece stems. These valves were the source of much of the experimental difficulty, but in all fairness it must be said that they were not used in the manner suggested by the manufacturer. The special requirements of this work made the successful operation of any valve of this design unlikely.

When the valves were received from Ruska, the stem threads and tips were generously coated with molybdenum disulfide lubricant. If they had been used in this condition, it is possible that no problems would have occurred. In the present work, however, absolute cleanliness was desired for all of the internal surfaces of the apparatus. To maintain this cleanliness, it was necessary to remove all of the excess lubricant which could later be carried into the system. At the same time it was necessary to leave enough of a lubricant coating to permit operation of the valves at 700 atm.

The design of the one-piece stem caused two problems. First, the stem threads were below the valve packing, so they could not be lubricated heavily without contaminating the system. Also, the rotation of the stem on the seat, following the initial contact between them, tended to gall the stem.

The first step in preparing the valves for use was to "work in" both the threads and the mating sealing surfaces before removing the lubricant. This was done by repeatedly operating the valve from full open to full closed, each time seating the stem on the seat very gently. After every few turns, the stem tip was inspected, and the lubricant was redistributed to coat the sealing circle. Eventually, the tip acquired a fine gray-black ring around it which could not be wiped off. The MoS_2 in the lubricant adhered to the stem and the seat at this sealing circle, and provided excellent lubrication for several hundred subsequent closures.

Unfortunately, the same success was not obtained with the threads. Even after several hundred such open-and-close cycles, the stem threads or the threads of the valve body would gall when the valve was operated following the removal of the lubricant. Several attempts were made to polish the threads, but to no avail. The only way to ensure successful valve operation at the highest pressures was to leave a light coating of the lubricant on the threads after

they were worked in and cleaned. Even then, the valves could not be operated many times at high pressure without requiring a repeat of the working-in procedure.

Repeated successful operation of the valves was possible only if the closures were made with just enough torque to perform the seal. The amount of torque required to do this was determined by practice--very few valves had to be reworked before the inadvisability of overtightening became quite fully appreciated.

Low Temperature Valves

Based on the original plans to operate at temperatures down to -183°C and at pressures between 0 and 700 atm, it was felt that any valves used in the cryostat would be a major source of trouble during the data accumulation. The two difficulties anticipated were: (1) galling of the stems caused by rotation of the stem on the seat when the seal was made, and (2) shrinkage of the packing at the low temperatures, allowing leakage of the gas.

The tendency toward galling was greatly reduced by using Autoclave Engineers valves which had two-piece non-rotating stems. When properly assembled and lubricated, these valves could be sealed with no rotation of the stem on the seat. This advantage was slightly offset by a disadvantage that was noticed during the work. After the valves had been used several times, they developed a little bit of "play" in the stem assembly. With the charging and

vent valves, this was of little consequence; at least one of the expansion valves, however, had to be capable of very precise adjustments. It had to give the operator a good, firm "feel" of its contact with the seat. Therefore, this valve had to be assembled so that the stem could be kept from rotating only by the combination of very heavy loading of the packing and an initial contact with the seat. Even with this adjustment, however, the valve developed some "play" after about one hundred open-and-close cycles, and had to be retightened. Also, the packing was tightened so much that the brass follower was deformed by the packing nut.

The threads on the stem were above the packing, so they could be lubricated without fear of contaminating the system. In order that the lubricant not freeze at low temperature, powdered molybdenum disulfide was used for lubrication of the threads.

Lubrication of the valves at the contact circle of the stem and seat was absolutely essential for the cryogenic valves, as it was for those outside the cryostat. Each of the valves was required to seal absolutely tight with 700 atm on one side of the valve and a few microns pressure on the other side.

The cryogenic valves were not leak-tight until they had been polished to a near-mirror finish. Following this polishing, they were worked-in in the same way the other valves had been. Even then, they had to be closed firmly

to provide a perfect seal. The two-piece stem construction kept this from galling the stem.

Because of the necessity to limit the present experimental investigations to the temperature range between -50 and 50°C , the shrinkage of the packing was not serious. No modifications to the valves were necessary to prevent leakage through the packing. When a final low-temperature check of some of the equipment was carried out following the data accumulation, however, a leak through the packing did occur at some temperature below -50° (temperature of this test was -183°). One of the possibilities mentioned for preventing this in future work was rather interesting, and will be mentioned to encourage its application. This is the use of Belleville washers as part of the packing of the valve. The hopeful result would be that at low temperature the Belleville washers would keep the packing heavily loaded as its shrinkage became progressively worse.

Effect of Temperature on Circuitry of Cryo-PNI

A characteristic of the cryogenic pressure null indicator which was rather annoying has already been mentioned in the discussion of experimental procedure, but a more detailed review of the problem might be of value. This annoying characteristic is the manner in which the properties of the indicator changed so much with temperature.

Part of the initial installation adjustment procedures recommended by the manufacturer included the

adjustment of a "trim pot" in the electronic null indicator, with a corresponding change of the zero adjustment control. These two adjustments were to be made until the minimum change in null reading occurred as the sensitivity control was rotated through its full range. At this point the maximum variation in null position was supposed to be less than ± 1 division.

As the proper adjustment was approached, a very small change in the setting of the trim pot caused a sizable upset to the circuitry, and a wait of 15 minutes to an hour was often required for the unit to settle down again. Eventually the setting was found which, after this preliminary waiting period, appeared to be the right one. At this time the unit was allowed to stand for another 6 to 12 hours to ensure its stability. If at the end of this time it still possessed the required characteristics listed above, the adjustment was considered complete; otherwise, the procedure was repeated until satisfactory results were obtained.

Unfortunately, the proper adjustment of the indicator at one temperature was an improper adjustment for other temperatures. When the control temperature in the cryostat didn't change between successive runs, no particular problems were presented by the cryo-PNI. After the above-mentioned adjustments had been made at the experimental temperature, all that was required before beginning a run was a slight adjustment of the zero adjustment control,

if even that much. Whenever the temperature was changed between runs, however, the complete adjustments had to be made again, causing a delay of from half a day to perhaps a day and a half. Only after the indicator exhibited its original stability at the new temperature for the new adjustments, could the next run begin.

The exact cause of the change in electrical characteristics of the indicator is not known, but it was thought to be related to a change in the mutual capacitance of the lead wires either inside the cell or between the cell and the null indicator, or both. Hoover's recent work (26) indicates such a possibility. In Hoover's words "... the wires in the coils of the differential transformer are connected to the lead-out wires and electrically insulated with a potting material.... Since the [PNI] primary signal is capacitance sensitive, anything that causes the relative positions of the lead wires to change, alters this signal. Pressure on the potting material does just that. Also, temperature affects the mutual capacitance of these wires. The magnitude of this change is about 0.1 psi/100°F."

Hoover also found that a change of the mutual capacitance of the vinyl-insulated lead wires between the indicator and the cryostat amounted to 0.000263 ± 0.000004 psi/°F as the room temperature varied. The room temperature in his laboratory changed by as much as $\pm 13^\circ\text{F}$, making possible a drift equal to 0.0068 psi over the course of a

complete run. Hoover said this problem was eliminated by replacing the vinyl-insulated wires with Teflon-insulated wires, which had a very low mutual capacitance change with temperature.

In the present work, room-temperature changes could be held to less than $\pm 0.5^{\circ}\text{C}$ during a run, and the resulting drift of the indicator was not felt to be excessive.

Overpressure Indication

Overpressure of the diaphragms of the pressure null indicators was not critical if it occurred only from the top, but if an overpressure of more than a couple of psi occurred from the bottom side, a permanent shift in null point resulted. Such a shift in null point could greatly increase the uncertainty of the pressure measurements, so all possible efforts were made to prevent overpressures from the bottom side.

Despite these efforts, a few overpressures did occur from the bottom. Most frequently they were caused by venting too much from the intermediate gas system following an expansion of the gas in the Burnett cell. In most cases the overpressure was very slight, amounting to less than the critical value which would cause a permanent deformation of the diaphragm. In these cases, all that had to be done to correct the situation was to increase the intermediate gas pressure by using the gas hand pump.

Unfortunately, there were a few cases in which the direction of overpressure was not known. As the overpressure

from either side of the diaphragm increased slowly from zero, the meter swung to the corresponding extremity, and then doubled back toward the null position, giving the same indication as for an exact pressure balance. Thus it was possible to obtain the same meter reading with an exact balance, a large overpressure from above the diaphragm, or a large overpressure from below it.

The differentiation between a pressure balance and a large overpressure was very simple. At balance, the sensitivity was quite high and a slight movement of the gas hand pump caused a distinctive change in the meter reading. If no meter change occurred with a movement of the hand pump, an overpressure was certain.

Distinguishing between an overpressure from the top and one from the bottom was more difficult, because a complete traverse of the hand pump often caused no significant movement of the indicator needle. The manufacturer recommended that in such a case, a reduction of the indicator's sensitivity would show which side had the higher pressure. This was often not the case, so some other means had to be used. In practice, if the overpressure ever occurred so rapidly that its direction was not known, the only sure way to eliminate it was to increase the pressure of the intermediate gas to a value at least as high as the cell pressure at the time, and see if the overpressure was eliminated. If this did not take care of it, the excess

gas was then vented until the overpressure, which was then from the top, was reduced to zero.

At the risk of being redundant, the point will be re-emphasized that the behavior of the pressure null indicators must be completely understood if the errors in pressure measurement are to be minimized.

CHAPTER VI

DATA ANALYSIS

Gases Used

The argon used in this work was Matheson's prepurified grade having a quoted purity of 99.998 mole percent, and the helium was U. S. Bureau of Mines Grade-A which had been specially selected for its high purity. The helium-argon mixtures were obtained from the Matheson Company in size 1-A cylinders at a pressure of 2200 psi.

Samples of both pure components and all mixtures were analyzed by the U. S. Bureau of Mines Helium Research Center in Amarillo, Texas. The helium was analyzed before being sent from Amarillo prior to the experimental work, and all of the other samples were analyzed at a later date. A summary of the composition analyses is given in Table 1. Included in this summary are the gas mixture analyses reported by Matheson. The experimental data treatment was based on the analyses reported by the Bureau of Mines.

The Bureau of Mines analyses of the pure argon and the mixtures were made by mass spectrometer, except for the helium content. This was determined by the modified Frost

TABLE 1
RESULTS OF COMPOSITION ANALYSES*
(Compositions Reported in Mole Percent)

	Mixture A	Mixture B	Mixture C	Mixture D	Argon
% He	80.00 (79.70)	59.35 (59.40)	41.05 (40.2)	21.99 (22.0)	0.10
% Ar	19.95 (20.30)	40.49 (40.60)	58.91 (59.8)	77.97 (78.0)	99.85 (99.998)
% N ₂	0.05	0.11	0.04	0.04	0.05
% O ₂	0.00	0.05	0.00	0.00	0.00

* Values in parentheses are the analyses reported by the Matheson Company; other values are those reported by the Bureau of Mines Helium Research Center.

Analysis of Impurities in Helium:

Component	Amount, parts per million
H ₂ O	0.4
Ne	1.0
N ₂	0.8
O ₂	0.2
Ar	0.0
CO ₂	0.0
	2.4
Total:	2.4 ppm

procedure for all the mixtures, and by the regular Frost procedure for the pure argon sample.

Calculation of the Pressures

As indicated in Appendix C, the pressure exerted by the gas in the experimental cell was calculated as the sum of several parts, each of which involved a chance for errors. For many of the pressure measurements, the calculation of a single pressure involved as many as 25 additions and subtractions, 7 multiplications, and one division. Generally, the terms varied from one pressure to the next, so the amount of data which would have been required as input for a computer calculation of the pressure was considered excessive. The pressures were therefore determined by means of a desk calculator.

This use of a desk calculator necessitated the later recalculation of the pressures by a different person. Consequently, they were all checked, and a few errors were found and corrected before the final treatment of the data was made. The deviations resulting from the curve-fitting of the experimental compressibilities proved to be a very effective means of checking the precision of the pressures.

Treatment of the Data

The raw data from a Burnett apparatus consist of isothermal series of pressure measurements. In order to obtain all the information included in these measurements,

they must be analyzed properly. Brief mention is made here of two of the methods which have been used previously to treat Burnett data, with comments on their value. The method used in the present work will then be described.

Previous Methods

The common method of treating Burnett data has been discussed in Chapter I. In that method, the value of the zero-pressure cell constant, N_{∞} , is obtained by extrapolating the ratio of successive pressures, P_j/P_{j-1} , to zero pressure. Corrections to this zero-pressure cell constant are made, to account for the deformation of the experimental apparatus with pressure (Appendix D). The products $P_j N_1 N_2 N_3 \dots N_j$ are then formed, and a second zero-pressure extrapolation of these products is made. This second extrapolation yields the ratio between the initial pressure and the initial compressibility factor, P_0/z_0 , which has been called the "run constant." Compressibility factors for the remainder of the experimental pressures of a run are determined by substitution of the cell constants and the run constant into Equation 11.

Prior to Canfield's work in 1962, compressibility factors determined in this way were considered to be the best available from the given experimental measurements. Canfield, on the other hand, showed that the low pressure values of $V(z-1)$ were quite sensitive to small variations in N_{∞} , so that whenever the value of N_{∞} was determined correctly,

the behavior of $V(z-1)$ plotted against $1/V$ would be linear at low $1/V$. This was a significant improvement over the earlier technique, in that it greatly reduced the error in the determination of N_∞ .

Even with this improvement, however, a relatively large error was still possible in the determination of the run constant, P_0/z_0 .

Hoover (26) has recently proposed a new method of treatment to be applied to Burnett data, which he calls the "direct method," as opposed to the "apparatus constant method" described above. Among the advantages claimed by Hoover for this method are the following (26, p. 25):

1. The small error in the determination of N_∞ is eliminated.
2. The larger and more significant error in determining P_0/z_0 is also eliminated.
3. A systematic error (usually about 0.01%) in the piston area tends to cancel
4. A precision better than 0.005% in determining B is possible. This is a full order of magnitude better than all previous methods.

He has also mentioned two disadvantages:

1. A first estimate of B and C [second and third virial coefficients in the reciprocal volume series] is needed to begin the iterative solution of [the equations involved in the method].

2. At $T_r < 0.75$, ... the pressures [must] be measured with such a high precision that B can no longer be determined to $\pm 1.0\%$ with present pressure measuring instruments.

Another disadvantage of the direct method has been pointed out in the paper by Hoover, et al. (27). The method is limited to pressures for which the volumetric behavior of the given gas can be represented adequately by the following equation:

$$z = 1 + B/V + C/V^2 \quad (17)$$

The direct method is an iterative procedure for determining B and C of Equation 17 without the requirement that the zero-pressure cell constant and the run constant be determined. Thus the errors inherent in these two values determined by extrapolation of analytically-fitted curves will be eliminated.

This direct method was not applied to the data of the present investigation because of the importance of virial coefficients higher than the third.

Present Method of Analysis

The present method of analysis consisted of two separate parts. The first part was the analysis of the preliminary data to determine corrections which were then applied to those preliminary data. The second part is the part of interest here. It involved a rather sophisticated

treatment of the corrected data, yielding not only the compressibility factors, but also virial coefficients.

The preliminary data could not be corrected for pressure head effects in the intermediate gas system until the volumetric behavior of the gases was known (Appendix C). Consequently, these preliminary data--which differed from the final data by no more than about a part in 5,000--were treated by the general method described in Chapter I in order to obtain the required information concerning the density of the gases as a function of temperature, pressure, and composition of the gas. When these corrections had been applied to the preliminary data, the second part of the method was begun.

Before the second part of the treatment is described, it will be of value to discuss a technique which will be mentioned in the later sections. This technique, which has been presented recently by Hall and Canfield (18), consists of the use of the method of least squares employing orthonormal functions to determine polynomial approximations for an infinite series. According to these authors, "criteria [were] established which indicate the polynomial whose coefficients are statistically nearest those of the series and the polynomial which statistically "fits" the series best." In the present application, the technique has been utilized to obtain the "best" fit of experimental compressibility data and the "optimal" virial coefficients associated

with that data. For convenience in the discussion to follow, this technique will be referred to by the name ORNOR. For proper appreciation and understanding of the ORNOR technique, the interested reader should consult the paper by Hall and Canfield.

The methods mentioned earlier for treating Burnett data have been restricted to the treatment of individual experimental runs. The information obtained from different runs at the same composition and temperature was considered to be related only within the single runs and not from one to the next--with the possible exception that the zero-pressure cell constants for these similar runs were generally assumed to be equal.

In reality, such data sets are closely related. The compressibility factors obtained from any number of runs which have been made at the same temperature and for the same composition must all satisfy the same virial equation. Therefore, the treatment of the data set from any one of these runs will be improved by utilizing the results of the other runs under similar conditions. Each additional run introduces perhaps thirteen additional known points (the experimentally measured pressures), and only two new unknowns (the cell constant and the run constant). The likelihood of a sufficiently good fit of the results is then increased with an increase in the number of sets of experimental data at the same conditions.

In order to account for this common basis of similar runs, the goodness of fit must be tested by some means which will relate the final, common results (the coefficients of the virial equation) to the experimental measurements of all of the similar runs. This cannot be done by minimizing the sum of the squares of the deviations between the "experimental" and the "calculated" compressibility factors. The reason for this is that the calculated compressibility factors are obtained from a fit of the "experimental" compressibility factors, which in turn are dependent upon the extrapolated values for the zero-pressure cell constant, N_∞ , and the run constant, P_0/z_0 , for each of the runs. Each of these constants will involve some error, but the fit will not take this into account. Thus the result could be a good fit of bad points.

In the present treatment, the quantity used to relate the experimental measurements and the final calculated results for all similar runs was

$$\sum_{n=2}^{I_1+I_2} \left(\frac{P_n}{P_{n-1}} - \frac{z_n \rho_n}{z_{n-1} \rho_{n-1}} \right)^2$$

where I_1 denotes the number of pressure measurements from the first run, and I_2 the number from the second run. The compressibility factors, z , and the densities, ρ , are those calculated by the method to be described below, and the pressures, P , are those measured experimentally. This

quantity, which will be called SUM for convenience, was used in conjunction with ORNOR to determine the best combination of cell constants $(N_{\infty})_1$ and $(N_{\infty})_2$ and run constants $(P_0/z_0)_1$ and $(P_0/z_0)_2$ for treatment of the similar runs.

During the time in which this author was completing the experimental work, a co-worker, Mr. K. R. Hall, was preparing a computer program which incorporated ORNOR in a method for treating Burnett data. This program, which at the time of this writing was still undergoing modifications, was used for the treatment of the data. The program was run on the University of Oklahoma's OSAGE computer, which could be thought of as roughly comparable to an IBM 7040 in speed, having a memory of 16,000 54-bit words. Because of the involved nature of the program, it could be run on OSAGE only after several simplifying shortcuts were made in it. This program and the general method of treatment of Burnett data used in this work are now being written up as a special report by Mr. Hall, of the School of Chemical Engineering and Materials Science, University of Oklahoma.

In brief, the program obtains approximate cell constants and run constants by a fit of the experimental data, and then utilizes a combination of optimum searching techniques for minimizing SUM, at the same time obtaining the best ORNOR fit of the resulting compressibility factors to yield the virial coefficients which best describe the system. As mentioned above, the program is still undergoing

modifications. Its results up to this time have indicated that when it has been properly refined, it will be better than any existing method for treating Burnett data.

Because of the incomplete success of the program at the time these data were treated, a certain amount of subjectivity was introduced into the treatment. The results indicated that the response surface over which the search was made was not unimodal, but possessed a "waviness" caused by either random or systematic error in the data. This caused the "optimal" results to be judged unsatisfactory in some cases on the basis of their non-linearity at low density, on a plot of $(z-1)V$ versus density. This non-linearity was generally quite small, but a judicious selection from the remainder of the computer output resulted in better agreement with this criterion, which was always used to ensure the validity of the final results.

The resulting coefficients in the best fit of $(z-1)$ versus ρ were then interpreted to be the coefficients which were statistically nearest the exact theoretical virial coefficients of the infinite series indicated by Equation 13. Thus according to the work by Hall and Canfield, the final ORNOR fit resulted in the "best" fit of the experimental compressibility data and the "optimal" virial coefficients associated with the data. These coefficients are presented in Table 8.

Experimental Compressibility Factors: The experimental compressibility factors determined with the best

combination of cell constants and run constants are presented in Tables 2 through 7, with the corresponding experimental pressures. Two series of expansions were made at each temperature for each composition, in order to define each isotherm accurately--particularly at the higher pressures. The first series of expansions was started with an initial pressure in the vicinity of 700 atm. The second series was initiated at a pressure approximately equal to the average of P_0 and P_1 from the first series.

The range of variables for the experimental compressibility factors was as follows: temperature, 50, 0, and -50°C ; pressure, 3 to 700 atm; and compositions, pure helium to pure argon with four evenly-spaced helium-argon mixtures. The compositions of these mixtures have been tabulated at the first of this chapter, in Table 1. The value used for the gas constant in the analysis of the data was 82.0558 cc-atm/gm-mole $^{\circ}\text{K}$.

CHAPTER VII

DISCUSSION OF RESULTS

The results of the preliminary treatment of the data are presented in this chapter. The reliability of the ORNOR fits of the data is discussed in terms of the number of parameters required for a "best fit" of the data and in terms of the deviations of the experimental points from the fitted curves. Compressibility factors determined in this work are compared with those from the literature. An error analysis is also included.

Reliability of the Fitted Equations

The compressibility factors determined in this work are presented in Tables 2 through 7, where they are listed with the corresponding experimental pressures. The coefficients of the "best fit" equations for describing the variation of the compressibility factors with density are listed in Table 8. The number of parameters required for a statistical "best fit" of the data according to Hall and Canfield (18) varied from three for the pure helium to five for the argon.

The values of the deviations of the experimental compressibility factors from those calculated from the

TABLE 2

THE COMPRESSIBILITY FACTORS FOR HELIUM
AT THE EXPERIMENTAL PRESSURES*

T = 323.15°K		T = 273.15°K		T = 223.15°K	
P (atm)	z=Pv/RT	P (atm)	z=Pv/RT	P (atm)	z=Pv/RT
674.837	1.28067	683.599	1.33969	695.239	1.42834
393.223	1.16782	391.213	1.19985	387.712	1.24653
237.310	1.10289	233.607	1.12121	228.108	1.14765
146.294	1.06407	143.091	1.07494	138.518	1.09064
91.4027	1.04028	89.0521	1.04689	85.7495	1.05649
57.5799	1.02548	55.9640	1.02957	53.7166	1.03553
36.4620	1.01617	35.3851	1.01874	33.8931	1.00225
23.1654	1.01029	22.4593	1.01191	21.4866	1.01428
14.7478	1.00656	14.2908	1.00758	13.6601	1.00909
9.4017	1.00418	9.1072	1.00484	8.7007	1.00579
5.9987	1.00267	5.8095	1.00309	5.5486	1.00370
3.8300	1.00171	3.7083	1.00197	3.5411	1.00236
540.204	1.22738	534.047	1.26914	544.678	1.34068
319.943	1.13754	312.114	1.16070	311.476	1.19971
195.008	1.08493	188.741	1.09837	185.986	1.12098
120.951	1.05312	116.508	1.06118	113.944	1.07479
75.8599	1.03349	72.8529	1.03843	70.9233	1.04681
47.9005	1.02122	45.9194	1.02429	44.5771	1.02953
30.3791	1.01349	29.0883	1.01541	28.1881	1.01871
19.3193	1.00859	18.4851	1.00980	17.8924	1.01190
12.3080	1.00548	11.7702	1.00625	11.3860	1.00758
7.8495	1.00349	7.5040	1.00398	7.2557	1.00483
5.0100	1.00223	4.7881	1.00254	4.6291	1.00308
3.1992	1.00143	3.0570	1.00162	2.9551	1.00197

* 0°C = 273.15°K

TABLE 3

THE COMPRESSIBILITY FACTORS FOR MIXTURE A
AT THE EXPERIMENTAL PRESSURES*

T = 323.15°K		T = 273.15°K		T = 223.15°K	
P (atm)	z=PV/RT	P (atm)	z=PV/RT	P (atm)	z=PV/RT
708.063	1.35525	709.477	1.41723	691.089	1.49123
401.181	1.20163	393.403	1.22991	372.914	1.25928
238.897	1.11974	231.773	1.13388	217.032	1.14695
146.291	1.07313	141.146	1.08074	131.431	1.08703
91.0776	1.04544	87.6161	1.04976	81.3583	1.05298
57.2623	1.02853	54.9891	1.03109	50.9966	1.03282
36.2204	1.01803	34.7467	1.01958	32.2009	1.02056
22.9964	1.01144	22.0476	1.01240	20.4240	1.01297
14.6347	1.00728	14.0255	1.00788	12.9901	1.00822
9.3274	1.00464	8.9369	1.00502	8.2763	1.00523
5.9504	1.00296	5.7003	1.00320	5.2785	1.00333
3.7986	1.00189	3.6384	1.00204	3.3691	1.00212
562.379	1.28266	559.029	1.32848	536.097	1.37841
326.052	1.16373	318.786	1.18546	299.782	1.20625
196.682	1.09847	190.692	1.10970	177.743	1.11922
121.345	1.06061	117.129	1.06680	108.731	1.07148
75.8825	1.03783	73.0678	1.04142	67.6913	1.04385
47.8397	1.02383	45.9998	1.02597	42.5704	1.02730
30.3110	1.01508	29.1217	1.01640	26.9344	1.01716
19.2654	1.00958	18.4992	1.01040	17.1052	1.01085
12.2684	1.00610	11.7772	1.00661	10.8874	1.00688
7.8224	1.00389	7.5081	1.00421	6.9399	1.00438
4.9922	1.00248	4.7905	1.00269	4.4275	1.00279
3.1873	1.00158	3.0583	1.00171	2.8267	1.00178

* 0°C = 273.15°K

TABLE 4

THE COMPRESSIBILITY FACTORS FOR MIXTURE B
AT THE EXPERIMENTAL PRESSURES*

T = 323.15°K		T = 273.15°K		T = 223.15°K	
P (atm)	z=Pv/RT	P (atm)	z=Pv/RT	P (atm)	z=Pv/RT
703.600	1.38156	698.784	1.43529	686.455	1.50211
390.316	1.19938	377.576	1.21362	356.348	1.22037
231.266	1.11206	221.649	1.11487	206.814	1.10832
141.644	1.06597	135.370	1.06559	126.101	1.05763
88.3151	1.04000	84.3493	1.03896	78.6662	1.03245
55.6086	1.02472	53.1168	1.02374	49.6165	1.01902
35.2148	1.01546	33.6457	1.01471	31.4721	1.01147
22.3764	1.00974	21.3847	1.00922	20.0232	1.00706
14.2486	1.00617	13.6192	1.00582	12.7615	1.00440
9.0849	1.00392	8.6848	1.00369	8.1414	1.00277
5.7974	1.00250	5.5424	1.00234	5.1969	1.00175
3.7012	1.00159	3.5388	1.00149	3.3186	1.00111
542.512	1.28692	538.299	1.32290	539.737	1.37423
311.209	1.15523	302.989	1.16515	294.022	1.17148
187.502	1.08920	181.346	1.09125	174.313	1.08685
115.855	1.05326	111.822	1.05304	107.317	1.04720
72.5840	1.03258	70.0278	1.03187	67.2596	1.02698
45.8304	1.02025	44.2188	1.01957	42.5218	1.01599
29.0711	1.01271	28.0546	1.01219	27.0052	1.00972
18.4910	1.00803	17.8482	1.00766	17.1941	1.00601
11.7815	1.00509	11.3738	1.00484	10.9632	1.00376
7.5149	1.00324	7.2556	1.00307	6.9960	1.00237
4.7966	1.00206	4.6315	1.00196	4.4669	1.00150
3.0629	1.00132	2.9579	1.00125	2.8532	1.00095

* 0°C = 273.15°K

TABLE 5

THE COMPRESSIBILITY FACTORS FOR MIXTURE C
AT THE EXPERIMENTAL PRESSURES*

T = 323.15°K		T = 273.15°K		T = 223.15°K	
P (atm)	z=Pv/RT	P (atm)	z=Pv/RT	P (atm)	z=Pv/RT
699.689	1.38311	702.417	1.43452	699.333	1.50245
380.141	1.17594	367.118	1.17324	341.949	1.14964
225.079	1.08955	215.431	1.07738	198.358	1.04346
138.456	1.04887	132.569	1.03757	122.621	1.00944
86.7238	1.02802	83.2498	1.01949	77.5692	0.99916
54.8072	1.01663	52.7436	1.01068	49.4565	0.99681
34.7992	1.01012	33.5550	1.00611	31.6106	0.99691
22.1533	1.00626	21.3903	1.00362	20.2158	0.99761
14.1234	1.00392	13.6499	1.00220	12.9286	0.99831
9.0124	1.00247	8.7156	1.00136	8.2667	0.99885
5.7542	1.00156	5.5672	1.00085	5.2850	0.99924
3.6751	1.00099	3.5566	1.00053	3.3784	0.99950
542.808	1.27836	538.288	1.30209	519.055	1.31754
307.628	1.13375	297.577	1.12631	275.819	1.09558
185.566	1.07017	178.688	1.05838	165.096	1.02613
115.135	1.03912	111.029	1.02911	103.231	1.00404
72.4201	1.02277	70.0142	1.01543	65.5608	0.99777
45.8675	1.01366	44.4427	1.00861	41.8539	0.99670
29.1556	1.00837	28.3000	1.00500	26.7614	0.99715
18.5739	1.00521	18.0495	1.00299	17.1144	0.99788
11.8465	1.00327	11.5208	1.00183	10.9444	0.99853
7.5612	1.00206	7.3573	1.00113	6.9979	0.99901
4.8287	1.00131	4.7000	1.00071	4.4738	0.99934
3.0841	1.00083	3.0028	1.00045	2.8601	0.99958

* 0°C = 273.15°K

TABLE 6

THE COMPRESSIBILITY FACTORS FOR MIXTURE D
AT THE EXPERIMENTAL PRESSURES*

T = 323.15°K		T = 273.15°K		T = 223.15°K	
P (atm)	z=PV/RT	P (atm)	z=PV/RT	P (atm)	z=PV/RT
713.392	1.38280	692.994	1.40615	703.821	1.48503
374.134	1.13482	345.496	1.09710	310.961	1.02670
221.565	1.05164	203.881	1.01311	181.598	0.93817
137.417	1.02070	127.442	0.99108	115.386	0.93290
86.7774	1.00857	81.1693	0.98773	74.8314	0.94665
55.1862	1.00366	51.9679	0.98958	48.5896	0.96183
35.1950	1.00162	33.3007	0.99232	31.4453	0.97399
22.4715	1.00075	21.3308	0.99468	20.2762	0.98273
14.3548	1.00036	13.6548	0.99643	13.0370	0.98870
9.1721	1.00018	8.7364	0.99765	8.3653	0.99268
5.8610	1.00010	5.5873	0.99847	5.3601	0.99528
3.7454	1.00006	3.5724	0.99901	3.4314	0.99696
544.264	1.25281	516.516	1.24012	505.634	1.24235
303.326	1.09264	280.178	1.05272	254.503	0.97856
183.837	1.03620	170.250	1.00100	154.899	0.93196
115.034	1.01470	107.447	0.98868	99.5075	0.93678
72.8948	1.00616	68.6257	0.98816	64.6247	0.95202
46.4218	1.00267	43.9621	0.99061	41.9219	0.96636
29.6222	1.00120	28.1683	0.99327	27.0946	0.97732
18.9176	1.00056	18.0389	0.99541	17.4517	0.98033
12.0857	1.00028	11.5450	0.99695	11.2118	0.99024
7.7222	1.00014	7.3856	0.99800	7.1901	0.99369
4.9347	1.00008	4.7233	0.99870	4.6053	0.99593
3.1533	1.00004	3.0198	0.99916	2.9474	0.99739

* 0°C = 273.15°K

TABLE 7

THE COMPRESSIBILITY FACTORS FOR PURE ARGON
AT THE EXPERIMENTAL PRESSURES*

T = 323.15°K		T = 273.15°K		T = 223.15°K	
P (atm)	z=Pv/RT	P (atm)	z=Pv/RT	P (atm)	z=Pv/RT
694.323	1.34270	705.042	1.38980	678.687	1.42544
347.180	1.05064	315.438	0.97320	246.958	0.81191
207.605	0.98313	188.168	0.90867	149.386	0.76899
131.153	0.97197	121.149	0.91566	100.887	0.81277
84.1240	0.97556	79.1368	0.93598	68.510	0.86441
54.1039	0.98182	51.5888	0.95501	45.9368	0.90682
34.7690	0.98736	33.4633	0.96959	30.3443	0.93778
22.3119	0.99151	21.6072	0.97989	19.8251	0.95915
14.2997	0.99441	13.9037	0.98687	12.8551	0.97346
9.1560	0.99636	8.9251	0.99150	8.2923	0.98286
5.8588	0.99765	5.7202	0.99452	5.3311	0.98898
3.7473	0.99849	3.6624	0.99648	3.4204	0.99293
528.889	1.19240	511.090	1.16819	489.168	1.14463
287.878	1.01569	261.606	0.93579	213.686	0.78266
176.807	0.97613	162.081	0.90754	135.430	0.77661
112.553	0.97245	105.223	0.92201	91.9892	0.82558
72.3139	0.97767	68.7430	0.94268	62.3366	0.87568
46.5050	0.98386	44.7440	0.96034	41.6185	0.91529
29.8713	0.98894	28.9758	0.97342	27.4090	0.94372
19.1604	0.99263	18.6865	0.98251	17.8703	0.96316
12.2751	0.99517	12.0133	0.98862	11.5702	0.97610
7.8577	0.99686	7.7072	0.99264	7.4559	0.98459
5.0269	0.99798	4.9381	0.99526	4.7909	0.99009
3.2149	0.99870	3.1607	0.99696	3.0720	0.99365

* 0°C = 273.15°K

TABLE 8*

COEFFICIENTS IN THE SERIES
 $z = PV/RT = 1 + B/V + C/V^2 + \dots$
 FOR V IN cm^3/mole

Helium			
	T = 323.15°K	T = 273.15°K	T = 223.15°K
$B \times 10^{-1}$	1.181663922	1.191108460	1.220554826
$C \times 10^{-2}$	0.9967595504	1.140165757	1.160545378
$D \times 10^{-3}$	0.8264348809	0.8009260627	1.165014776
Mixture A: 80.00% Helium, 20.00% Argon			
	T = 323.15°K	T = 273.15°K	T = 223.15°K
$B \times 10^{-1}$	1.318095151	1.256274345	1.151617139
$C \times 10^{-2}$	1.876910250	2.035929626	2.368335719
$D \times 10^{-3}$	2.963669381	3.149323015	2.017716584
$E \times 10^{-4}$			3.739192712
Mixture B: 59.35% Helium, 40.65% Argon			
	T = 323.15°K	T = 273.15°K	T = 223.15°K
$B \times 10^{-1}$	1.137679615	0.9413277698	0.6057187925
$C \times 10^{-2}$	3.328286224	3.535735002	4.026530595
$D \times 10^{-3}$	4.351391998	4.310984546	3.191755228
$E \times 10^{-4}$	6.946132111	8.898908591	13.01921700

* 0°C = 273.15°K

Pressure Range: 0-700 atm

TABLE 8 (CONTINUED)

Mixture C: 41.05% Helium, 58.95% Argon			
	T = 323.15°K	T = 273.15°K	T = 223.15°K
$B \times 10^{-1}$	0.7103828152	0.3275123468	-0.2808433716
$C \times 10^{-2}$	5.222491434	5.537413307	5.766774884
$D \times 10^{-3}$	3.251839767	3.194902135	9.475420874
$E \times 10^{-5}$	2.635865173	2.870815008	-0.9502703876
$F \times 10^{-6}$			8.030220385
Mixture D: 21.99% Helium, 78.01% Argon			
	T = 323.15°K	T = 273.15°K	T = 223.15°K
$B \times 10^{-1}$	0.02932478639	-0.6314676281	-1.631571871
$C \times 10^{-2}$	6.877019783	7.774112273	8.628079742
$D \times 10^{-3}$	10.99523531	8.443774213	14.05078437
$E \times 10^{-5}$	0.08919536057	0.3345783163	-4.515329097
$F \times 10^{-7}$	1.329545675	1.392048140	2.481703933
Argon			
	T = 323.15°K	T = 273.15°K	T = 223.15°K
$B \times 10^{-1}$	-1.084026609	-2.166793619	-3.790121491
$C \times 10^{-2}$	9.805359555	12.47145291	15.24394041
$D \times 10^{-3}$	12.50172188	-2.046250752	2.215337652
$E \times 10^{-5}$	-0.1955656150	2.343556245	-9.307016611
$F \times 10^{-7}$	3.236609033	3.427254236	6.451270815

fitted equations are presented in Tables 9 through 14. These deviations apply to the compressibility factors listed in Tables 2 through 7, and are listed in the same order to allow easy comparison. A summary of the average deviations is given in Table 15, where they are summarized first for each composition at the three experimental temperatures, and then for all compositions at all temperatures. That table shows that for all the gases except argon, the average deviations were approximately 0.2 to 0.3×10^{-4} . The values for argon at 0 and -50°C are abnormally large. No explanation for this has been possible as a result of the preliminary treatment. The average overall deviation of 0.32×10^{-4} is still felt to be an indication that the isotherms of all the gases are well represented to 700 atm by the fitted equations. As another indication of the goodness of fit, the root-mean-square deviation for the fits has been included in Table 15.

Comparison with Other Investigators

The values of the compressibility factors used in the comparison have been calculated from the "best fit" coefficients listed in Table 8. The values from the literature have been calculated from similar reported equations. The only gases which can be compared directly are helium and argon. The comparisons for argon are shown in Table 16, and those for helium in Table 17. A comparison of the virial coefficients will be presented in Chapter VIII.

TABLE 9*

DIFFERENCES BETWEEN THE EXPERIMENTAL COMPRESSIBILITY
FACTORS AND THOSE CALCULATED FROM THE
FITTED EQUATIONS FOR PURE HELIUM

$\Delta = (z_{\text{exp}} - z_{\text{calc}}) \times 10^5$				
Pressure No.	T = 323.15°K	T = 273.15°K	T = 223.15°K	
	0	0	5	1
	1	-1	5	0
	2	2	10	1
	3	-9	-7	-7
High	4	0	-4	-4
Pressure	5	4	-2	7
Runs	6	6	-2	2
	7	6	-2	7
	8	0	0	2
	9	-3	1	-2
	10	-6	2	-1
	11	1	5	-2
	0	-1	-13	-2
	1	1	-1	3
	2	5	7	5
	3	-6	-4	-6
Low	4	-3	-2	-2
Pressure	5	2	-1	2
Runs	6	3	0	3
	7	0	2	-2
	8	2	1	4
	9	-4	-3	-6
	10	-1	-1	2
	11	3	5	5
	$\frac{1}{n} \sum \Delta $	2.8	3.7	3.2
	$\frac{1}{n-1} \sqrt{\sum \Delta^2}$	0.8	1.0	0.8

* This table is to be used in conjunction with Table 2. The data are listed in exactly the same order in both tables. The coefficients for the fitted equations are given in Table 8.

TABLE 10*

DIFFERENCE BETWEEN THE EXPERIMENTAL COMPRESSIBILITY
FACTORS AND THOSE CALCULATED FROM THE
FITTED EQUATIONS FOR MIXTURE A

$$\Delta = (z_{\text{exp}} - z_{\text{calc}}) \times 10^5$$

Pressure No.	T = 323.15°K	T = 273.15°K	T = 223.15°K	
	0	0	3	
	1	2	-4	
	2	3	5	
	3	-9	-7	
High	4	-2	3	
Pressure	5	1	0	
Runs	6	5	0	
	7	5	3	
	8	3	2	
	9	1	1	
	10	-2	-2	
	11	1	0	
	0	-1	-5	
	1	-1	5	
	2	4	7	
	3	-6	-7	
Low	4	-1	-5	
Pressure	5	3	-3	
Runs	6	5	1	
	7	6	-1	
	8	1	0	
	9	-4	3	
	10	3	1	
	11	-1	2	
	$\frac{1}{n} \Sigma \Delta $	3.0	3.0	2.2
	$\frac{1}{n-1} \sqrt{\Sigma \Delta^2}$	0.8	0.8	0.6

* This table is to be used in conjunction with Table 3. The data are listed in exactly the same order in both tables. The coefficients for the fitted equations are given in Table 8.

TABLE 11*

DIFFERENCES BETWEEN THE EXPERIMENTAL COMPRESSIBILITY
FACTORS AND THOSE CALCULATED FROM THE
FITTED EQUATIONS FOR MIXTURE B

$\Delta = (z_{\text{exp}} - z_{\text{calc}}) \times 10^5$				
Pressure No.	T = 323.15°K	T = 273.15°K	T = 223.15°K	
	0	1	1	0
	1	0	2	-5
	2	3	0	4
	3	-9	-9	-6
High	4	-2	-3	1
Pressure	5	2	3	3
Runs	6	3	6	7
	7	2	6	5
	8	2	2	5
	9	2	0	2
	10	3	-3	-5
	11	-1	-5	-11
	0	-2	-4	0
	1	3	3	4
	2	3	4	3
	3	-5	-6	-8
Low	4	-1	0	-1
Pressure	5	2	2	0
Runs	6	5	4	0
	7	2	3	0
	8	0	-1	0
	9	1	-3	-3
	10	0	-5	-3
	11	2	3	4
	$\frac{1}{n} \Sigma \Delta $	2.4	3.2	3.3
	$\frac{1}{n-1} \sqrt{\Sigma \Delta^2}$	0.6	0.8	0.9

* This table is to be used in conjunction with Table 4. The data are listed in exactly the same order in both tables. The coefficients for the fitted equations are given in Table 8.

TABLE 12*

DIFFERENCES BETWEEN THE EXPERIMENTAL COMPRESSIBILITY
FACTORS AND THOSE CALCULATED FROM THE
FITTED EQUATIONS FOR MIXTURE C

$\Delta = (z_{\text{exp}} - z_{\text{calc}}) \times 10^5$				
Pressure No.	T = 323.15°K	T = 273.15°K	T = 223.15°K	
	0	0	2	0
	1	-1	3	-4
	2	1	1	4
	3	-5	-11	-4
High	4	1	-2	0
Pressure	5	3	2	1
Runs	6	2	5	3
	7	2	4	3
	8	-1	1	4
	9	-2	0	1
	10	-3	3	-2
	11	2	2	-2
	0	0	-6	2
	1	0	5	1
	2	3	0	3
	3	-2	-4	-3
Low	4	2	1	-3
Pressure	5	3	2	-2
Runs	6	-6	3	3
	7	-1	5	-1
	8	-2	0	-3
	9	-3	-1	-1
	10	7	2	0
	11	2	2	12
	$\frac{1}{n} \Sigma \Delta $	2.1	2.9	2.6
	$\frac{1}{n-1} \sqrt{\Sigma \Delta^2}$	0.6	0.8	0.8

* This table is to be used in conjunction with Table 5. The data are listed in exactly the same order in both tables. The coefficients for the fitted equations are given in Table 8.

TABLE 13*

DIFFERENCES BETWEEN THE EXPERIMENTAL COMPRESSIBILITY
FACTORS AND THOSE CALCULATED FROM THE
FITTED EQUATIONS FOR MIXTURE D

$\Delta = (z_{\text{exp}} - z_{\text{calc}}) \times 10^5$				
Pressure No.	T = 323.15°K	T = 273.15°K	T = 223.15°K	
	0	0	0	0
	1	1	-2	1
	2	1	1	6
	3	-4	-6	-6
High	4	1	1	-1
Pressure	5	2	3	-1
Runs	6	1	3	0
	7	-1	3	-1
	8	-3	1	0
	9	0	0	2
	10	1	-2	1
	11	2	-1	2
	0	0	1	0
	1	-3	0	-4
	2	5	5	-2
	3	-3	-2	3
Low	4	0	-1	1
Pressure	5	1	-2	2
Runs	6	1	-2	1
	7	0	-3	0
	8	-1	-5	-1
	9	-2	-1	0
	10	2	6	-2
	11	-1	9	-2
	$\frac{1}{n} \Sigma \Delta $	1.5	2.5	1.6
	$\frac{1}{n-1} \sqrt{\Sigma \Delta^2}$	0.4	0.7	0.5

* This table is to be used in conjunction with Table 6. The data are listed in exactly the same order in both tables. The coefficients for the fitted equations are given in Table 8.

TABLE 14*

DIFFERENCES BETWEEN THE EXPERIMENTAL COMPRESSIBILITY
FACTORS AND THOSE CALCULATED FROM THE
FITTED EQUATIONS FOR PURE ARGON

$\Delta = (z_{\text{exp}} - z_{\text{calc}}) \times 10^5$				
Pressure No.	T = 373.15°K	T = 273.15°K	T = 223.15°K	
	0	0	1	2
	1	1	2	7
	2	2	-3	-13
	3	-3	-5	3
High	4	1	10	11
Pressure	5	2	6	2
Runs	6	0	0	-10
	7	-1	-4	-19
	8	-2	-7	-11
	9	-2	-9	-4
	10	1	-6	8
	11	5	-1	39
	0	0	-2	-5
	1	-3	5	4
	2	3	-8	-8
	3	-3	2	6
Low	4	0	8	14
Pressure	5	2	5	3
Runs	6	0	-4	-11
	7	1	-7	-13
	8	-2	-12	-8
	9	-1	-11	-5
	10	-2	1	19
	11	2	4	32
	$\frac{1}{n} \Sigma \Delta $	1.7	5.2	10.7
	$\frac{1}{n-1} \sqrt{\Sigma \Delta^2}$	0.4	1.3	3.0

* This table is to be used in conjunction with Table 7. The data are listed in exactly the same order in both tables. The coefficients for the fitted equations are given in Table 8.

TABLE 15

AVERAGE DIFFERENCES BETWEEN THE EXPERIMENTAL
COMPRESSIBILITY FACTORS AND THOSE CALCULATED
FROM THE FITTED EQUATIONS

	$\frac{1}{n} \Sigma \Delta \times 10^4$	$\frac{1}{n-1} \sqrt{\Sigma \Delta^2} \times 10^4$
Helium	0.32	0.087
Mixture A	0.27	0.072
Mixture B	0.30	0.079
Mixture C	0.25	0.070
Mixture D	0.18	0.054
Argon	0.58	0.157
OVERALL	0.32	0.104

Error Analysis

The error analysis used in estimating maximum possible error limits for the present work is the same as the one presented by Canfield et al. (8). That analysis will be summarized here briefly.

The only measured quantities in the Burnett method are pressure and temperature. As a result of this, all errors except those caused by inconsistencies between the experimental procedure and the analytical expressions describing the Burnett method must be related to these two quantities. The errors due to the inconsistencies are caused by incomplete evacuation of V_b before an expansion,

TABLE 16

COMPARISON OF THE EXPERIMENTAL ARGON COMPRESSIBILITY
FACTORS WITH THOSE OF OTHER INVESTIGATORS

P, atm	Reference	T = 273.15°K
50	This Work	0.9562
	Crain (13)	0.9571
	Levelt (34)	0.9570
	Michels (35)	0.9568
	Onnes (42)	0.9614
	Holborn (23)	0.9566
	Whalley (50)	0.9563
100	This Work	0.9244
	Crain (13)	0.9253
	Levelt (34)	0.9253
	Michels (35)	0.9253
200	This Work	0.9108
	Crain (13)	0.9140
	Levelt (34)	0.9114
	Michels (35)	0.9121
400	This Work	1.0521
	Crain (13)	1.0518
	Levelt (34)	1.0500
	Michels (35)	1.0514

TABLE 17

COMPARISON OF THE EXPERIMENTAL HELIUM COMPRESSIBILITY
FACTORS WITH THOSE OF OTHER INVESTIGATORS

P, atm	Reference	T = 273.15°K	T = 223.15°K
25	This Work	1.01324	1.0166
	Canfield (6)	1.01346	1.0169
	White (51)	1.01379	
	Holborn (23)	1.01312	1.0164
	Schneider (46)	1.01313	
50	This Work	1.0264	1.0331
	Canfield (6)	1.0268	1.0336
	Holborn (23)	1.0262	1.0329
	Schneider (46)	1.0263	
100	This Work	1.0526	1.0657
	Canfield (6)	1.0533	1.0666
	Holborn (23)	1.0525	1.0633
200	This Work	1.1041	1.1299
	Canfield (6)	1.1053	1.1312
	Holborn (23)	1.1049	
300	This Work	1.1544	1.1926
	Canfield (6)	1.1561	1.1942
400	This Work	1.2042	1.2540
	Canfield (6)	1.2059	1.2559
500	This Work	1.2527	1.3142
	Canfield (6)	1.2546	1.3164

variation in the temperature during an experimental run, and incorrect proportioning of the gas between V_a and V_b .

The error due to incomplete evacuation is analyzed in Appendix A, where it is seen to be negligible.

The error caused by a variation in the temperature during a run can be estimated by repeating the development of the Burnett equations (pages 2 through 4) without assuming the temperatures to be equal. In such a case, Equation 11 will become

$$z_j = P_j N_1 N_2 N_3 \dots N_j \left(\frac{z_0}{P_0} \right) \left(\frac{T_0}{T_j} \right) \quad (18)$$

In the present work, the bath temperature was controlled to $\pm 0.004^\circ\text{C}$ of the desired temperature. The maximum difference between T_0 and T_j was therefore 0.008°C , which would cause a maximum error of 0.0036 percent in the compressibility factor.

The error due to incorrect proportioning of the gas between V_a and V_b will be reflected in the value for the zero-pressure cell constant. The source of this type of error has been discussed in Chapter IV, where it was seen to be related to the position of the diaphragm of the cryogenic pressure null cell at the time of closure of the expansion valve following the pressure measurement. Its magnitude is very small, and it is included in the error estimate for the zero-pressure cell constant.

The errors associated with the experimental pressure measurements can be estimated by first rearranging Equation 11 to the form

$$z_j = \frac{P_0}{z_0} = P_j N_1 N_2 N_3 \dots N_j \quad (19)$$

and then differentiating this equation totally (at constant temperature) to get

$$\begin{aligned} z_j d\left(\frac{P_0}{z_0}\right) + \left(\frac{P_0}{z_0}\right) dz_j &= N_1 N_2 \dots N_j dP_j + P_j N_2 N_3 \dots N_j dN_1 + \\ &P_j N_1 N_3 \dots N_j dN_2 + P_j N_1 N_2 \dots N_j dN_3 + \dots + \\ &P_j N_1 N_2 \dots N_{j-1} dN_j \end{aligned} \quad (20)$$

For small errors, the differentials can be replaced by delta quantities. The successive cell constants N_1 , N_2 , etc., are all approximately equal (Appendix D), so that the quantity $N_1 N_2 \dots N_j$ can be simplified to N^j . When these changes are made and the equation rearranged slightly, the result is

$$(\Delta z_j)_T = \frac{N^j \Delta P_j + P_j N^j \left(\frac{\Delta N_1}{N_1} + \frac{\Delta N_2}{N_2} + \dots + \frac{\Delta N_j}{N_j} \right) - z_j \Delta(P_0/z_0)}{P_0/z_0} \quad (21)$$

where the delta quantities are the differences between the true values and those calculated in the experimental treatment.

The error in the run constant, $\Delta(P_0/z_0)$, is dependent upon the errors in the cell constants, ΔN_j , and those in the pressures, ΔP_j , because of the relationship

$$P_0/z_0 = \lim_{P_j \rightarrow 0} P_j N_1 N_2 \dots N_j \quad (22)$$

Extrapolation of these values from the lowest experimental pressure to zero pressure introduces another error. If this latter error is denoted by E_{P_0/z_0} , Equation 22 can be used to estimate the error in P_0/z_0 .

$$\Delta(P_0/z_0) = N^n \Delta P_n + P_n N^n \left(\frac{\Delta N_1}{N_1} + \frac{\Delta N_2}{N_2} + \dots + \frac{\Delta N_n}{N_n} \right) + E_{P_0/z_0} \quad (23)$$

In this equation, n denotes the total number of pressure measurements in an experimental run.

When Equation 23 is substituted into Equation 21, the result is an expression for the error in z_j due to errors in the pressure measurements and the analytical treatment of these measurements,

$$(\Delta z_j)_T = \left(\frac{N^j \Delta P_j - z_j N^n \Delta P_n}{P_0/z_0} \right) - z_j \left(\frac{\Delta N_{j+1}}{N} + \dots + \frac{\Delta N_n}{N} \right) + \frac{z_j E_{P_0/z_0}}{P_0/z_0} \quad (24)$$

where the approximations have been made that

$$z_n = 1$$

$$P_j N^j = z_j P_0 / z_0$$

$$N_1 = N_2 = \dots = N_n$$

In addition to the errors caused by pressure uncertainties, there are also errors caused by uncertainties in the temperature. The effect of temperature uncertainty, ΔT , upon the compressibility factor is seen to be

$$(\Delta z_j)_P = \left(\frac{\partial z}{\partial T} \right)_P \Delta T \quad (25)$$

The value of $\left(\frac{\partial z}{\partial T} \right)_P$ can be obtained from the experimental data.

The combination of Equations 24 and 25 will be the total error in the compressibility factor,

$$\Delta z_j = \frac{N^j \Delta P_j - z_j N^n \Delta P_n}{P_0 / z_0} - z_j \left(\frac{\Delta N_{j+1}}{N} + \dots + \frac{\Delta N_n}{N} \right) + \frac{z_j E_{P_0 / z_0}}{P_0 / z_0} + \left(\frac{\partial z}{\partial T} \right)_P \Delta T \quad (26)$$

Estimated Errors

The error in the pressures, ΔP_j , is estimated to be

$$\Delta P_j = \pm (10^{-4} P_j + 10^{-4} + 2 \times 10^{-4}) \text{ atm} \quad (27)$$

where the first term represents the uncertainty in the calibrated area of the piston gages; the second term, errors

in the barometric pressure; and the third term, errors in the hydraulic head values (Appendix C). The last two of these terms can be combined to give an overall estimated uncertainty in the pressures of

$$\Delta P_j = \pm(10^{-4}P_j + 3 \times 10^{-4}) \text{ atm} \quad (28)$$

where P_j is in atmospheres.

The uncertainty in the cell constant, ΔN_j , is a function of pressure because of the manner in which the cells deform elastically as pressure is applied. The possibility of a shift in the null point of the cryogenic pressure null indicator during a run is also a potential source of uncertainty in the cell constant. This combined uncertainty has been estimated in Appendix D, and is assumed to be accurate to at least 20 percent. Because of the double-wall construction of the Burnett cell, the total deformation is so small that an uncertainty of 20 percent is negligible in the present case. The principal remaining uncertainty in the cell constants is then the uncertainty in the value of the zero-pressure cell constant, which is estimated to be no more than 0.005 percent. Therefore the maximum estimated uncertainty in the cell constants can be represented as

$$\frac{\Delta N_j}{N} = \pm 5 \times 10^{-5} \quad (29)$$

The error involved in the extrapolation to get the run constant, E_{P_0/z_0} , is estimated to vary between 0.02 atm for helium at 50°C to 0.05 atm for argon at -50°C.

The maximum estimated uncertainty in the temperature is

$$\Delta T = \pm 0.01^\circ\text{C} \quad (30)$$

based on the maximum difference between the temperature observed with a calibrated platinum resistance thermometer, and the International Temperature Scale.

When these maximum estimated uncertainties are substituted into Equation 26, the results are the estimated maximum error limits of the experimental compressibility factors. This has been done for four selected conditions, with the following results:

<u>System</u>	<u>Maximum Error in z</u>
Argon, -50°C , 679 atm	0.08%
Argon, -50°C , 3.0 atm	0.03%
Helium, 50°C , 675 atm	0.07%
Helium, 50°C , 3.0 atm	0.03%

The actual errors expected in the experimental compressibility factors are much less than these estimated maximum errors.

CHAPTER VIII

APPLICATIONS OF THE DATA

This chapter is devoted to the theoretical analysis of the data presented in the previous chapter. As part of this analysis, the second virial coefficients, the interaction second virial coefficients, the third virial coefficients, and the interaction third virial coefficients are discussed, summarized, and compared with corresponding values reported by other investigators.

Even though the virial coefficients determined as indicated in Chapter VI are the values resulting from a preliminary treatment only, the comparisons indicate that the present results are reasonable.

Second Virial Coefficients

Pure-Component and Mixture Second Virial Coefficients

The discussion in Chapter VI showed that there are more ways than one to obtain the second virial coefficients. Canfield has presented an interesting discussion of several methods utilized in determining the coefficients; he has summarized some of these methods in the following manner (6, p. 93):

Method 1. Curve fitting:

$$A. \quad z = 1 + B/V + C/V^2 + \dots$$

$$B. \quad z = 1 + B'P + C'P^2 + \dots$$

$$C. \quad z = e^{\alpha P + \beta P^2 + \dots} \quad \text{where } \alpha = B'$$

Method 2. Limiting Procedures:

$$A. \quad B = \lim_{1/V \rightarrow 0} [V(z-1)]$$

$$B. \quad B = \lim_{1/V \rightarrow 0} \left(\frac{\partial z}{\partial (1/V)} \right)_T$$

$$C. \quad B' = \lim_{P \rightarrow 0} \left(\frac{z-1}{P} \right)$$

$$D. \quad B' = \lim_{P \rightarrow 0} \left(\frac{\partial z}{\partial P} \right)_T$$

All of these methods except 2-D were investigated by Canfield in the evaluation of his data. For all the reasons he listed, he chose Method 2-A for the evaluation of the second virial coefficients in his work. He evaluated these coefficients graphically, "with very little weight given to the low pressure data points."

In the present work, the second virial coefficients were obtained as indicated in Chapter VI, pages 100-105. The equations obtained by the ORNOR fit of the data were checked for linearity of the extrapolation of a plot of $V(z-1)$ versus $1/V$ as added assurance of a satisfactory fit. As another check, the standard deviations of the

coefficients calculated by the ORNOR fitting program were used as a guide in determining whether the overall program for treating Burnett data had picked the best combination of cell constants and run constants for the two runs at the same temperature and for the same composition. In some cases the combination picked by the program was not the one yielding the minimum standard deviations of the coefficients. In those cases, it was found that the standard deviations could be used as a criterion for picking the proper fit.

The second virial coefficients for the pure components and the mixtures are presented in Table 18. A comparison with several values reported in the literature is given in Table 19. For the conditions in which comparison is possible, the results of the present work agree reasonably well with previous results.

TABLE 18*
SECOND VIRIAL COEFFICIENTS FOR HELIUM, ARGON,
AND FOUR MIXTURES, IN cm^3/mole

System	T = 323.15°K	T = 273.15°K	T = 223.15°K
Helium	11.82	11.91	12.21
Mixture A	13.18	12.56	11.52
Mixture B	11.38	9.41	6.06
Mixture C	7.10	3.28	-2.81
Mixture D	0.29	-6.32	-16.32
Argon	-10.84	-21.67	-37.90

* 0°C = 273.15°K

TABLE 19

COMPARISON OF SELECTED VALUES FOR THE SECOND VIRIAL
COEFFICIENTS OF HELIUM AND ARGON

Helium			
Reference	T = 373.15°K	T = 273.15°K	T = 223.15°K
This Work	11.82	11.91	12.21
Holborn (23)	11.73	11.86	11.93
Michels (36)	11.57	11.87	
Wiebe (52)	11.43	11.70	
Tanner (48)	11.39	11.70	
Keesom (28)	11.30	11.48	11.59
Canfield (6)		12.09	12.46
White (51)		12.08	
Schneider (46)		11.77	

Argon			
Reference	T = 373.15°K	T = 273.15°K	T = 223.15°K
This Work	-10.84	-21.67	-37.90
Holborn (23)	-11.02	-21.91	-37.80
Michels (35)	-11.26	-21.45	-37.08
Whalley (50)	-11.20	-22.40	-36.79
Getzen (17)	-11.40	-21.51	
Crain (13)		-21.18	

Interaction Second Virial Coefficients

Information about the interaction of two unlike molecules in a binary gas mixture can be obtained by evaluation of the interaction second virial coefficient, B_{12} , which is defined by the Lennard-Jones and Cook equation

$$B_M = X_1^2 B_{11} + 2X_1 X_2 B_{12} + X_2^2 B_{22} \quad (31)$$

The value of B_{12} can be determined from known values of the pure-component second virial coefficients, B_{11} and B_{22} , and the value of B_M for one mixture. Four values for the mixture second virial coefficients were available from the present investigation, so it was desirable to choose a method for getting the best value of B_{12} at each temperature. The method selected was an ORNOR fit of the experimental values of B_M versus composition to Equation 31. As mentioned before, the ORNOR fit was a least-squares fit employing orthonormal polynomials. The values of B_{12} obtained in this way are listed in Table 20.

TABLE 20
THE SECOND INTERACTION VIRIAL COEFFICIENT, B_{12} ,
FOR HELIUM-ARGON MIXTURES

$T, \text{ }^\circ\text{K}$	$B_{12} \text{ (cm}^3\text{/mole)}$
323.15	18.57
273.15	18.27
223.15	17.04

Figure 12 shows the temperature dependence of B_{12} , and it also indicates the comparison of the present values with values from the literature. Figure 13 shows the values of B_M versus composition, with the least-squares curve plotted for each temperature.

The interaction second virial coefficient at 90°K (30) has been recalculated, using Fender and Halsey's second virial coefficient for pure argon (16). The value of B_{12} was originally reported as 6.6 cm³/mole; the recalculated value is 0.65 cm³/mole.

Third Virial Coefficients

As mentioned in Chapter I, the third virial coefficient describes the interaction between three molecules of a gas in the limit of zero macroscopic density. Evaluation of third virial coefficients for pure components or mixtures requires very precise data. Evaluation of the interaction third virial coefficients, which offer information concerning the behavior of unlike molecules in a gas mixture, is even more critically dependent upon high quality data.

Pure-Component and Mixture Third Virial Coefficients

The third virial coefficients for the pure components and the mixtures were obtained at the same time as the second virials, by the optimization program described in Chapter VI. Their values are tabulated in Table 21. Figures 14, 15, and 16 show the variation of C_M with composition.

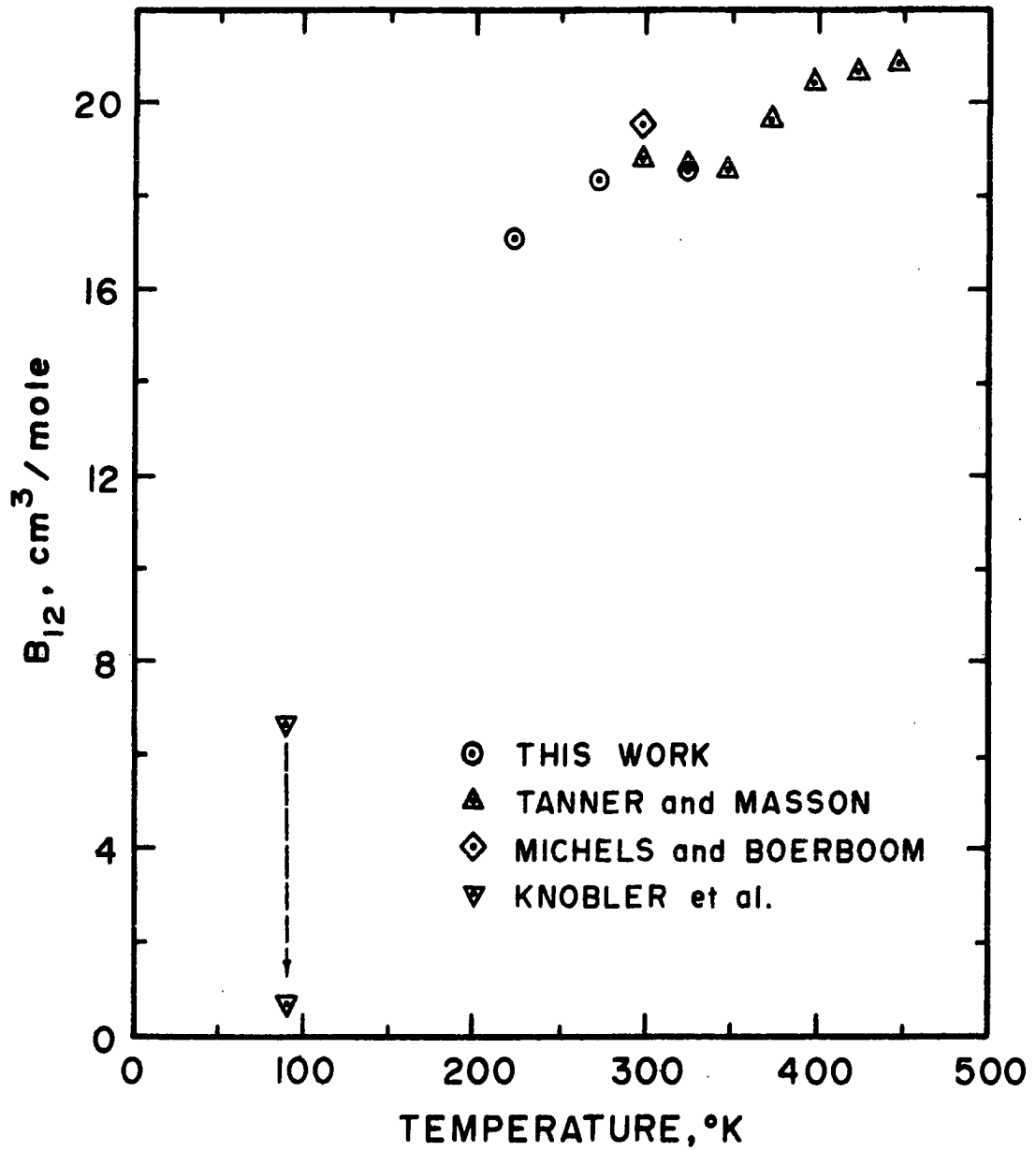


Figure 12. Temperature Dependence of the Helium-Argon Interaction Second Virial Coefficient

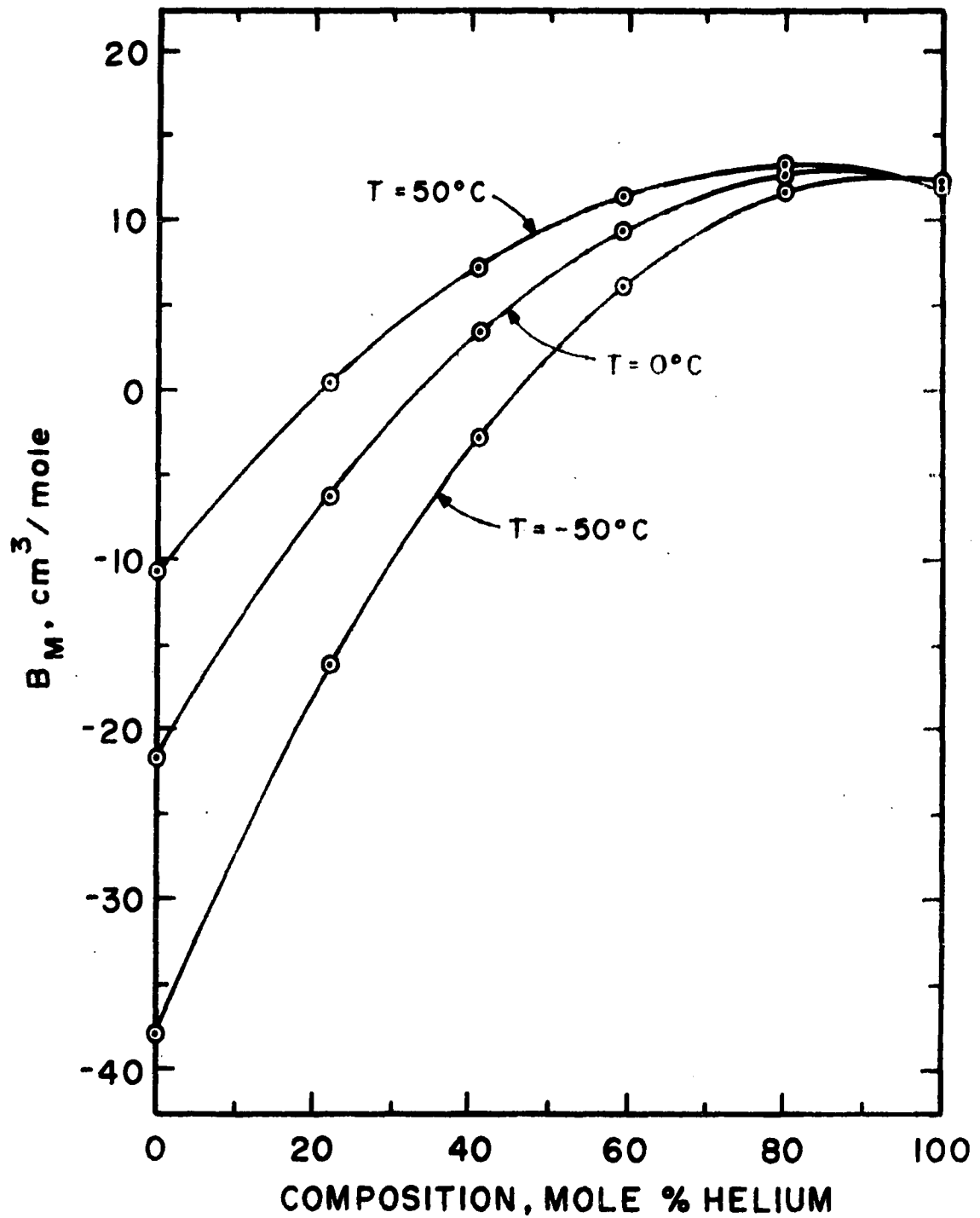


Figure 13. Variation of the Helium-Argon Mixture Second Virial Coefficient with Composition

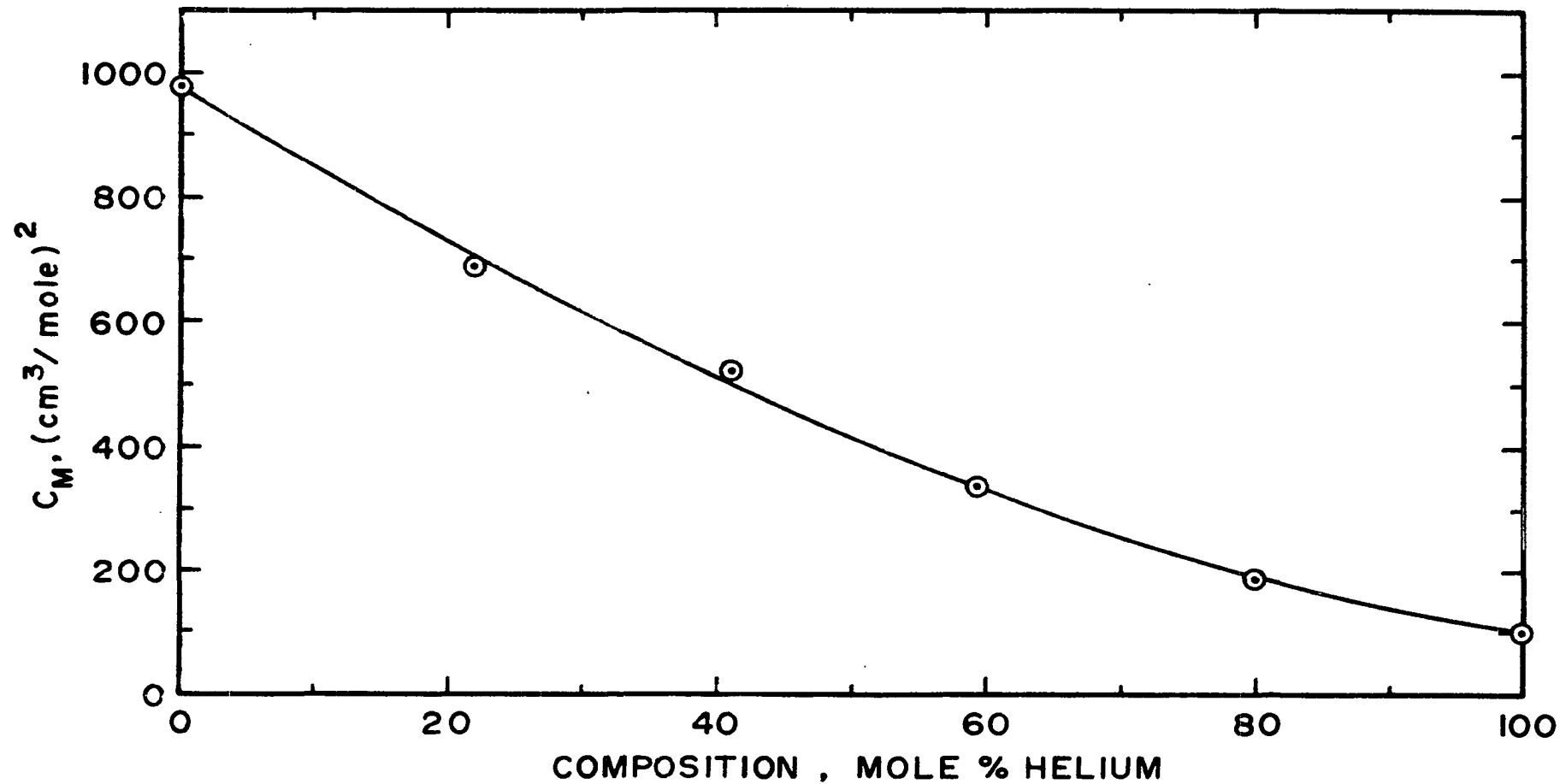


Figure 14. Variation of the Helium-Argon Mixture Third Virial Coefficient with Composition at 50°C

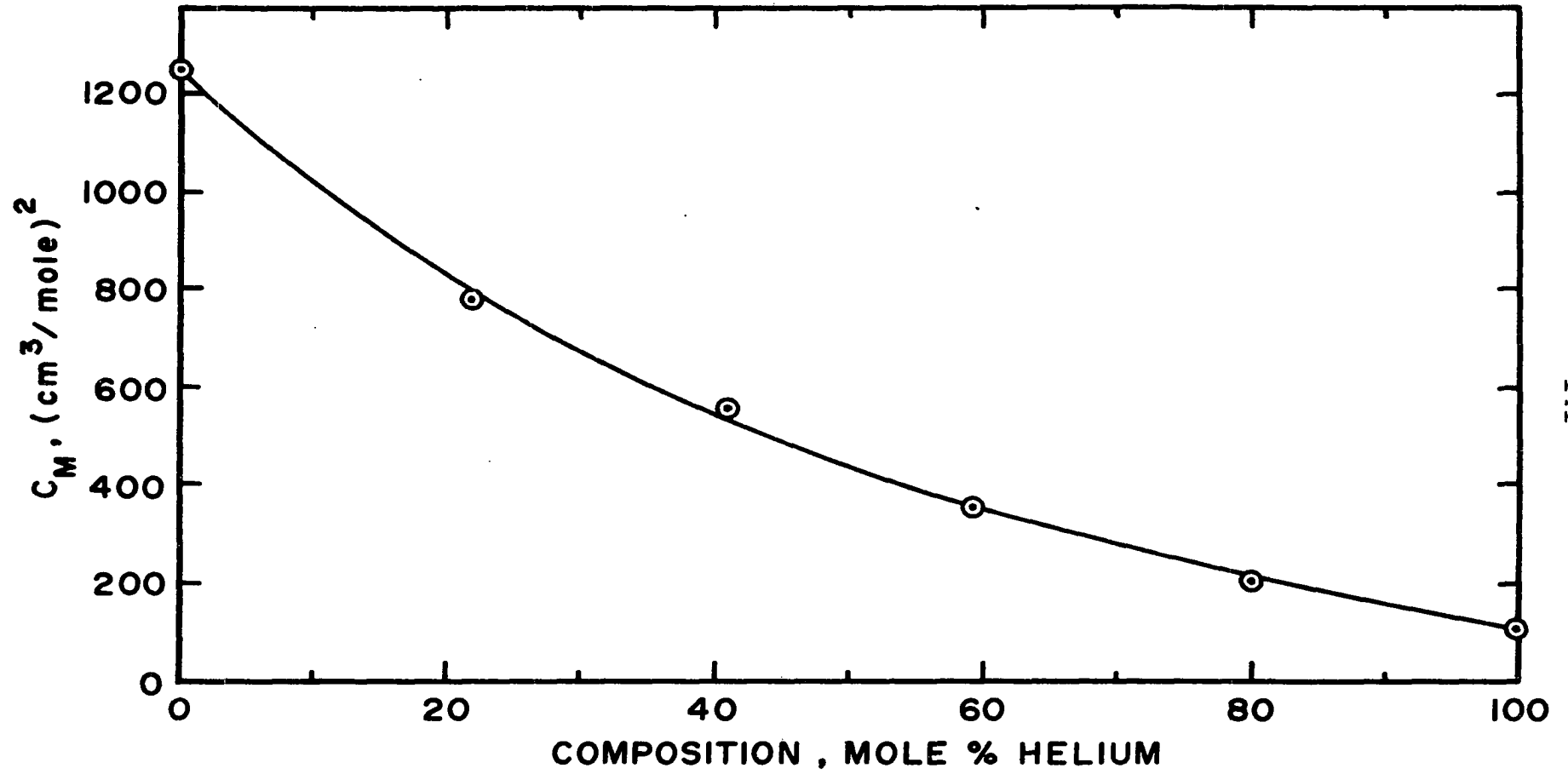


Figure 15. Variation of the Helium-Argon Mixture Third Virial Coefficient with Composition at 0°C

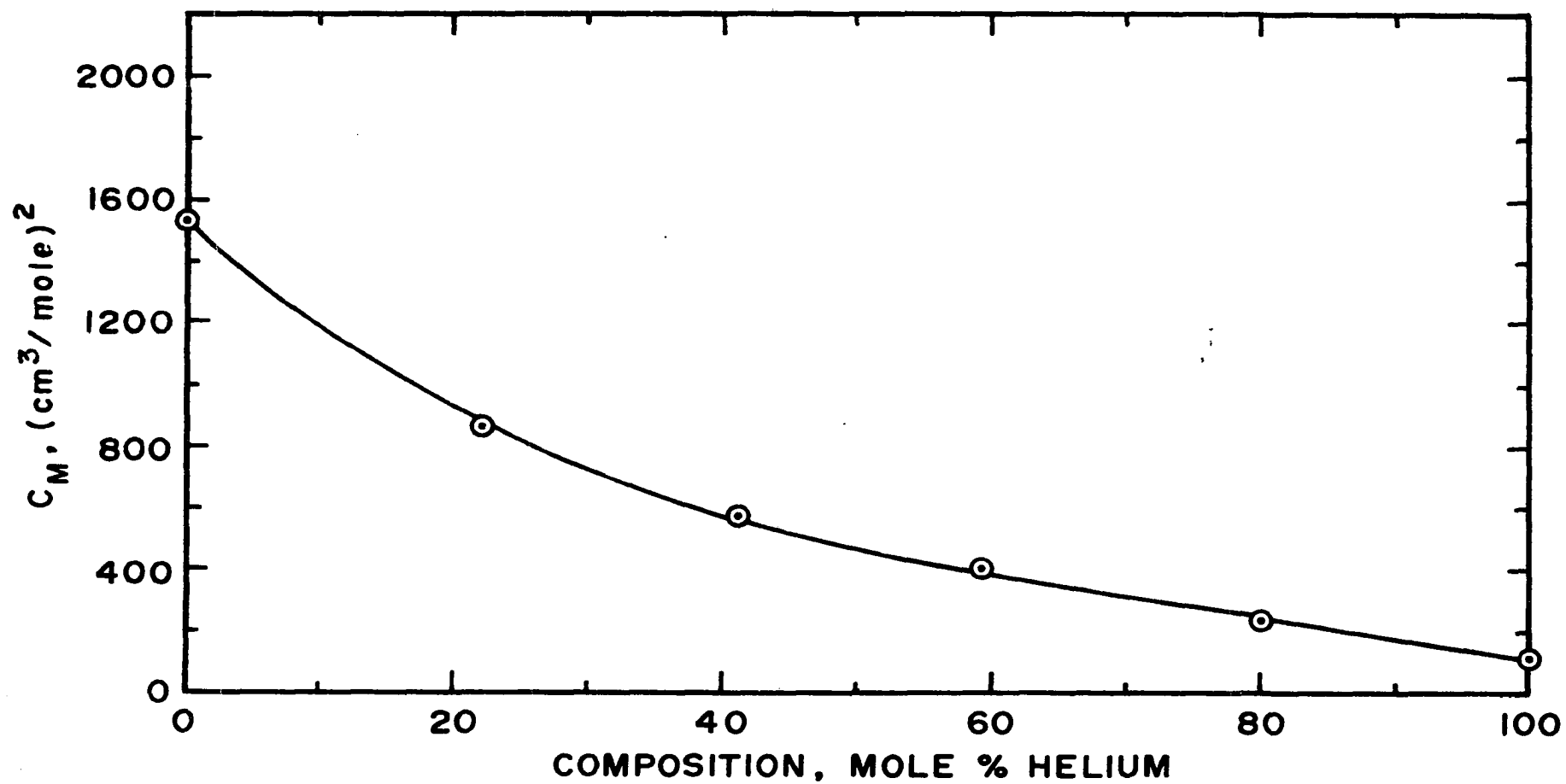


Figure 16. Variation of the Helium-Argon Mixture Third Virial Coefficient with Composition at -50°C

TABLE 21*

THIRD VIRIAL COEFFICIENTS FOR HELIUM, ARGON,
AND FOUR MIXTURES, IN (cm³/mole)²

System	T = 323.15°K	T = 273.15°K	T = 223.15°K
Helium	100	114	116
Mixture A	188	204	237
Mixture B	333	354	403
Mixture C	522	554	577
Mixture D	688	777	863
Argon	981	1247	1524

* 0°C = 273.15°K

Interaction Third Virial Coefficients

The interaction third virial coefficients, C_{112} and C_{122} , are defined by the following equation for a binary mixture:

$$C_M = x_1^3 C_{111} + 3x_1^2 x_2 C_{112} + 3x_1 x_2^2 C_{122} + x_2^3 C_{222} \quad (32)$$

Values of C_{112} and C_{122} were obtained from the present data by an ORNOR fit of C_M versus composition. The values of C_{112} and C_{122} are presented for the three experimental temperatures in Table 22.

The least-squares line from the ORNOR fit of the third virial coefficients is shown in Figures 14, 15, and 16, along with the experimental values.

TABLE 22

THE THIRD INTERACTION VIRIAL COEFFICIENTS,
 $C_{\text{He-He-Ar}}$ AND $C_{\text{He-Ar-Ar'}}$ IN
(cm^3/mole)²

T, °K	$C_{\text{He-He-Ar}}$	$C_{\text{He-Ar-Ar}}$
323.15	220	535
273.15	278	436
223.15	424	276

LITERATURE CITED

1. Baxter, G. P., and Starkweather, H. W., "Density, Compressibility, and Atomic Weight of Argon," Proc. Natl. Acad. Sci. U.S., 14, 57 (1928).
2. Baxter, G. P., and Starkweather, H. W., "Density, Compressibility, and Atomic Weight of Argon," Proc. Natl. Acad. Sci. U.S., 15, 441 (1929).
3. Blancett, A. L., and Canfield, F. B., "Gas Bath Cryostat for Wide Range Temperature Control," Adv. Cryo. Eng., 11, 612 (1965).
4. Bridgman, P. W., "The Compressibility of Five Gases to High Pressures," Proc. Am. Acad. Arts Sci., 59, No. 8, 173 (1924).
5. Burnett, E. S., "Compressibility Determination without Volume Measurements," J. Appl. Mech., Trans. ASME, 58, A136 (1936).
6. Canfield, F. B., "The Compressibility Factors and Second Virial Coefficients for Helium-Nitrogen Mixtures at Low Temperature and High Pressure," Ph.D. Thesis, Rice University, Houston, Texas (1962).
7. Canfield, F. B., "Volumetric Behavior of Gas Mixtures at Low Temperature and High Pressure," Final Report, University of Oklahoma Research Institute, NSF Grant (1965).
8. Canfield, F. B., Leland, T. W., and Kobayashi, R., "Compressibility Factors for Helium-Nitrogen Mixtures," J. Chem. Eng. Data, 10, 92 (1965).
9. Canfield, F. B., Watson, J. K., and Blancett, A. L., "Electromagnetic Gas Pump for Low Temperature Service," Rev. Sci. Inst., 34, 1431 (1963).
10. Comings, E. S., High Pressure Technology, McGraw-Hill Book Company, Inc., New York, 1956.

11. Cook, G. A., (ed.), Argon, Helium, and the Rare Gases, Vol. I, Interscience Publishers, New York, 1961, Ch. VIII.
12. Cragoe, C. S., Temperature, Reinhold, New York, 1941, p. 89, cited by Whalley, et al., Can. J. Chem., 31, 722 (1953).
13. Crain, R. W., "The P-V-T Behavior of Nitrogen, Argon, and Their Mixtures," Ph.D. Thesis, University of Michigan, Ann Arbor, Michigan (1965).
14. Cross, J. L., "Reduction of Data for Piston Gage Measurements," Nat. Bur. Stds. Monograph 65 (1963).
15. Din, F., Thermodynamic Functions of Gases, Vol. 2: Air, Acetylene, Ethylene, Propane, and Argon, Butterworths, London, 1956.
16. Fender, B. E. F., and Halsey, G. D., Jr., "Second Virial Coefficients of Argon, Krypton, and Argon-Krypton Mixtures at Low Temperatures," J. Chem. Phys., 36, 1881 (1962).
17. Getzen, F. W., "The Compressibility of Gaseous Argon," Thesis, Massachusetts Institute of Technology (1956).
18. Hall, K. R., and Canfield, F. B., "Optimal Recovery of Virial Coefficients from Experimental Compressibility Data," to be published in Physica.
19. "Heating and Pickling Huntington Alloys," Technical Bulletin T-20, Huntington Alloy Products Division of the International Nickel Company, Inc.
20. Heuse, W., and Otto, J., "Über eine Neubestimmung des Grenzwertes der Ausdehnungs- und Spannungskoeffizienten von Helium, Wasserstoff und Stickstoff. (Concerning a New Determination of the Critical Value of the Expansion and Voltage Coefficients of Helium, Hydrogen and Nitrogen)," Ann. Physik, (5) 2, 1012 (1929).
21. Hirschfelder, J. O., Curtiss, C. F., and Bird, R. B., Molecular Theory of Gases and Liquids, 2nd ed., John Wiley, New York, 1964.
22. Holborn, L., and Otto, J., "Über die Isothermen Einiger Gase bis 400 Grad und Ihre Bedeutung für das Gas-thermometer. (On Isotherms of Several Gases up to 400 Degrees and Their Importance for the Gas Thermometer)," Z. Physik, 23, 77 (1924).

23. Holborn, L., and Otto, J., "Über die Isothermen einiger Gase Zwischen $+400^{\circ}$ und -183° . (Isotherms of Several Gases between $+400^{\circ}$ and -183°)," Z. Physik, 33, 1 (1925).
24. Holborn, L., and Otto, J., "Über die Isothermen von Helium, Stickstoff und Argon unterhalb 0 Grad. C. (Isotherms for Helium, Nitrogen, and Argon below 0 Degrees C)," Z. Physik, 30, 320 (1924).
25. Holborn, L., and Schultze, H., "Über die Druckwage und die Isothermen von Luft, Argon, und Helium zwischen 0 und 200 Grad. (Concerning the Pressure Balance and the Isotherms of Air, Argon and Helium between 0 and 200 Degrees C)," Ann. Physik, 47, 1089 (1915).
26. Hoover, A. E., "Virial Coefficients of Methane and Ethane," Ph.D. Thesis, Rice University, Houston, Texas (1965).
27. Hoover, A. E., Canfield, F. B., Kobayashi, R., and Leland, T. W., Jr., "Determination of Virial Coefficients by the Burnett Method," J. Chem. Eng. Data, 9, 568 (1964).
28. Keesom, W. H., Helium, Elsevier, Amsterdam, 1942: Reprinted without revision, 1959.
29. Kerr, E. C., "I. The Second Virial Coefficient of Argon at Low Temperatures and Low Pressures. II. The Heat Capacity of Liquid Nitric Oxide above its Boiling Point," Ph.D. Thesis, Ohio State University, Columbus, Ohio (1957).
30. Knobler, C. M., Beenakker, J. J. M., and Knaap, H. F. P., "The Second Virial Coefficients of Gaseous Mixtures at 90°K ," Physica, 25, 909 (1959).
31. Magasanik, D., "Unlike-Molecule Interactions from Second Virial and Joule-Thomson Coefficients," Ph.D. Thesis, Institute of Gas Technology, Chicago, Illinois (1963).
32. Masson, I., and Dolley, L. G. F., "The Pressures of Gaseous Mixtures," Proc. Roy. Soc. (London), A103, 524 (1923).
33. Michels, A., and Boerboom, A. J. H., "The Volume Change on Mixing Two Gases at Constant Pressure," Bull. Soc. Chim. Belg., 62, 119 (1953).
34. Michels, A., Levelt, J. M. and De Graaff, W., "Compressibility Isotherms of Argon at Temperatures between -25 and -155 Degrees C and at Densities up to 640 Amagat. (Pressures up to 1050 Atmospheres)," Physica, 24, 659 (1958).

35. Michels, A., Wijker, Hub., and Wijker, Hk., "Isotherms of Argon between 0 and 150 Degrees C and Pressures up to 2900 Atmospheres," Physica, 15, 627 (1949).
36. Michels, A., and Wouters, H., "Isotherms of Helium between 0° and 150°C up to 200 Amagat," Physica, 8, 923 (1941).
37. Miks, Claude, Ruska Instrument Company, Houston, Texas. Personal Communications.
38. Mueller, W. H., "Volumetric Properties of Gases at Low Temperatures by the Burnett Method," Ph.D. Thesis, Rice Institute, Houston, Texas (1959).
39. National Bureau of Standards Cryogenic Data Center, "A Bibliography of References for the Thermophysical Properties of Helium-4, Hydrogen, Deuterium, Hydrogen Deuteride, Neon, Argon, Nitrogen, Oxygen, Carbon Dioxide, Methane, Ethane, Krypton, and Refrigerants 13, 14, and 23," NBS Report 8808, 1965.
40. Oishi, Jiro, "0 Degrees and 100 Degrees Isotherms of Helium, Hydrogen, Neon, Argon, Air and Carbon Dioxide at Pressures below 2 Atmospheres and Absolute Temperature of 0 Degrees C," J. Sci. Research Inst. (Tokyo), 43, 220 (1949).
41. Onnes, H. K., "Isotherms of Monatomic Gases and Their Binary Mixtures. I. Isotherms of Helium between +100°C and -217°C," Comm. Phys. Lab. Univ. Leiden, 102a (1908).
42. Onnes, H. K., and Crommelin, C. A., "Isotherms of Monatomic Gases and of Their Binary Mixtures. VII. Isotherms of Argon between 20 and -150 Degrees C," Comm. Phys. Lab. Univ. Leiden, 118B (1911).
43. Onnes, H. K., and Crommelin, C. A., "Isotherms of Monatomic Gases and of Their Binary Mixtures. IX. The Behavior of Argon with Regard to the Law of Corresponding States," Comm. Phys. Lab. Univ. Leiden, 120a (1911); X., 128 (1921).
44. Popov, E. P., Mechanics of Materials, Prentice-Hall, Inc., Englewood Cliffs, New Jersey, 1952, pp. 415-19.
45. Rogovaya, I. A., and Kaganer, M. G., "The Compressibility of Argon at Low Temperatures up to 200 Atmospheres," Russ. J. Phys. Chem. USSR, 35, 1049 (1961); trans. from Zhur. Fiz. Khim., 35, 2135 (1961).

46. Schneider, W. G., and Duffie, J. A. H., "Compressibility of Gases at High Temperatures. II. The Second Virial Coefficient of Helium in the Temperature Range 0°C to 600°C," J. Chem. Phys., 17, 751 (1949).
47. Stroud, L., Miller, J. E., and Brandt, L. W., "Compressibility of Helium at -10° to 130°F and Pressures to 4,000 psia," J. Chem. Eng. Data, 5, 51 (1960).
48. Tanner, C. C., and Masson, I., "The Pressure of Gaseous Mixtures. Part III," Proc. Roy. Soc. (London), A126, 268 (1930).
49. Whalley, E., "Thermodynamic Properties of Argon in the Temperature Range -100 to 600 Degrees C and Pressure Range 0 to 80 Atmospheres," Can. J. Technol., 33, 111 (1955).
50. Whalley, E., Lupien, Y., and Schneider, W. G., "The Compressibility of Gases. VII. Argon in the Temperature Range 0 to 600 Degrees C and the Pressure Range 10 to 80 Atmospheres," Can. J. Chem., 31, 722 (1953).
51. White, D., Rubin, T., Camky, P., and Johnston, H. L., "The Virial Coefficients of Helium from 20 to 300°K," J. Phys. Chem., 64, 1607 (1960).
52. Wiebe, R., Gaddy, V. L., and Heins, C., Jr., "The Compressibility Isotherms of Helium at Temperatures from -70° to 200° and at Pressures to 1,000 Atmospheres," J. Am. Chem. Soc., 53, 1721 (1931).
53. Wilde, D. J., Optimum Seeking Methods, Prentice-Hall, Inc., Englewood Cliffs, New Jersey, 1964.
54. Witonsky, R. J., and Miller, J. G., "Compressibility of Gases. IV. The Burnett Method Applied to Gas Mixtures at Higher Temperatures. The Second Virial Coefficients of the Helium-Nitrogen System from 175° to 475°," J. Am. Chem. Soc., 85, 282 (1963).
55. Yntema, J. L., and Schneider, W. G., "Compressibility of Gases at High Temperatures. III. The Second Virial Coefficient of Helium in the Temperature Range 600°C to 1200°C," J. Chem. Phys., 18, 641 (1950).

APPENDIX A

EFFECT OF INCOMPLETE EVACUATION OF V_b

One of the steps included in the experimental procedure of the Burnett method is the evacuation of chamber V_b before each expansion. The equations used for describing the method are based on the assumption that the number of moles in V_a before an expansion is equal to the number of moles in both V_a and V_b following that expansion.

The evacuation of V_b is never complete, and as a result, this assumption is not exactly correct. The error introduced by incomplete evacuation can be estimated, and is seen to be negligible if the pressure in V_b before an expansion is sufficiently low.

This error source has been discussed previously by Mueller (38). It is re-examined here, and found to be of more importance than Mueller reported for his work. Part of the difference is due to the effect of the greater number of expansions per run in the present work. This will be seen later to be of major importance in the size of the error in the low pressures of the run.

In order to simplify the discussion of this error estimation, the following definitions are made:

n_x = moles of gas in V_b after evacuation

P_x = pressure in V_b after evacuation

z_x = compressibility factor at P_x

n_j = moles of gas in V_a after j expansions

P_j = pressure in V_a after j expansions

z_j = compressibility factor at P_j

n_0 = moles of gas in V_a before first expansion

P_0 = pressure in V_a before first expansion

z_0 = compressibility factor at P_0

It is assumed that V_b is evacuated to the same pressure before each expansion, so that n_x is the same for all expansions. It is also assumed that the cell constant, N , does not change with pressure.

Following the first expansion, the system contains $n_0 + n_x$ total moles. The fraction of this gas remaining in V_a is $1/N$. When the expansion valves are closed prior to evacuation of V_b , the gas in chamber b is no longer a part of the system, so the number of moles of gas in the system after the first complete expansion cycle is n_1 , where

$$\begin{aligned} n_1 &= \frac{1}{N} (n_0 + n_x) & (A-1) \\ &= n_0 \left(\frac{1}{N}\right) + n_x \left(\frac{1}{N}\right) \end{aligned}$$

The number of moles after the second cycle, n_2 , is

$$\begin{aligned} n_2 &= \frac{1}{N} (n_1 + n_x) \\ &= n_0 \left(\frac{1}{N}\right)^2 + n_x \left(\frac{1}{N^2} + \frac{1}{N}\right) & (A-2) \end{aligned}$$

In like manner, the general equation for the number of moles after j expansions will be

$$\begin{aligned} n_j &= \frac{1}{N} (n_{j-1} + n_x) \\ &= n_0 \left(\frac{1}{N}\right)^j + n_x \left(\frac{1}{N^j} + \frac{1}{N^{j-1}} + \dots + \frac{1}{N}\right) \end{aligned} \quad (\text{A-3})$$

which may be simplified to

$$n_j = \frac{n_0}{N^j} + n_x \left[\frac{1}{N^j} \left(\frac{N^j - 1}{N - 1} \right) \right] \quad (\text{A-4})$$

or

$$n_j = \frac{n_0}{N^j} \left[1 + \frac{n_x}{n_0} \left(\frac{N^j - 1}{N - 1} \right) \right] \quad (\text{A-5})$$

The quantities in Equation A-5 are related to the pressures, volumes, and temperatures of the experimental run by the following equations:

$$n_0 = \frac{P_0 V_a}{z_0 RT} \quad (\text{A-6})$$

$$n_j = \frac{P_j V_a}{z_j RT} \quad (\text{A-7})$$

$$\begin{aligned} n_x &= \frac{P_x V_b}{z_x RT} \\ &= \frac{P_x V_a (N-1)}{z_x RT} \end{aligned} \quad (\text{A-8})$$

Substitution of Equations A-6, A-7, and A-8 into Equation A-5 yields

$$P_j = \frac{P_0 z_j}{z_0 N^j} \left[1 + \frac{P_x z_0}{P_0 z_x} (N^j - 1) \right] \quad (\text{A-9})$$

which can be rearranged to express z_j in terms of all the other quantities.

$$z_j = \frac{P_j N^j}{P_0/z_0} \left[1 + \frac{P_x z_0}{P_0 z_x} (N^j - 1) \right]^{-1} \quad (\text{A-10})$$

The second term inside the brackets of Equation A-10 will always be small, so the expression can be approximated closely by

$$z_j = \frac{P_j N^j}{P_0/z_0} \left[1 - \frac{P_x z_0}{P_0 z_x} (N^j - 1) \right] \quad (\text{A-11})$$

When Equation A-11 is compared with the corresponding equation for calculating the z_j if the evacuation is complete,

$$z_j \approx \frac{P_j N^j}{P_0/z_0} \quad (\text{A-12})$$

It is seen that the relative error in z_j caused by incomplete evacuation is

$$E_{\text{evac.}} = \frac{P_x z_0}{P_0 z_x} (N^j - 1) \quad (\text{A-13})$$

The pressure P_x is always close to zero, so that the corresponding compressibility factor, z_x , is approximately unity. Thus the error is approximated by

$$E_{\text{evac.}} = P_x \frac{z_0}{P_0} (N^j - 1) \quad (\text{A-14})$$

For a given pressure P_x and cell constant, N , the error will thus depend upon both z_0/P_0 and the number of expansions, j . In the present work, the worst combination of these two factors yielded a maximum possible error of

$$E_{\text{evac.}} \approx 0.73 P_x \quad (\text{A-15})$$

where P_x is expressed in atmospheres. The data treatment included only those pressures for the first eleven expansions, so the maximum error in that treated data, caused by incomplete evacuation, was less than that indicated in Equation A-15, by a factor of N^2 , or about 2.45. The corresponding maximum error was therefore

$$E_{\text{evac.}} \approx 0.30 P_x \quad (\text{A-16})$$

The evacuation of V_b was always carried out to less than 20 microns, and for the last several expansions of each run, the pressure before the expansion was less than 10 microns. Thus in the above case, the error in z_{11} caused by incomplete evacuation was less than

$$E_{\text{evac.}} \approx 0.30 \left(\frac{0.01}{760} \right) \\ \approx 4 \times 10^{-6} \quad (\text{A-15})$$

or an error in z of approximately 0.0004 percent. All other compressibility factors were less uncertain and their errors due to incomplete evacuation were negligible.

This amount of error, although larger than Mueller's values by more than an order of magnitude, is negligible in comparison with other errors inherent in the pressure measurements.

APPENDIX B

TEMPERATURE MEASUREMENT

The components of the temperature measuring system have been described in Chapter III. There it was seen that the temperature of the Burnett cell in the cryostat was determined by using a Leeds & Northrup G-2 Mueller Bridge to measure the resistance of a Leeds & Northrup Model 8164 capsule-type platinum resistance thermometer which was inserted into a thermowell in the upper end of the cell.

This appendix presents more detailed information concerning calibrations and certifications of these components.

Thermometer

The International Temperature Scale is defined between 630.5 and -183°C by four fixed temperatures and a formula which gives the temperature-resistance relation of a standard strain-free platinum resistance thermometer calibrated at these fixed temperatures. The fixed temperatures are: (1) the normal boiling point of oxygen, -182.97°C ; (2) the melting point of ice, 0°C ; (3) the normal boiling point of water, 100°C ; (4) the normal boiling point of sulfur, 444.600°C .

Below 0°C, the Callendar-Van Dusen Equation is used to define the temperature:

$$t(^{\circ}\text{C}) = \frac{R_t - R_0}{\alpha R_0} + \delta \left(\frac{t}{100} - 1 \right) \frac{t}{100} + \beta \left(\frac{t}{100} - 1 \right) \left(\frac{t}{100} \right)^3 \quad (\text{B-1})$$

Above 0°C, the Callendar Equation is used:

$$t(^{\circ}\text{C}) = \frac{R_t - R_0}{\alpha R_0} + \delta \left(\frac{t}{100} - 1 \right) \frac{t}{100} \quad (\text{B-2})$$

The constants in the first equation are determined from the above four calibration points, and the constants in the second equation are determined from the last three points.

Certifications of Thermometers

As mentioned in Chapter III, two thermometers were used in the cryostat when the steady-state gradients were determined between the upper and lower ends of the Burnett cell. Each of these thermometers had been calibrated by the National Bureau of Standards. The thermometer which remained in the cryostat throughout the experimental phase of this work possessed the following values for the constants to be used in Equations B-1 and B-2:

Serial Number 1617523

Date of Calibration: May 17, 1963

$$\alpha = 0.0039266_{19}$$

$$\delta = 1.491_{36}^*$$

* Estimated value.

$$\beta = \begin{array}{ll} 0.110_{35} & (t \text{ below } 0^{\circ}\text{C}) \\ 0 & (t \text{ above } 0^{\circ}\text{C}) \end{array}$$

The thermometer which was used only for the determination of gradients was, at that time, calibrated only between 200 and -50°C , and only the constants α and δ were reported:

Serial Number 1628421

Date of Calibration: February 17, 1964

$$\alpha = 0.003926634$$

$$\delta = 1.49222$$

A later check with the NBS revealed that an approximate value of β could be obtained which should give the temperature within 0.005° to -183°C . This was based on the fact that the product $\alpha\beta$ is more constant, from one thermometer to the next, than either α or β , and approximately equal to 4.327×10^{-4} . Using this relationship and the reported value for α , the value for β was estimated to be 0.11020. A recalibration by NBS in January of 1966 reports the value of 0.11007 for β .

Ice Point Resistances: One value listed in the reports of calibration was not included above. In order that the reason for this omission may be understood more clearly, some comments are included from "Notes to Supplement Resistance Thermometer Certificates," which accompanied the reports of calibration from NBS.

The certificate for a resistance thermometer gives the constants, α and δ , which were found to apply to the resistor of that particular thermometer. Another constant, β , is given when temperatures below 0°C are to be determined. These constants are characteristic of the material in the particular resistor but do not depend on the magnitude of its resistance. To determine temperature with a platinum thermometer it is necessary to refer to some known and reproducible fixed temperature (fixed point) which is readily available whenever it is needed. This fixed temperature is most commonly the ice point, and a measurement of the resistance of the thermometer in a suitable ice bath will give R_0 . The value of R_0 is purposely given only approximately in the certificate, since precision temperature determinations with any thermometer should be based upon a value of R_0 determined from measurements with the bridge which is to be used.

Any known and reproducible fixed point, such as the triple point of water, may be used in place of the ice point. The choice of the fixed point will depend upon the accuracy and reproducibility of its temperature and upon the temperature range in which measurements are to be made. If a fixed point other than the ice point is used, a value of R_0 may be computed from the calibration constants of the thermometer and the measured resistance at the known temperature....

Certain precautions must be observed if reliable temperature determinations are to be made with a resistance thermometer.... It is important that the thermometer be protected from mechanical shocks which might produce some change in the characteristics of the wire in the platinum resistor. The characteristic constants of a thermometer may change as a result of changes in the dimensions of the wire, strains in the wire, or the subjection of the thermometer to excessive temperatures. If the measured resistance at a reliable fixed point is found to have changed by a significant amount after use and the change cannot be attributed to the bridge, recalibration of the thermometer is advisable.

With these points in mind, a review of the calibration history of the two thermometers is of interest.

The ice point resistance for the first of the two thermometers listed above was reported (NBS, May 1963) as

$$R_0 = 25.550 \text{ Abs. Ohms}$$

Following the preliminary work with temperature control in the empty cryostat, all the equipment (including this thermometer) was moved from the original laboratory to a new laboratory. Just before the actual data accumulation was started (June 1965), the triple point resistance of this thermometer was determined with a Trans-Sonics Equiphase Type 130 Triple Point of Water cell, serial number 52810. This measured triple point resistance was used to calculate R_0 , which was

$$R_0 = 25.5509 \text{ Bridge Units}$$

The relationship between absolute ohms and bridge units is discussed below.

The reported ice point resistance for the second of the two thermometers was first given as

$$R_0 = 25.5758 \text{ Abs. Ohms}$$

in the NBS calibration of February 1964. Measurement of the triple point resistance in this laboratory in June of 1965 yielded

$$R_0 = 25.5762 \text{ Bridge Units}$$

A second NBS calibration in January 1966 reported

$$R_0 = 25.5772 \text{ Abs. Ohms}$$

A measurement of the ice point resistance of the second thermometer was made in March 1966, by M. Y. Shana'a, of this laboratory. The resulting value was

$$R_0 = 25.5775 \text{ Bridge Units}$$

The triple point cell and the ice bath used in this laboratory were both prepared very carefully according to standard instructions, and the resistance measurements were reproducible to better than 0.0001 Bridge Units. These measurements were felt to be correct, so the following values of R_0 for the two thermometers were used:

$$\#1617523: \quad R_0 = 25.5509 \text{ Bridge Units} \quad (\text{B-3})$$

$$\#1628421: \quad R_0 = 25.5762 \text{ Bridge Units} \quad (\text{B-4})$$

The temperatures of the experimental cell were determined by relating the resistances at the given temperatures to these resistances at the ice point, using Equations B-1 and B-2.

Resistance Bridge

Equations B-1 and B-2 can be rearranged to show that temperatures can be determined with only ratios of resistances. The rearrangement of Equation B-2 yields

$$\frac{R_t}{R_0} = 1 + At + Bt^2 + C(t-100)t^3 \quad (\text{B-5})$$

where $A \equiv \alpha \left(1 + \frac{\delta}{100}\right)$

$$B \equiv -\alpha\delta/100^2$$

$$C \equiv - \alpha\beta/100^4$$

The rearranged form of Equation B-1 is the same as this, except with the constant C equal to zero. Thus it is seen that as long as the bridge used in the measurement is self-consistent, the units of resistance may be absolute ohms, international ohms, or any arbitrary unit.

The resistance bridge used in this work was tested by the Leeds & Northrup Company in February 1963, and a calibration certificate was issued which gave the corrections to be applied to the bridge readings in order to express the resistances in absolute ohms. At the time of the test, the corrections were sufficient for determining a resistance or a change in resistance greater than 1 ohm to about 2 parts in 100,000. A later check of these corrections in this laboratory showed no significant difference in the corrections reported by L&N and those determined later.

The "bridge unit" introduced above was arbitrarily defined as one-tenth of the sum of the resistance of the ten 1-ohm resistors in the 1-ohm decade. The relationship between one bridge unit and one absolute ohm was determined by comparison of the bridge with a standard resistor, Leeds & Northrup Number 8070-B, serial No. 1617199. The resistance of this standard resistor, as measured in February 1963, was 10.0100 ohms, specified to be accurate to 0.005 percent. When the comparison was made, the resulting relationship was

$$\text{One Bridge Unit} = 1.000014 \text{ Absolute Ohms} \quad (\text{B-6})$$

This is outside the accuracy of the calibrating resistor, and is therefore of little value for expressing the measured resistances of the thermometer in absolute ohms. The importance of the result is that future calibrations can be compared with this to assure no change in the characteristics of the bridge.

APPENDIX C

PRESSURE MEASUREMENT

The pressure measurements listed in Tables 2 - 7 represent pressures exerted by the gas in the experimental cell. Each of these values consists of not only the barometric pressure and the additional pressure imposed with a piston gage, but also corrections to account for difference in heights at different points of the pressure measuring system and for the behavior of the pressure null indicators in the system.

In order to isolate the experimental gas from the external pressure-measuring system, two diaphragm pressure null indicators were used. The cell of the first one was located in the cryostat and its diaphragm separated the experimental gas, which was a constant temperature, from the intermediate gas which led out of the cryostat to the second null indicator. The second diaphragm separated this intermediate gas from the oil used in the piston gages. A physical description of the two pressure null indicators has been presented in Chapter III. The nomenclature used for describing these indicators in the present work is also defined there, and information concerning sensitivities of the two null indicators is presented.

When a pressure measurement was made, the pressure of the gas in the Burnett cell was not transmitted directly to the piston gage. The most obvious reason for this was the difference in heights of the cell and the gage. Another reason which was less obvious was the existence of a slight pressure differential across the diaphragm of each of the pressure null indicators when the indicator meter was at the null position. This pressure difference, which has been called the "zero shift," will be discussed thoroughly at the end of this appendix. The essential point to be mentioned here is that the zero shift was found to be a function of both pressure and temperature. The magnitude of the zero shift was a small percentage of the total pressure, but all of the experimental pressures were corrected to account for it.

The difference in height between different points of the system contributed a pressure effect because of the density of the fluids in the lines of the pressure system.

The total pressure of the gas in the Burnett cell is expressible as the sum of all the above-mentioned parts,

$$P = P_G + P_B + \Delta P_H + \Delta P_{ZSR} + \Delta P_{ZSC} \quad (C-1)$$

where P is the total pressure exerted by the gas, P_G is the pressure exerted by the piston gage, P_B is the barometric pressure acting on the piston, ΔP_H is the sum of the static head pressures, and ΔP_{ZSR} and ΔP_{ZSC} are the zero shifts for the room-temperature and the cryogenic pressure null indicators.

In the following paragraphs these component parts of the total pressure measurement are discussed individually. Reference should be made to Figure 8 in Chapter III for best understanding.

Piston Gage Pressure Measurements

When a piston gage is in equilibrium with a pressure system, the pressure, P_G , measured at the piston gage reference level is

$$P_G = F_e/A_e \quad (C-2)$$

where F_e = the effective force due to the weight load
on the piston

A_e = the effective area of the piston.

For accurate determinations of pressure, several variables affecting the weight load and the piston area must be taken into account. Obvious sources of error are those arising from the uncertainty of the masses of the loading weights and the measurement of the area of the piston-cylinder combination. Other sources include the effects of thermal expansion and elastic deformation of the piston and cylinder, fluid buoyancy on the piston, the value of local gravity, and the fluid heads involved. These effects and others of smaller magnitude are discussed in the National Bureau of Standards Monograph 65 (14).

The corrections applied in this section are those concerned with temperature, pressure, gravity, and fluid

heads. Uncertainty in the masses of the weights and in the measured cross-sectional area of the piston are also discussed.

Effective Piston Area

According to Equation C-2, a change in the total weight load would be expected to cause a proportionate change in the total pressure. This does not occur, however, in a piston gage, because a change of pressure causes a change in the effective area of the piston. Moreover, the piston area also changes with temperature. Thus both temperature and pressure must be considered when the pressure exerted by a piston gage is to be determined.

Temperature and Pressure Effects: In accordance with the instructions in the test report accompanying the piston gages, the effective area of the piston-cylinder combination was calculated by means of the relation

$$A_e = A_{0,25} (1 + C\Delta T)(1 + bP) \quad (C-3)$$

where A_e = the effective area at the working pressure and temperature

$A_{0,25}$ = the effective area at atmospheric pressure and 25°C, indicated in the test report

C = the coefficient of superficial expansion, indicated in the test report

ΔT = the difference between the working temperature and 25°C

b = the fractional change in area per unit change in pressure, indicated in the test report

T = the working temperature of the piston gage

P = the operating pressure of the piston gage

Piston Gage Area Calibration: A large part of the uncertainty in the pressure measurements with a piston gage arises from the uncertainty of the effective area of the piston-cylinder assembly of the gage. Several methods are available for determining this area. Canfield (6) discussed four methods for determining it, and obtained areas by three of those methods. First, he measured the vapor pressure of CO_2 at 0°C ; second, he obtained direct measurements of the diameter profile of the cylinder; third, he arranged to have his gage calibrated against a set of piston gages which had been calibrated at the National Bureau of Standards. Quite understandably, he did not calibrate the gage by comparison with a mercury column several meters high. On the basis of Canfield's calibrations by three different methods, he concluded that the NBS calibration was probably the most accurate, and he used the results of that calibration for the calculation of his experimental pressures.

Both of the piston gages used in the present work were calibrated against the same set of piston gages that had been used to calibrate Canfield's gages. The areas calculated from these calibrations were assumed to be the most accurate values possible at the present time, so no further calibrations were made. Those areas were then used in the calculations of the experimental pressures.

Results of these calibrations are presented in Table C-1. These areas are the ones substituted into Equation C-3 as $A_{0,25}$, the area at atmospheric pressure and 25°C.

TABLE C-1
INSTRUMENT CONSTANTS FOR PISTON GAGES¹

	High Pressure Gage	Low Pressure Gage
Effective Area at Atmospheric Pressure and 25°C, square inches	0.0260430	0.130220
Coefficient of Superficial Thermal Expansion, (°C) ⁻¹	1.7×10^{-5}	1.7×10^{-5}
Fraction Change of Area per Unit Change of Pressure, (psi) ⁻¹	-3.6×10^{-8}	-4.8×10^{-8}
Resolution ²	< 5 PPM	< 5 PPM
Plane of Reference	0.04 inch below line on sleeve weight	0.10 inch below line on sleeve weight

¹This calibration was made by intercomparing the above piston gages with Ruska Instrument Corporation Laboratory Master Dead weight Gage No. 7544, which has been calibrated by the National Bureau of Standards. The piston area is reported by the National Bureau of Standards to be correct to one part in 10,000 at 25°C.

²Resolution is defined as the smallest change in the weight load on the test gage that will produce a measurable change in the equilibrium condition of the two gages. The numerical value of resolution is expressed as the ratio of change in mass to the total mass.

Piston Gage Weights

The effective force F_e (Equation C-2) on the piston gages was applied with calibrated stainless steel weights. The weights were calibrated by the manufacturer by comparison with another set of weights which had been calibrated against Class S standards*. Results of the calibration are presented in Table C-2. The values for "tare low" and "tare high" are the weights of the piston assemblies in the two piston gages. Division of the tare weight by the effective piston area yields the tare-pressure--the minimum pressure which the gage is capable of measuring.

Buoyancy: The heading "Apparent Mass vs Brass" in Table C-2 indicates that the masses listed in that column are those which the weights appear to have when compared against normal brass standards in air under normal conditions, with no correction being made for the buoyant effect of air. The masses used for the brass standards are their true masses, however, so an air buoyancy correction must be made to account for this fact. This correction was made for air having a density of 1.2 mg/cm^3 and brass having a density of 8.4 gm/cm^3 . Using these values, the weight in air was found to be

$$W = \left(1 - \frac{0.0012}{8.4}\right) \frac{g}{g_c} M_A \quad (\text{C-4})$$

where W = weight in air at local gravity

*A National Bureau of Standards Classification; see NBS Circular 547.

TABLE C-2
 CALIBRATION DATA FOR PISTON GAGE WEIGHTS

Weight Letter Designation	Apparent Mass vs Brass (M_A), Pounds
A	26.03576
B	26.03564
C	26.03567
D	26.03569
E	26.03575
F	26.03500
G	26.03511
H	26.03504
I	26.03513
J	26.03543
K	26.03552
L	13.01812
M	5.20716
N	5.20718
O	2.60351
P	1.30167
Q	0.52073
R	0.52075
S	0.26034
T	0.13018
U	0.05207
V	0.05206
W	0.02603
X	0.01302
\bar{A}	0.00521
\bar{A}	0.00521
\bar{B}	0.00260
\bar{C}	0.00130
Tare High	0.78104
Tare Low	0.78107

g = local gravity

g_c = dimensional constant

M_A = apparent mass determined in the calibrations

Gravity: The value of the force exerted by a given mass is dependent on the local value of gravity, which varies over the surface of the earth. The value chosen for local gravity in the present calculations was*

$$g = 979.7608 \text{ cm/sec}^2$$

When this value for local gravity is divided by the dimensional constant g_c expressed in units of standard gravity, the correction factor to be applied to the piston gage weights and the barometric reading is seen to be

$$\frac{g}{g_c} = \frac{979.7608}{980.665} = 0.999078$$

Substitution of this value into Equation C-4 yields the relationship used in calculating the weight load on the piston gages for given combinations of the calibrated weights.

$$W = \left(1 - \frac{0.0012}{8.4}\right) (0.999078) M_A$$

$$= 0.998935 M_A$$

(C-5)

* Personal Communication: Prof. J. A. E. Norden, School of Geology, University of Oklahoma.

If the piston gage is leveled so that this weight load is applied perfectly vertically on the piston-cylinder area, the weight load will be the effective force F_e of Equation C-2.

Barometric Pressure

The barometric pressure was determined with a marine barometer which had been calibrated in 1962. The scale on the barometer could be read to 0.002 inches by means of a vernier. A gimbal joint supporting the barometer eliminated the necessity of leveling the instrument. The temperature of the mercury column was determined by a thermometer which was mounted near the middle of the barometer.

Temperature and gravity corrections were made to express the direct reading in international atmospheres, or the pressure exerted by 760 mm of mercury at 0°C and standard gravity. The temperature corrections were obtained from a table supplied by the manufacturer, and the gravity correction was the same as was used in the piston gage weight calculations.

The direct reading from the barometer and the temperature correction to that reading were in inches, so that the temperature-corrected reading was divided by the inch equivalent of 760 mm, or 29.9213 inches. Thus the corrected barometric pressure in international atmospheres was

$$\begin{aligned}
 P_B &= (R-r) \frac{0.999078}{29.9213} \\
 &= 0.0333902 (R-r) \qquad \qquad \qquad (C-6)
 \end{aligned}$$

where P_B = barometric pressure, int. atm
R = barometer reading, inches
r = correction which reduces the mercury column height at room temperature to the equivalent height at 0°C.

Head Pressure Corrections

The total contribution of head pressure to the reported pressures was made up of a number of components. Figure 8 indicates the sources of the head corrections. The line between the piston gages and the room-temperature pressure null cell was filled with oil. The line between this cell and the one in the cryostat was filled with gas of the same composition as that inside the Burnett cell. The portion of this gas in the line outside the cryostat was at one density, and that inside the cryostat was at another. At some conditions, the density of the gas in the Burnett cell was great enough to necessitate consideration of the height of the cell.

The reference level for all of the head corrections was picked to be the height of the diaphragm in the room-temperature pressure null cell. The location of this diaphragm was indicated by a scribe mark on the outside of the cell. The principal reason for picking this particular reference level was that the pressure null cell was firmly attached to the instrument table at a point which did not flex noticeably when the pressure gages were loaded with

their weights. The scribe mark was easily seen from a point where all the other components could also be seen.

Piston Gage Oil System

In this discussion, the piston gage oil system includes all of the components of the pressure measurement system from the piston gage to the diaphragm of the room-temperature pressure null cell. Head corrections in this part of the total system must take into account the location of the reference plane of each of the piston gages and the height of the oil manometer scale zero in relationship to the reference level indicated by the scribe mark on the pressure null cell.

Reference Plane of Piston Gage: The pressure indicated by a piston gage is valid at only one point, called the reference plane. The pressure at any other point in the system must be determined by measuring the vertical distance of the other point from the reference plane of the gage. All points higher in elevation than those of the reference plane will have a pressure less than the indicated pressure at the reference plane by an amount equal to the difference in elevation multiplied by the density of the oil. The density of oil in the gage system is approximately 0.85 gm/cc, which corresponds to a pressure gradient of 0.031 psi for each inch of vertical dimension of the system. This concept is no different from normal hydraulic head effects, but it is mentioned here because it is not quite as obvious as the more usual corrections.

The location of the plane of reference for the piston gage is determined from the dimensions of the submerged portion of the piston. The pistons of the two gages used in this work had an enlarged section submerged in the fluid, so that the reference plane of the gage was determined by dividing the volume of the enlarged section by the piston and adding the result to the bottom of the piston as an increased length.

The reference plane of each of the piston gages was related to the remainder of the system by means of a post mounted on the base plate of the gage. This post had an index line on it, and the sleeve weight of the gage also had an index line around its circumference. When the index line of the sleeve weight and that of the post coincided during the slow fall of the piston, the reference plane of the piston was referenced directly to the system.

This reference plane's location is indicated in Table C-1, for each of the two gages. The indication that the plane of reference for the high pressure gage is 0.04 inch below the index line on the sleeve weight simply means that the pressure indicated by the piston gage (P_G of Equations C-1 and C-2) is valid only at that point. Thus by measuring the heights of all other components in the pressure measurement system, relative to the index line of the post attached to the base of the gage, the components may be related directly to the reference plane of the piston.

Oil Manometer Scale Zero: An oil manometer which was included in the piston gage oil system allowed the null point of the room-T PNI to be checked before each run, and between expansions within a run if necessary. With reference to Figure 8, this manometer had a movable scale attached to it which could be adjusted so that the zero mark of the scale would be in the same horizontal plane as the scribe mark of the room-T PNC. With the scale adjusted in this manner, the valve between the manometer and the remainder of the oil system could be opened and the oil level adjusted to the scale zero to apply atmospheric pressure above the diaphragm of this cell. At the same time, the vent valve in the line below the diaphragm could be opened so that atmospheric pressure would be applied below the diaphragm.

When the oil manometer was zeroed and the vent valve opened as described, the diaphragm had a zero pressure differential across it at atmospheric pressure. The PNI readout was then set at a null meter reading. Whenever a null reading of the indicator was obtained at any other pressure, the pressure difference across the diaphragm was equal to the zero shift, which is discussed later in this appendix.

During the early stages of this experimental work, the manometer scale was adjusted to approximate height required for its zero mark to be aligned with the PNC scribe

mark. The ease of making an exact adjustment of the scale, compared with the later nuisance of making a head correction because of different heights of the manometer scale zero and the PNC scribe mark, was not fully appreciated. Consequently, these two levels (h_{OM} and h_D of Figure 8) differed by 0.05 cm, causing a head correction of 4.2×10^{-5} atm which had to be applied to all of the pressure measurements. As a matter of convenience, these two levels should be made exactly equal if possible.

Combined Hydraulic Head Effects: The total hydraulic head correction in the piston gage oil system was composed of three parts: (1) the pressure difference due to the difference in the height of the PNC scribe mark and the index line on the post of the piston gage base; (2) the pressure difference due to the difference in height of this index line and the reference plane of the piston gage; (3) the "zero correction" caused by the difference in level of the PNC scribe mark and the oil manometer level when the pressure null indicator was zeroed.

The pressure effect of a hydraulic head can be represented by the following equation:

$$P_h = \rho_i h_i (g/g_c) \quad (C-7)$$

where P_h is the pressure effect, ρ_i is the fluid density, and h_i is the height of the hydraulic head. Using the nomenclature of Figure 8, the correction necessary to account for the hydraulic head is thus

$$\Delta P_H' = \rho_{oil} (g/g_c) [(h_{PGR} - h_{PGI}) + (h_{PGI} - h_D)] \quad (C-8)$$

where $\Delta P_H'$ = hydraulic head correction

h_{PGR} = relative height of piston gage reference plane

h_{PGI} = relative height of piston gage index mark

h_D = relative height of diaphragm (chosen as 0.0)

g = local acceleration of gravity

g_c = dimensional conversion constant

ρ_{oil} = density of oil

The zero correction of the oil manometer is, in a similar manner,

$$\Delta P_Z = \rho_{oil} (g/g_c) (h_{OM} - h_D) \quad (C-9)$$

where ΔP_Z = zero correction

h_{OM} = relative height of meniscus of oil manometer when pressure null indicator is zeroed

The effective hydraulic head is equal to the hydraulic head represented by Equation C-8 minus the zero correction,

$$\Delta P_{H-Z} = \Delta P_H' - \Delta P_Z \quad (C-10)$$

When Equations C-8 and C-9 are substituted into Equation C-10, the effective hydraulic head is obtained as

$$\Delta P_{H-Z} = \rho_{oil} (g/g_c) [(h_{PGR} - h_{PGI}) + (h_{PGI} - h_D) - (h_{OM} - h_D)] \quad (C-11)$$

The value for the difference $h_{PGR} - h_{PGI}$ is given in the test report for the piston gages; from Table C-1 the value is seen to be -0.04 inch for the high pressure gage and -0.10 inch for the low pressure gage. A measurement of $h_{PGI} - h_D$ with a cathetometer showed its value to be -0.15 cm for the high pressure gage and -0.44 cm for the low pressure gage. Incidentally, these values changed only insignificantly as the piston gages were loaded. The value of $h_{OM} - h_D$ was 0.05 cm. When these values were substituted into Equation C-11, the results were:

for the high pressure gage ($P > 2400$ psi),

$$\Delta P_{H-Z} = -0.00025 \text{ atm} \quad ; \quad (C-12)$$

for the low pressure gage ($P < 2400$ psi),

$$\Delta P_{H-Z} = -0.00061 \text{ atm} \quad (C-13)$$

Each of the experimental pressure measurements was corrected by the proper amount to account for this hydraulic head effect in the piston gage oil system. The result obtained was the pressure exerted on the top of the diaphragm of the room-temperature pressure null cell. Obtaining the actual pressure of the gas in the Burnett cell required further consideration of both the zero shift for each pressure null cell and the static head of the gas in the tubing between them.

Gaseous Head Corrections

As mentioned earlier, the term "intermediate gas" is the name applied to the gas contained in the tubing between the two pressure null cells. This gas was always of the same composition as the gas in the Burnett cell. As the pressure in the lines changed during a run, the density of the intermediate gas changed correspondingly, and the head correction to be applied to the pressure measurement therefore changed. As the control temperature inside the cryostat changed, the same density and head correction changes occurred. As a consequence, the head corrections in this part of the pressure measurement system varied both with temperature and with pressure. This is the reason for treating the gas head corrections separately from the head corrections in the oil system, which were constant.

Intermediate Gas: Head corrections for the intermediate gas must be divided into two parts because of the temperature difference between the inside of the cryostat and the outside. The density of the gas in the line outside the cryostat is assumed to be the density of that gas at room temperature (approximately 23°C) and at the experimental pressure P_j . For the immediate purpose, the gas inside the cryostat is assumed to be of the same density from the top of the cryostat to the bottom of the cell, that density being equal to the density obtained for the gas by a treatment of the data without head corrections, at the experimental control temperature in the cryostat.

The important difference in level that must be considered in treating the intermediate gas head corrections is $(h_C - h_D)$ (Figure 8), the difference in height between the top outer surface of the cryostat and the diaphragm in the pressure null cell. That height difference was 120 cm.

Gas in the Cryostat: The head correction for the gas in the cryostat could be made without regard to the presence of the diaphragm in the cryogenic pressure null cell, because the densities above and below were assumed to be equal. The only remaining problem was then one of determining the proper level in the Burnett cell to account for head differences in the experimental gas. This level was picked as the level of average density inside the pressure bomb, assuming the density to vary linearly with height. Before the first expansion, this height was in one place, and on all succeeding pressure measurements it was lower because of the presence of gas in both cells after the first expansion. Thus the proper differences $(h_C - h_{B_0})$ and $(h_C - h_{B_j})$ (Figure 8) were found to be 59.7 cm and 63.4 cm.

Total Gas Head Corrections: When the head corrections are expressed according to Equation C-7, the total correction for the gas head is

$$\Delta P_{gh} = (g/g_C) [(\rho_g)_o (h_D - h_C) + (\rho_g)_i (h_C - h_B)] \quad (C-14)$$

where ΔP_{gh} = total gas head correction

$(\rho_g)_o$ = density of gas outside the cryostat, at
room temperature and experimental pressure

- $(\rho_g)_i$ = density of gas inside the cryostat, at the experimental temperature and pressure
- h_D = relative height of room-T PNC diaphragm
- h_C = relative height of top surface of cryostat
- h_B = relative height of the location of average density in the Burnett cell; h_{B_0} before the first expansion and h_{B_j} for each successive measurement.

Substitution of the appropriate values in the expression, with the correct conversion of units, yields the following results:

Before the first expansion in a run:

$$\Delta P_{gh} = (\text{M.W.}) [(-0.116)(\rho_g)_o + (0.0578)(\rho_g)_i] \quad (\text{C-15})$$

For all subsequent measurements in a run:

$$\Delta P_{gh} = (\text{M.W.}) [(-0.116)(\rho_g)_o + (0.0613)(\rho_g)_i] \quad (\text{C-16})$$

where ΔP_{gh} = gas head correction, atm

M.W. = molecular weight of the gas mixture in the system during the run, gm/g-mole

ρ_g = density of the gas mixture as specified above, g-moles/cc

Combined Hydraulic and Gas Head Corrections

The total head correction (ΔP_H of Equation C-1) is found by combining Equations C-12, C-13, C-15, and C-16.

The result is:

before the first expansion of a run,

$$\Delta P_H = -0.00025 + (\text{M.W.})[(-0.116)(\rho_g)_o + (0.0578)(\rho_g)_i] \quad (\text{C-17})$$

for subsequent measurements with the high-pressure gage,

$$\Delta P_H = -0.00025 + (\text{M.W.})[(-0.116)(\rho_g)_o + (0.0613)(\rho_g)_i] \quad (\text{C-18})$$

for subsequent measurements with the low-pressure gage,

$$\Delta P_H = -0.00061 + (\text{M.W.})[(-0.116)(\rho_g)_o + (0.0613)(\rho_g)_i] \quad (\text{C-19})$$

- where ΔP_H = total combined head correction in the
pressure measurement system, atm
- M.W. = molecular weight of the gas in the system
during the pressure measurements, gm/g-mole
- $(\rho_g)_o$ = density of the gas in the lines outside the
cryostat, g-moles/cc
- $(\rho_g)_i$ = density of the gas in the system inside the
cryostat, g-moles/cc

Zero Shift Corrections

Part of the procedure that was followed before beginning any experimental run was the zeroing of the pressure null indicators. Except for a slight head correction (explained in the previous section) necessitated by the misplacement of the oil manometer scale, the room-T PNI could be zeroed at atmospheric pressure by means of an oil manometer in the system above the diaphragm, and a vent valve in the lines below it. This could be done without contaminating the system with air.

Zeroing of the cryo-PNI was accomplished by opening the charge valve and the other valve between the lower and upper chambers of the null cell in the cryostat (Figure 2). As described in Chapter IV, this was done only after the Burnett cell had been evacuated and purged, the cryostat temperature stabilized, and the final adjustments to the circuitry of the electronic null indicator made. In order to prevent contamination of the study gas, the Burnett cell was never vented completely down to atmospheric pressure for the zeroing, but rather, a gage pressure of a few psi was maintained. Thus the zeroing pressure was only approximately atmospheric.

Whenever the proper pressure balance had been made for the null indicators, their meters were adjusted to the null position. The hopeful extension of this zeroing procedure would be the expectation of a null reading for the same pressure balance at any other pressure. Unfortunately, this was not the case. When the meter had been nulled at the low pressure, an increase of pressure caused it to indicate a pressure unbalance even when the pressure differential across the diaphragm was exactly zero. This effect has been called the "null-point shift," or "null shift" by Canfield (6), and will be called that in this discussion.

In order to get a null reading on the meter it was then necessary to apply a slight excess of pressure on the

appropriate side of the diaphragm to return the meter to a null position. The amount of this pressure excess has been called the "zero shift," and is defined by the equation

$$\Delta P_{ZS} = P_L - P_U \quad (C-20)$$

where ΔP_{ZS} = zero shift at meter null
 P_L = pressure in lower chamber of PNC at meter null
 P_U = pressure in upper chamber of PNC at meter null

Significance of Zero Shift

The existence of this zero shift was significant not only because of the correction that had to be made in the pressure measurements, but also because the position of the diaphragm was different at different pressures when the meter null was obtained. Such changes of position of the diaphragm in the cryo-PNC caused volume changes which had to be taken into account in the calculation of the effect of pressure on the cell constant.

The test report accompanying each of the pressure null indicators included a graphical representation of the relationship between zero shift and total pressure. According to the comments by Claude Miks (37), these curves had been obtained by a somewhat indirect method. First, the sensitivity of each PNI was determined at atmospheric pressure. Following an adjustment of the meter to obtain a null reading at atmospheric pressure, the pressure in the PNC was then increased stepwise to a maximum of 10,000 psi, always

maintaining a pressure balance across the diaphragm. At each of these steps, the microamp output of the electronic null indicator was measured. These values were then multiplied by the sensitivity in psi/microamp (determined at atmospheric pressure) to get corresponding values of pressures which were called the zero shift values for those pressures.

The microamp output was actually a measure of the null-point shift rather than the zero shift because it was made with zero pressure differential across the diaphragm. Thus it was an indirect measurement of the zero shift and could be called the zero shift only by making the assumption that the sensitivity of the PNI remained constant with changing pressure.

Although the present experimental equipment could not be used to make direct measurements of sensitivity at pressures other than atmospheric, the sensitivity of the room-T PNI appeared, during the pressure-measuring phases of the experimentation, to be essentially the same at all pressures. Therefore, the relationship between zero shift and total pressure that was reported by Ruska was accepted as the true behavior for this unit:

$$\Delta P_{ZSR} \approx 1.91 \times 10^{-6} P \quad (C-21)$$

where ΔP_{ZSR} and P are in consistent units, e.g., atm.

For the cryo-PNI, however, Ruska's reported curve could not be used because the sensitivity was found to

change slightly with temperature, and their curve had been based on the sensitivity at room temperature. Thus it was necessary to make measurements of the zero shift as a function of pressure at each of the three experimental temperatures.

Measurement of Zero Shift

The zero shift measurements were made by what might be thought of as a backwards technique. No measurements were ever made of the actual zero shift, which was earlier seen to be the pressure difference across the diaphragm at a meter null. Instead of direct measurement, an indirect method was used: (1) measure the pressure above (and below) the diaphragm at an exact pressure balance; (2) close the external valve between the upper and lower chambers of the PNC; (3) measure the pressure above the diaphragm at a meter null.

The results of these measurements indicated zero shift values greatly exceeding those reported by Ruska, sometimes by as much as a factor of forty. At -50°C , not only were the measured values large, but also they were of opposite algebraic sign. During an attempt to verify these results by repeating the measurements, a composition dependence of the measured values soon became apparent. The values obtained with pure argon in the system were much larger than those obtained with pure helium, and with a mixture of 78% argon-22% helium the values were intermediate.

This composition dependence of the measured zero shift eventually led to the explanation of the discrepancy between the measured values and Ruska's reported values.

The essential point on which the analysis was based was the fact that, for any finite volume connected to the lower chamber of the PNC, a movement of the diaphragm would cause a change of pressure of the gas in that volume. The Burnett cell's upper volume had been connected to the lower chamber of the PNC during these zero shift measurements; thus the pressure change in the Burnett cell caused by a movement of the diaphragm during the adjustment of the intermediate gas pressure (to give a null reading) caused the cell pressure at null to be different from the cell pressure at balance. The extent of this pressure change below the diaphragm was related not only to the total volume below the diaphragm and the pressure change above it, but also to the "stiffness" of the diaphragm and the volumetric properties of the gas in the volume below it.

Although the procedure for back-calculating the actual zero shift from the measured zero shift was fairly straightforward, it can be understood more easily with the help of a few of the more important equations involved. The first of these equations was obtained by relating the actual zero shift (Equation C-20) to the measured or known quantities mentioned above.

$$\Delta P_{ZSC} \equiv (P_L - P_U)_n \quad (C-22a)$$

$$\Delta P_{ZSC} = (P_L)_n - (P_L)_b + (P_L)_b - (P_U)_n \quad (C-22b)$$

$$= (P_n)_L - (P_b)_L + (P_b)_L - (P_n)_U \quad (C-22c)$$

$$= (P_n - P_b)_L + (P_b - P_n)_U \quad (C-22d)$$

$$= \Delta P_{dm} + M.Z.S. \quad (C-22e)$$

where ΔP_{ZSC} = Actual zero shift for the cryogenic pressure null indicator

$(P_L)_n \equiv (P_n)_L$ = pressure in the lower chamber at null

$(P_L)_b \equiv (P_b)_L$ = pressure in the lower chamber at balance

$(P_U)_n \equiv (P_n)_U$ = pressure in the upper chamber at null

$(P_U)_b \equiv (P_b)_U$ = pressure in the upper chamber at balance

ΔP_{dm} = pressure change below diaphragm due to diaphragm movement

M.Z.S. = Measured zero shift

This equation shows that the only thing needed for determining the actual zero shift from known values of the measured zero shift was the pressure change in the volume connected to the lower chamber of the cryo-PNC. This pressure change, ΔP_{dm} , depended on the deflection of the diaphragm, which in turn was related to the magnitude of the actual zero shift.

For the relationship between the actual zero shift and the diaphragm deflection, the results given by Canfield

(6) were used. Canfield determined the amount of diaphragm deflection that would occur when a pressure difference was applied across the diaphragm at atmospheric pressure. His results were expressed by

$$\Delta P_{ZS} \approx 9d \quad (C-23)$$

where d = diaphragm deflection, inches

ΔP_{ZS} = corresponding pressure difference across
the diaphragm, atmospheres

The volume change corresponding to a deflection d was estimated by making two assumptions: (1) at a pressure balance, the diaphragm is perfectly flat; (2) when a pressure difference is applied across the diaphragm, it will deform into a spherical segment of height d . With these assumptions, the volume change could then be expressed as

$$\Delta V_{dm} = (\pi d/6) (3r^2 + d^2) \quad (C-24)$$

where ΔV_{dm} = change of volume due to diaphragm movement

d = deflection of diaphragm

r = effective free radius of diaphragm

The effective radius of the diaphragm was 1.00 inch and the deflection was never more than 0.015 inches (maximum cavity depth on either side of diaphragm), so d^2 could be neglected in comparison with $3r^2$. The equation could thus be simplified to

$$\begin{aligned} \Delta V_{dm} &\approx \pi r^2 d/2 \\ &\approx 1.571 d \end{aligned} \quad (C-25)$$

where ΔV was in cubic inches and d was in inches. Combination of Equations C-23 and C-25 then gave the relationship between the actual zero shift at a meter null and the volume change caused by deflection of the diaphragm as the pressure above the diaphragm was adjusted to obtain that null.

$$\Delta V_{dm} \approx (0.1745) (\Delta P_{ZSC}) \quad (C-26)$$

where ΔP_{ZSC} is expressed in atmospheres.

The principal problem remaining was to relate the pressure change inside the Burnett cell, ΔP_{dm} , to ΔV_{dm} and the volumetric properties of the gas in the cell during the zero shift measurements. Fortunately, the early measurements had shown that if the adjustment of the external pressure was made in just a few seconds, the measured zero shift values were quite reproducible; a delay of a few seconds, however, caused problems that were apparently due to the transfer of heat between the gas and the cell. All further measurements were made as rapidly as possible, and as a result, the analysis of the problem could be simplified by the assumption that the actual change of pressure in the cell could be approximated satisfactorily by an adiabatic reversible change.

As a consequence of this assumption, the pressure change in the cell could be related to the volume change.

$$\Delta P_{dm} \approx \left(\frac{\partial P}{\partial V} \right)_S \Delta V_{dm} \quad (C-27)$$

where ΔV_{dm} = change in specific volume of the gas in the cell during the expansion.

The number of moles of gas in the cell remained constant during the change, so that ΔV_{dm} was simply $(1/n)(\Delta V_{dm})$, or $(V/V)(\Delta V_{dm})$. Introduction of Equation C-26, along with the value of 10.4 in^3 for the volume below the diaphragm, then yielded the equation

$$\Delta V_{dm} = \frac{0.1745 (\Delta P_{ZSC})}{10.4/V} \approx 0.0168 \underline{V} (\Delta P_{ZSC}) \quad (C-28)$$

which could be substituted back into Equation C-27 to give

$$\Delta P_{dm} \approx 0.0168 \underline{V} \left(\frac{\partial P}{\partial V} \right)_S (\Delta P_{ZSC}) \quad (C-29)$$

The partial derivative in this equation was expressed in terms of measurable properties and the resulting expression was applied in Equation C-22e. That equation was then rearranged to give the final form which was used in calculating the actual zero shift values from the measured values.

$$\Delta P_{ZSC} \approx \frac{\text{M.Z.S.}}{1 + .0168 \underline{V} \left[\frac{\frac{C_P}{T} \left(\frac{\partial T}{\partial V} \right)_P}{\frac{C_P}{T} \left(\frac{\partial T}{\partial P} \right)_V - \left(\frac{\partial V}{\partial T} \right)_P} \right]} \quad (C-30)$$

where the unit of pressure is atmospheres.

The curves of actual zero shift versus pressure at the three experimental temperatures were calculated in this way, for the three compositions used. The results of the

corrections are shown in Figure C-1, along with the curve reported by Ruska. A temperature dependence is obvious, and even though the evaluation of some of the thermodynamic quantities was only approximate (11,15), the agreement among all the measurements at a single temperature is quite acceptable when considered as a percentage of the total pressure. As would be hoped, Ruska's curve, which was determined at room temperature, falls between the curves for 0° and 50°C. A possible reason for the difference in curvature in the high-pressure region might be a change in sensitivity of the PNI with pressure, which would modify Ruska's curve.

As a close look at Figure C-1 will show, the final results for actual zero shift versus pressure are of interest principally because of their existence and not because of their magnitude. At 0 and -50° the actual zero shift never exceeds a part in 500,000 of the total pressure, and at 50° it is always less than a part in 250,000. Pressure corrections to account for zero shift are therefore almost meaningless, but corrections for volume changes of the Burnett apparatus due to diaphragm distortion are important compared with other, much less certain, estimates of pressure deformation of the remaining equipment.

Even though the zero shift corrections were small, all of the experimental pressures were still corrected to account for zero shift. The corrections for the room-T PNI were determined according to Equation C-21, and those

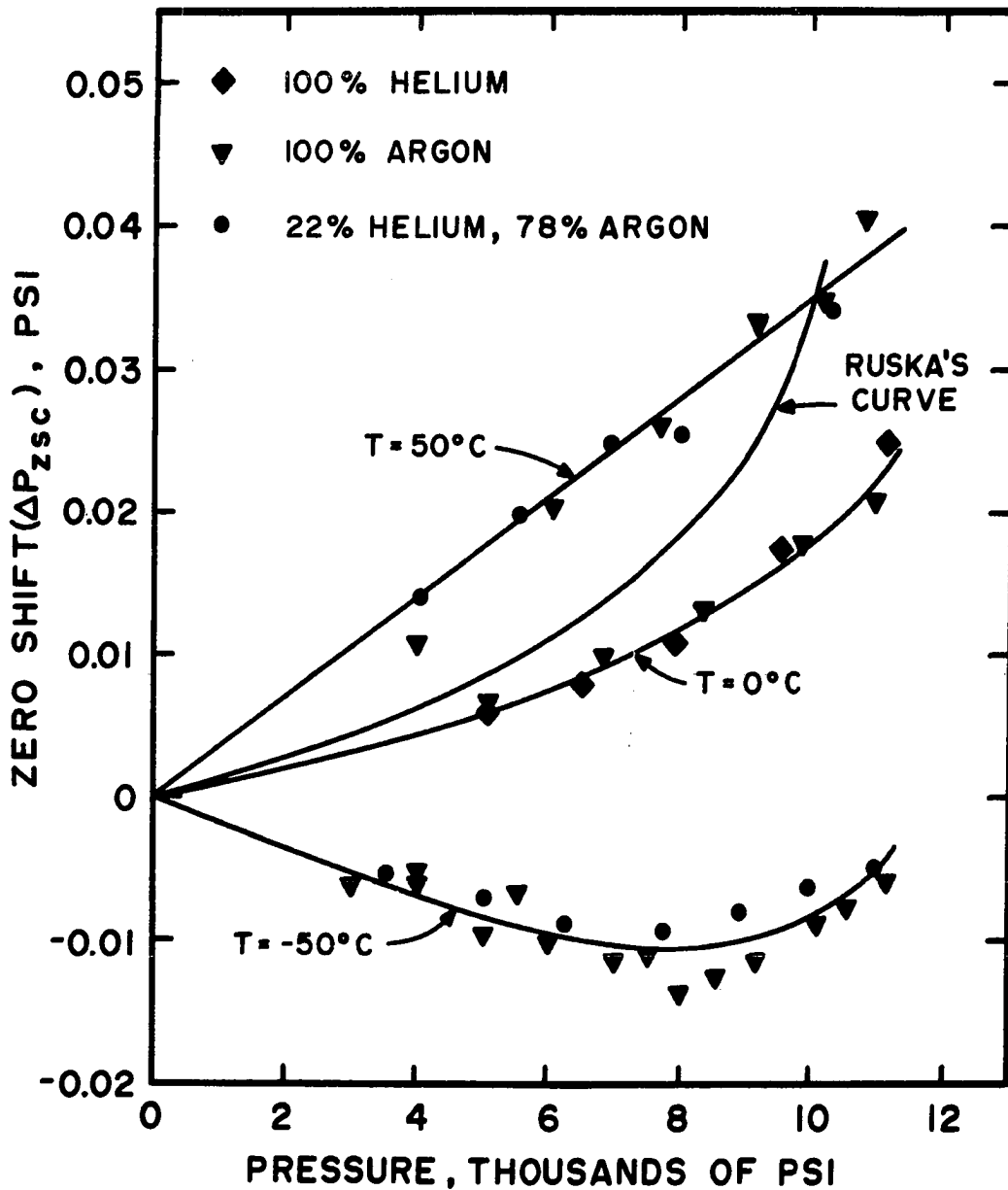


Figure C-1. Zero Shift of Cryogenic Pressure Null Indicator as a Function of Pressure for Three Temperatures. Room-Temperature Curve Presented by Ruska is Included for Comparison.

for the cryo-PNI were taken from the smooth curves of Figure C-1. Approximate equations for these curves were used for calculating volume changes in the Burnett apparatus caused by deflection of the cryo-PNI diaphragm. These are presented in Appendix D.

As an interesting sidelight, the question of determining the sensitivity of the PNI at high pressure should be raised. During the actual phases of data accumulation in this work, the behavior of the PNI indicated a decrease of sensitivity with increasing pressure. This apparent decrease was determined by balancing the pressures to get a null reading on each of the PNI's, and then incrementing the weights on the piston gage by a very small amount to get a change in the cryo-PNI reading while holding the room-T PNI at null. A similar technique has been reported recently by Hoover (26). In light of the above discussion showing the relationship between measured zero shift and actual zero shift, this method of determining sensitivity is clearly seen to be misleading unless the results are carefully analyzed and interpreted. In any case, the measured sensitivities will always be worse than the actual ones for the same reasons mentioned in the zero shift discussion.

Summary

The pressure exerted by the gas inside the Burnett cell was determined by measurement of the gage pressure with a piston gage, measurement of the barometric pressure with

a marine barometer, and corrections to account for static head effects and zero shifts of the two pressure null indicators. Some of these corrections were very small in magnitude, but were still considered in the treatment of the data.

APPENDIX D

EFFECT OF PRESSURE ON THE CELL CONSTANT

One of the quantities which arises repeatedly in the treatment of Burnett data is often called the cell constant or apparatus constant N_j , which was defined earlier by Equation 7:

$$N_j \equiv \frac{(V_a + V_b)_j}{(V_a)_{j-1}} \quad (7)$$

In this equation V_a represents the total volume occupied by the gas before an expansion, and $V_a + V_b$ is the total volume occupied by the same amount of gas following the expansion. These volumes include not only the internal volumes of the two cells of the Burnett pressure bomb, but also the internal volume of the expansion valves, the tubing, the magnetic pump used to circulate the gas, and the lower cavity of the pressure null indicator cell in the cryostat.

Treatment of the Burnett data yields the zero-pressure cell constant N_∞ , where the subscripted ∞ denotes that this cell constant is the limiting volume ratio as the number of expansions becomes infinite, or in other words, when the pressure goes to zero. Unfortunately, the N_j 's are not

equal to N_{∞} , but they change with increasing pressure because of the deformation of all the volumes mentioned above. Since maximum accuracy in the final results of the experimental work is attainable only if the cell constant for each expansion is known very closely, the deformation of these volumes must be estimated as well as possible to minimize the uncertainty in the cell constants for the various experimental pressures.

The formulas normally used to calculate deformations of thick-walled vessels involve an uncertainty which, as a rough approximation, might be considered to be a percentage of the total change. Thus if the deformation is reduced to a small enough level, this uncertainty will then become negligible with respect to other irreducible experimental errors.

Deformation of the valves, tubing, magnetic pump, and pressure null indicator cell must be accepted as they are; the two cell volumes of the pressure bomb, however, are such a large part of the total system volume that a substantial decrease in their change with pressure is quite significant in reducing the uncertainties in the cell constant. Such an improvement is made possible by surrounding the cells with an outer jacket which will allow the inner and outer pressures to be equalized. As discussed in Chapter III, that approach is the one that was taken in this work--each of the two cells of the pressure bomb had equal internal and external pressure over about 99 percent of their surface.

An estimate of the deformation of the entire Burnett system as a function of pressure is made below, and the results are applied to the description of the change of the cell constant with pressure. The effect is seen to be non-negligible, although it is considerably less than it would have been without the double-wall feature in the Burnett cell.

Deformation of Thick-Walled Cylinders

The deformation of the two cells in the pressure bomb, the magnetic pump, and the tubing can be estimated by application of the Lamé equations (10, pp. 160-165; 44). In the case of the Burnett cells, the assumption is made that the ratio of length to diameter is sufficiently large to make the non-uniformities of the longitudinal stress distribution insignificant. The cells can then be treated as long, thick-walled cylinders, closed at both ends, with balanced internal and external pressure. It is felt that the balanced pressure on the cells makes this assumption of uniform stress distribution acceptable (10, p. 180). The magnetic pump is treated as a combination of three long, thick-walled cylinders with closed ends and internal pressure only, and the tubing as a long thick-walled cylinder with closed ends and internal pressure only.

The application of internal and external pressure to a thick-walled cylinder with closed ends causes both a radial and a longitudinal deformation, which can be expressed

in terms of the pressures, the original dimensions of the cylinder, and the properties of the material used for the cylinder,

$$\frac{\delta L}{L} = \frac{P_i}{E} \left\{ \frac{R_i^2(1-2\mu) + R_e^2[2\mu(P_e/P_i)]}{R_e^2 - R_i^2} \right\} \quad (D-1)$$

$$\frac{\delta R_i}{R_i} = \frac{P_i}{E} \left\{ \frac{R_i^2(1-2\mu) + R_e^2[1+\mu-2(P_e/P_i)]}{R_e^2 - R_i^2} \right\} \quad (D-2)$$

where L = length of the cylinder
 δL = increase in the length of the cylinder
caused by the application of pressure
 P_i = internal pressure
 P_e = external pressure
 R_i = inner radius of the cylinder
 R_e = outer radius of the cylinder
 δR_i = increase in the inner radius of the cylinder
caused by the application of pressure
 E = modulus of elasticity
 μ = Poisson's ratio

When the external pressure is zero, these equations reduce to

$$\frac{\delta L}{L} = \frac{P_i}{E} \left[\frac{R_i^2(1-2\mu)}{R_e^2 - R_i^2} \right] \quad (D-3)$$

$$\frac{\delta R_i}{R_i} = \frac{P_i}{E} \left[\frac{R_i^2(1-2\mu) + R_e^2(1+\mu)}{R_e^2 - R_i^2} \right] \quad (D-4)$$

Equations D-1 and D-2 will be applicable to the determination of the volume change of the Burnett cells, and D-3 and D-4 will apply to the magnetic pump and the tubing. In order to obtain the expression for these volume changes, the equation for the volume of a cylinder,

$$V_c = \pi R_i^2 L \quad (D-5)$$

can be differentiated to give

$$dV_c = 2\pi R_i L dR_i + \pi R_i^2 dL \quad (D-6)$$

For small changes of volume, the derivatives can be replaced by delta quantities so that Equation D-6 will become

$$\delta V_c = 2\pi R_i L \delta R_i + \pi R_i^2 \delta L \quad (D-7)$$

Division by Equation D-5 will then yield the general expression for the ratio of the volume change and the initial volume.

$$\frac{\delta V_c}{V_c} = 2 \frac{\delta R_i}{R_i} + \frac{\delta L}{L} \quad (D-8)$$

When Equations D-1 and D-2 are substituted into this expression, the relationship is obtained by which the volume change of the Burnett cells can be calculated for any internal and external pressure,

$$\frac{\delta V_c}{V_c} = \frac{P_i}{E} \left\{ \frac{3R_i^2(1-2\mu) + 2R_e^2[1+\mu+(\mu-2)(P_e/P_i)]}{R_e^2 - R_i^2} \right\} \quad (D-9)$$

For the situation of immediate interest, in which the internal and external pressure are equal, this relationship simplifies to

$$\frac{\delta V_c}{V_c} = \frac{P_i}{E} \left[\frac{(1-2\mu)(3R_i^2 - 2R_e^2)}{R_e^2 - R_i^2} \right] \quad (D-10)$$

To obtain the analogous equation for the tubing and magnetic pump, Equations D-3 and D-4 can be substituted into Equation D-8, giving

$$\frac{\delta V_c}{V_c} = \frac{P_i}{E} \left[\frac{3R_i^2(1-2\mu) + 2R_e^2(1+\mu)}{R_e^2 - R_i^2} \right] \quad (D-11)$$

Equation D-11 can be seen to follow immediately from Equation D-9 when the external pressure is zero.

Equations D-10 and D-11 are the equations to be used in the following calculation of the cylinder deformations.

Deformation of the Burnett Cells

For the calculation of cell deformations by means of Equation D-10, the following values are appropriate for each cell:

$$R_i = 0.875 \text{ in.}$$

$$R_e = 1.3125 \text{ in.}$$

D-7

$$E \approx 1.77 \times 10^6 \text{ atm.}$$

$$\mu \approx 0.32$$

The internal length of the larger cell was 4.0 inches, and of the smaller, 2.0 inches. Substitution of these values into Equation D-10 gives

$$\frac{\delta V}{V} \approx -2.44 \times 10^{-7} P \quad (D-12)$$

where P is the pressure in atmospheres. Multiplication of both sides of this equation by the volume of each cell yields the relationship between pressure and change of volume in each of the cells.

$$(\delta V)_{\text{larger cell}} \approx -2.35 \times 10^{-6} P \quad (D-13)$$

$$(\delta V)_{\text{smaller cell}} \approx -1.17 \times 10^{-6} P \quad (D-14)$$

Deformation of the Magnetic Pump

An estimate of the deformation of the magnetic pump can be obtained by dividing the pump into three parts and applying Equation D-11 to each part. The dimensions of interest for this calculation are

$$\text{for the bottom part, } R_i = 0.250 \text{ in.}$$

$$R_e = 0.4375 \text{ in.}$$

$$L = 2.125 \text{ in.}$$

$$\text{for the middle part, } R_i = 0.158 \text{ in.}$$

$$R_e = 0.3125 \text{ in.}$$

$$L = 1.8125 \text{ in.}$$

D-8

for the top part, $R_i = 0.1406$ in.

$R_e = 0.3125$ in.

$L = 0.5625$ in.

for all parts, $E \approx 1.77 \times 10^6$ atm.

$\mu \approx 0.32$

Substitution of the appropriate values into Equation

D-11 yields

$$\frac{\delta V}{V} \approx 2.51 \times 10^{-6} P \quad (\text{bottom}) \quad (\text{D-15})$$

$$\frac{\delta V}{V} \approx 2.21 \times 10^{-6} P \quad (\text{middle}) \quad (\text{D-16})$$

$$\frac{\delta V}{V} \approx 2.03 \times 10^{-6} P \quad (\text{top}) \quad (\text{D-17})$$

and multiplication of these ratios by their respective volumes yields

$$(\delta V)_{\text{bottom}} \approx 1.05 \times 10^{-6} P \quad (\text{D-18})$$

$$(\delta V)_{\text{middle}} \approx 3.14 \times 10^{-7} P \quad (\text{D-19})$$

$$(\delta V)_{\text{top}} \approx 7.1 \times 10^{-8} P \quad (\text{D-20})$$

The total deformation of the pump as a function of pressure will then be

$$(\delta V)_{\text{magnetic pump}} \approx 1.44 \times 10^{-6} P \quad (\text{D-21})$$

Deformation of Tubing

The deformation of the tubing can be estimated by

substitution of the tubing dimensions and properties into Equation D-11.

$$R_i \approx 0.055 \text{ in.}$$

$$R_e \approx 0.094 \text{ in.}$$

$$E \approx 1.97 \times 10^6 \text{ atm.}$$

$$\mu \approx 0.30$$

$$L_1 \approx 77 \text{ in.}$$

$$L_2 + L_1 \approx 127 \text{ in.}$$

The total length of tubing included in the volume of the system before an expansion is denoted by L_1 , and the total length after an expansion is $L_1 + L_2$. For each of these two lengths, the resulting relationship becomes

$$\frac{\delta V}{V} \approx 2.32 \times 10^{-6} P \quad (\text{D-22})$$

Multiplication of this relationship by the two separate volumes then gives

$$(\delta V)_{L_1} \approx 1.70 \times 10^{-6} P \quad (\text{D-23})$$

$$(\delta V)_{L_1+L_2} \approx 2.81 \times 10^{-6} P \quad (\text{D-24})$$

Volume Change of Cryogenic Pressure Null Cell

The volume change below the diaphragm of the cryogenic pressure null cell must be divided into two parts. The first part is analogous to the deformations calculated

in the previous sections, and is just the change caused by the deformation of the cell body with pressure. The other part is more complicated and has to do with an apparent change in the null-point position of the diaphragm with changing pressure.

Deformation of the Cell Due to Pressure

This volume change is very difficult to calculate because of the physical dimensions of the cell. Since the total volume in the cell, below the diaphragm, is only about 0.037 cubic inches, however, the amount of volume change caused by pressure changes is considered negligible in this work.

Volume Change Due to Null-Point Shift of the Indicator

This effect has been discussed thoroughly in Appendix C, where it was seen to be very small. A few points will be borrowed from that discussion and applied here. First, the assumption is made that no deflection of the diaphragm will occur as long as there is no pressure differential across it, regardless of the total pressure. The logical extension from this assumption is that whenever the meter of the PNI is nulled, the pressure difference (actual zero shift) across the diaphragm will cause a deflection of the diaphragm.

This deflection of the diaphragm will cause a change in the volume of the Burnett apparatus, and the volume

change will be related to the actual zero shift according to Equation C-26:

$$\delta V_{dm} \approx 0.1745 (\Delta P_{ZSC}) \quad (C-26)$$

where δV_{dm} is expressed in in^3 and ΔP_{ZSC} is in atmospheres. As seen in Figure C-1, the relationship between the actual zero shift and the pressure is linear only at 50°C of the three experimental temperatures studied here. That relationship is expressed by the equation

$$\Delta P_{ZSC} \approx 3.5 \times 10^{-6} P \quad (D-25)$$

where ΔP_{ZSC} and P are in consistent units, e.g., atmospheres. Substitution of Equation D-25 into Equation C-26 then gives

$$(\delta V_{dm})_{50^\circ\text{C}} \approx 6 \times 10^{-7} P \quad (D-26)$$

where δV_{dm} is in cubic inches and P is in atmospheres. At 0 and 50°C the variation of zero shift with pressure is non-linear, but each of the two curves can be approximated by two straight line segments. At 0°C ,

$$\Delta P_{ZSC} \approx \begin{cases} 1.4 \times 10^{-6} P & , P \leq 500 \text{ atm} \\ -1.1 \times 10^{-3} + 3.6 \times 10^{-6} P, & 500 \leq P \leq 750 \text{ atm} \end{cases} \quad (D-27)$$

Substitution of these relationships into Equation C-26 gives

$$(\delta V_{dm})_{0^\circ\text{C}} \approx \begin{cases} 2.44 \times 10^{-7} P & , P \leq 500 \text{ atm} \\ -1.92 \times 10^{-4} + 6.28 \times 10^{-7} P, & 500 \leq P \leq 750 \text{ atm} \end{cases} \quad (D-28)$$

Similarly, at -50° ,

$$\Delta P_{ZSC} \approx \begin{cases} -1.5 \times 10^{-6} P & , P \leq 500 \text{ atm} \\ -1.45 \times 10^{-3} + 1.4 \times 10^{-6} P, & 500 \leq P \leq 750 \text{ atm} \end{cases} \quad (\text{D-29})$$

Substitution into Equation C-26 gives

$$(\delta V_{dm})_{-50^\circ C} \approx \begin{cases} -2.62 \times 10^{-7} P & , P \leq 500 \text{ atm} \\ -2.53 \times 10^{-4} + 2.44 \times 10^{-7} P, & 500 \leq P \leq 750 \text{ atm} \end{cases} \quad (\text{D-30})$$

Volume Change of Cryogenic Valves

The four valves in the cryostat will undergo a slight deformation as the pressure increases in the system. The volume change below the seat will be entirely negligible, but the change of volume of the upper part may or may not be. The uncertainty is caused by the fact that the Teflon packing ring in the valve compresses and extrudes as pressure is applied. Because of the uncertainty of the magnitude of this very small possible change, it has been entirely neglected in comparison with all other pressure deformation effects. Thus for the cryogenic valves, the volume change with pressure is assumed to be zero.

Total Effect of Pressure on the Cell Constant

With the above estimates of pressure deformation of the components in the system, the combined effect of pressure on the cell constant can be estimated. As mentioned at the first of this appendix, the cell constant for a given

expansion is defined as the ratio of the total volumes before and after that expansion. By this same definition, the cell constant at zero pressure is then

$$N_{P=0} \equiv N_{\infty} = \frac{(V_a + V_b)_{\infty}}{(V_a)_{\infty}} = \frac{(V_a + V_b)_{P=0}}{(V_a)_{P=0}} \quad (D-31)$$

The volume at a pressure P_j is equal to the volume at zero pressure plus the change in volume caused by the pressure,

$$(V_a + V_b)_j = (V_a + V_b)_{P=0} + \Delta(V_a + V_b)_j \quad (D-32)$$

$$(V_a)_{j-1} = (V_a)_{P=0} + \Delta(V_a)_{j-1} \quad (D-33)$$

Substitution of Equations D-31, D-32, and D-33 into Equation 7 gives

$$N_j = N_{\infty} \frac{\left[1 + \frac{\Delta(V_a + V_b)_j}{(V_a + V_b)_{P=0}} \right]}{\left[1 + \frac{\Delta(V_a)_{j-1}}{(V_a)_{P=0}} \right]} \quad (D-34)$$

The value of $\Delta(V_a + V_b)_j$ is approximated by the sum of Equations D-13, D-14, D-21, D-24, and one of the group D-26, D-28, and D-30, depending on the temperature. The value of $\Delta(V_a)_{j-1}$ is approximated by the sum of Equations D-13, D-23, and one of the group D-26, D-28 and D-30. From these estimated values of the volume changes and the dimensions of the components of the system, the expressions for the cell constant N_j are:

at 50°C,

$$N_j = N_\infty \left[\frac{1 + 8.1 \times 10^{-8} P_j}{1 - 4.8 \times 10^{-9} P_{j-1}} \right] \text{ for all pressures; (D-35)}$$

at 0°C,

$$N_j = N_\infty \left[\frac{1 + 5.9 \times 10^{-8} P_j}{1 - 3.8 \times 10^{-8} P_{j-1}} \right] \text{ if } P_{j-1} \leq 500 \text{ atm (D-36)}$$

$$= N_\infty \left[\frac{1 + 5.9 \times 10^{-8} P_j}{1 - 1.82 \times 10^{-5} - 1.9 \times 10^{-9} P_{j-1}} \right]$$

if $P_{j-1} > 500$ atm; (D-37)

at -50°C,

$$N_j = N_\infty \left[\frac{1 + 2.9 \times 10^{-8} P_j}{1 - 8.7 \times 10^{-8} P_{j-1}} \right] \text{ if } P_j \leq 500 \text{ atm (D-38)}$$

$$= N_\infty \left[\frac{1 + 2.9 \times 10^{-8} P_j}{1 - 2.41 \times 10^{-5} - 3.9 \times 10^{-8} P_{j-1}} \right]$$

if $P_j > 500$ atm (D-39)

As a point of clarification, mention should be made of the fact that in no case was the pressure following an expansion,

P_j , greater than 500 atmospheres. Thus it follows that only for the runs having initial pressures greater than this do the second of the equations listed above for 0 and 50° need to be considered, and even for these runs the high-pressure equation applies only for the first expansion.

An interesting result of the double-wall design of the Burnett cell is the manner in which the decrease in the cell volume is almost balanced by the increase of the volume for the remainder of the system, leading to very small pressure effects in the cell constant expressions.

The magnitude of these effects can be evaluated by assuming reasonable values for typical pressure measurements. For instance, if the initial pressure (P_0) is assumed to be 700 atm, a reasonable value for P_1 would be 400 atm, and for P_2 , 250 atm. When these values are substituted into Equations D-35 through D-39, the following results are obtained for the change in cell constant with pressure:

$$\text{At } 50^\circ\text{C: } N_1/N_\infty \approx 1.0000358$$

$$N_2/N_\infty \approx 1.0000221$$

$$\text{At } 0^\circ\text{C: } N_1/N_\infty \approx 1.0000431$$

$$N_2/N_\infty \approx 1.0000300$$

$$\text{At } -50^\circ\text{C: } N_1/N_\infty \approx 1.0000630$$

$$N_2/N_\infty \approx 1.0000421$$

Thus in the worst case, at -50°C , the change only amounts to approximately 0.0063 percent. By comparison, Canfield estimated a maximum change of 0.05 percent for an expansion between 500 and 250 atm (6, p. D-2).